The Occurrence and Behavior of Rainfall-Triggered Landslides in Coastal British Columbia

by

Richard Hamilton Guthrie

A thesis
presented to the University of Waterloo
in the fulfillment of the
thesis requirement for the degree of
Doctor of Philosophy
in
Earth Science

Waterloo, Ontario, Canada, 2009

Author's Declaration

I hereby declare that I am the sole author of this thesis. This is a true copy of the thesis, including any required final revisions, as accepted by my examiners.

I understand that my thesis may be made electronically available to the public.

Abstract

This thesis seeks to analyze the occurrence and behavior of rainfall-triggered landslides in coastal British Columbia. In particular, it focuses on the analysis of landslide temporal and spatial distributions occurrence and their magnitudes, and considers the major factors that influence regional landslide behavior. Implicit in the research is the understanding that the landscape of coastal BC is managed, and that landslides, in addition to occurring naturally may be caused by, and certainly impact, resources that are important to humankind. Underlying each chapter is the rationale that by better understanding the causes of, and controls on landslide occurrence and magnitude, we can reduce the impacts and lower the associated risk. Statistical magnitude-frequency relationships are examined in coastal BC. Observations suggest that landslides in coastal British Columbia tend to a larger size until about 10,000 m^2 in total area. At this point larger landslides are limited by landscape controls according to a power law. Probabilistic regional hazard analysis is one logical outcome of magnitude-frequency analysis and a regional mass movement hazard map for Vancouver Island is presented. Physiographic controls on statistical magnitude-frequency distributions are examined using a cellular automata based model and results compare favorably to actual landslide behavior: modeled landslides bifurcate at local elevation highs, deposit mass preferentially where the local slopes decrease, find routes in confined valley or channel networks, and, when sufficiently large, overwhelm the local topography. The magnitude-frequency distribution of both the actual landslides and the cellular automata model follow a power law for magnitudes higher than 10,000 m^2 - 20,000 m^2 and show a flattening of the slope for smaller magnitudes. The results provide strong corroborative evidence for physiographic limitations related to slope, slope distance and the distribution of mass within landslides. The physiographic controls on landslide magnitude, debris flow mobility and runout behavior is examined using detailed field and air photograph analysis. The role of slope on deposition and scour is investigated and a practical method for estimating both entrainment and runout in the field, as well as in the GIS environment, is presented. Further controls on landslide mobility, including the role of gullies and stream channels, roads and benches and intact forests, are considered. The

role of landslides in controlling landscape physiography is also examined. In particular, it is determined that moderate-sized landslides do the most work transporting material on hillslopes, defined by a work peak, and that magnitude varies based on local physiography and climate. Landslides that form the work peak are distinct from catastrophic landslides that are themselves formative and system resetting. The persistence time for debris slides/debris flows and rock slides/rock avalanches is calculated over six orders of magnitude and an event is considered catastrophic when it persists in the landscape ten times longer than the population of landslides that form the work peak. A detailed case study examines meteorological controls on landslide occurrence and the role of extreme weather is considered. A critical onset of landslide triggering rainfall intensity is determined to be between 80 mm and 100 mm in 24 hours and wind is determined to result in increased local precipitation. The role of rain-on-snow is also evaluated and determined to be crucial to landslide occurrence. Finally, a conceptual model of landslide-induced denudation for coastal mountain watersheds spanning 10,000 years of environmental change is presented. Recent human impacts are calculated for landslide frequencies over the 20th century. The impact of logging during the last 100 years is unambiguous; logging induced landslides almost doubles the effect frequency of the wettest millennia in the last 10,000 years. This suggests that the impact of logging outpaces that of climatic change. Debris slides and debris flows are estimated to have resulted in a landscape lowering of 0.7 m across the Vancouver Island during the last 10,000 years.

Acknowledgements

No body of research is done in isolation and in writing this thesis I owe a debt of gratitude to several people and institutions:

The Natural Sciences and Engineering Research Council of Canada is one of three major federal granting agencies that support research in Canada, and indeed, this research was supported by an Alexander Graham Bell Canada Graduate Scholarship (CGS D). The funding provided by NSERC was crucial to the successful completion of my PhD, and allowed me to learn from and collaborate with colleagues around the world. If this thesis succeeds in advancing the science of landslide research, much of that success is owed to NSERC.

Additional financial support came from the University of Waterloo in the form of a President's Graduate Scholarship award. Again, I am grateful for the support.

I approached Dr. Stephen Evans and the Department Earth Sciences just over 4 years ago with a genuine interest in, and a vision for, this research, but with some restrictions as well, specifically the need to spend most of my time on the west coast with my family. I am sincerely grateful for the accommodations that have been made that made that have allowed me to do just that. I am proud to be associated with the University of Waterloo and this great group of scientists.

I wish to thank my employer, the British Columbia Ministry of Environment, who also stepped up to the plate and were accommodating of my efforts. It sounds redundant to say that the work would not be completed without the support of yet another group, but it is nonetheless true. Specifically, I'd like to thank Judy Teskey for her unfailing support, and Dick Heath, who perceived benefit in both this work, and my continued role at the ministry.

I had several opportunities over the course of my research that changed my world view. These experiences are not explicitly part of my thesis, but they were nonetheless a big part of my program. I wish to acknowledge the International School of Landslide Risk Assessment and Mitigation (LARAM), the premiere course of its kind held annually in Ravello Italy, for the opportunity to participate, and learn firsthand from some of the world's most renowned landslide scientists. I wish to acknowledge Canadian Foreign

Affairs for their support of scientific outreach and assistance to the Philippines in 2006, following the deadliest single landslide worldwide in over a decade. I wish to acknowledge the warm hospitality of the Geotechnical Engineering Office in Hong Kong who recently celebrated 30 years of dedicated slope safety practice, and from whom so much can be learned.

A huge thank you to the many friends and colleagues who have listened to me, sometimes bemused, as I got excited about yet another landslide or idea.

Life has a tendency to take one by surprise, and upheavals are almost guaranteed. The upheavals in my own life that ultimately led to this undertaking were made smoother by the patient advice from my father, and the buoying support of my brother. To you both, I wish I could tell you how important this has been. Thank you will have to suffice.

Finally, I wish to thank my friend and mentor, Steve Evans. Steve began pushing me to take on a PhD a few years before I actually made the choice. He has been at various times collegial, paternal, editorial, unyielding, encouraging, co-conspiring, accommodating, patient and supportive. I have never met anyone with a greater enthusiasm for landslide research, or anyone with whom I felt such an affinity for the intellectual side of this discipline. I have always come away from our discussions feeling inspired. Steve and I have travelled the world together, and I've rarely had more fun than we have had in any of our several misadventures! Importantly, Steve has always been an advocate for me and my research. He has several strengths, but one of them is undoubtedly his ability to increase the personal worlds of those around him. Words are once again insufficient and, once again, thank you will have to suffice.

Dedication

To my father, Richard Hamilton Guthrie II, and to my brother, Mark Ryan Guthrie, with thanks.

Contents

List of Figures

List of Tables

Chapter 1: Introduction

1.1 CONTEXT

Coastal British Columbia is dominated by an unbroken mountain chain, the Coast Mountains, extending from its southern border some 1500 km northward to the provincial boundary and varying in width between 50 and 160 km (Holland, 1976) and the Insular Mountains of Vancouver Island and the Queen Charlotte Islands. In all cases the terrain is rugged, glacially over-steepened and dissected. Sediments tend to be thin over steep volcanic or granitic slopes, glacially derived and frequently subject to failure. Runoff is rapid in this dynamic environment that receives more rain, typically upwards of 2.5 $m \cdot y^{-1}$ on average, than anywhere else in British Columbia (Figure 1.1, Rodenhuis *et al.* 2007; Wang *et al.*, 2006). Steep terrain and a wet environment combine to produce a landscape that is highly susceptible to landslides. In particular, the occurrence of shallow rainfall-induced landslides: debris slides, debris avalanches and debris flows of the Varnes' (1978) classification, dominate the terrain of coastal British Columbia (Howes, 1981; Schwab, 1983; Rood, 1984; Rollerson *et al.* 1997; Millard, 1999; Guthrie, 2005).

The same dramatic terrain, due in part to the high levels of precipitation, yields a dense coniferous forest typically co-dominated by Western Red-cedar (*Thuja plicata*) and Western Hemlock (*Tsuga hterophylla*), mature examples of which reach lofty heights of 30-60 m above the ground (Fenger *et al.*, 2006). Not surprisingly, logging is the spatially dominant industry in coastal British Columbia and forest harvesting and road building have long been known to increase landslide frequency by several times (Howes and Sondheim, 1988; Rollerson, 1992; Rollerson *et al.*, 1998; Jakob, 2000; Guthrie, 2002; Chatwin 2005). These landslides, both natural and logging-related, have a variety of costly effects including: destroying roads, bridges and other public infrastructure, threatening human lives and private property, removing timber from the managed land base, burying streams and destroying aquatic habitat. As a consequence, British Columbia (BC) has invested considerable resources trying to understand the relationships between landslides, terrain and land management.

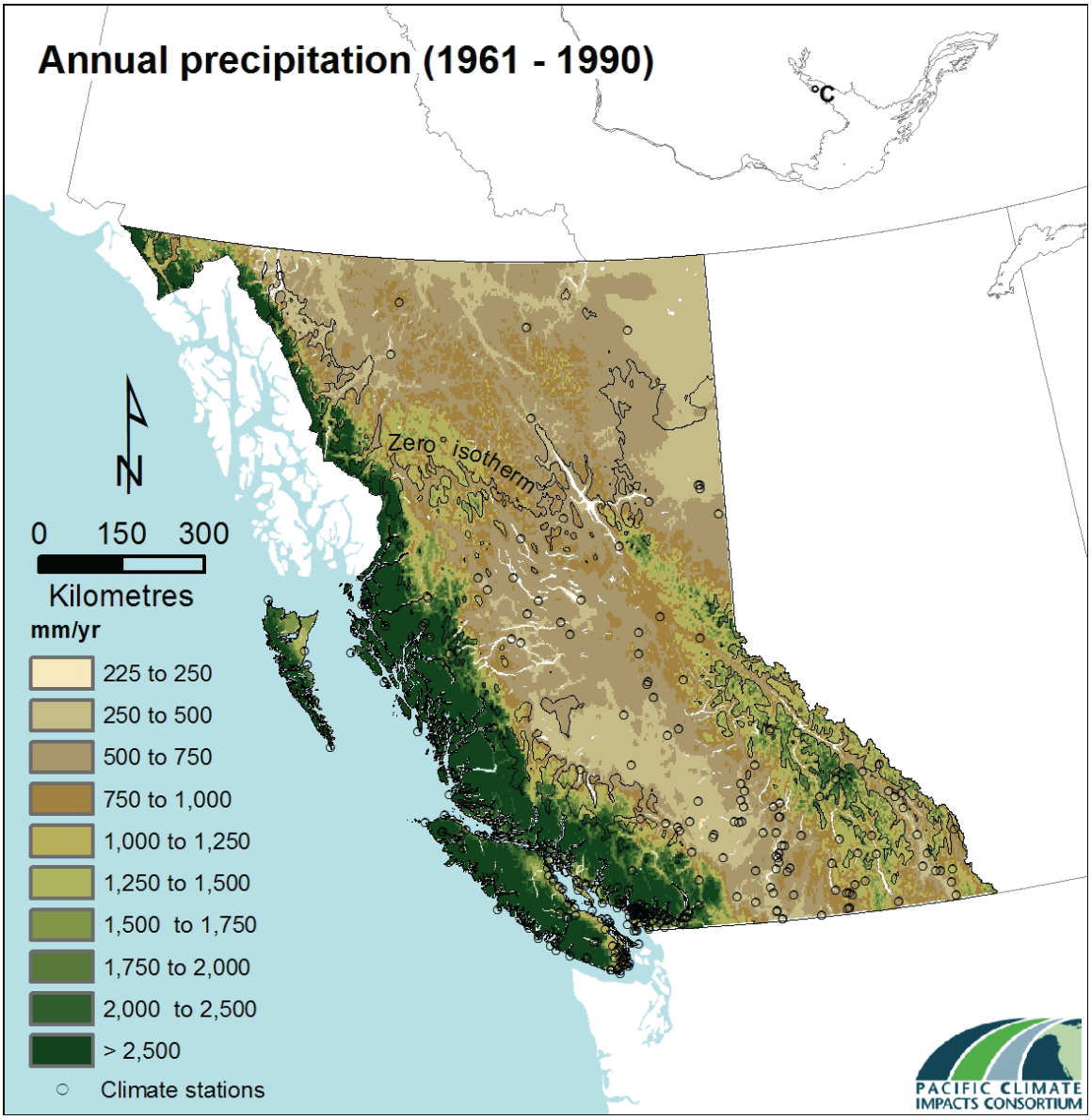

Figure 1.1 Mean annual precipitation for coastal British Columbia (from Rodenhuis *et al.*, 2007). Coastal British Columbia typically receives in excess of 2500 mm of precipitation annually.

Landslide studies in coastal BC have historically focused on establishing regional inventories (Howes, 1981; Rood, 1984; Sauder *et al.*, 1987; Thomson, 1987; Gimbarzevsky, 1988; Hartman *et al.*, 1996; Millard, 1999; Jakob, 2000; Guthrie 2002), landslide process (Hungr *et al.*, 1984; Lister *et al.*, 1984; VanDine, 1985; Fannin and Rollerson, 1993), landslide triggers (Schwab, 1983; Guthrie, 1997; Millard, 1999; Guthrie and Evans, 2004a, 2004b), landslide recovery (Smith *et al.*, 1986), and terrain

susceptibility or preparatory factors (Howes, 1987; Howes and Sondheim, 1988; Rollerson 1992; Rollerson *et al.*, 1997, 1998, 2002; Chung *et al.*, 2002; Guthrie, 2005). Overwhelmingly, the majority of the aforementioned studies also focused on the role played by forestry in the context of each of the other landslide factors: inventories, triggers, recovery, susceptibility and hazard mapping. Historical work contributed to major legislative changes in British Columbia including the Forest Practices Code, now the Forest and Range Practices Act (Government of British Columbia, 2004), and several guidebooks produced to help identify landslide prone terrain and guide land managers to reduce the impacts of landslides around the province (e.g. Chatwin *et al.*, 1994; Howes and Kenk, 1997; British Columbia Ministry of Forests and Ministry of Environment, 1999, Association of Professional Engineers and Geoscientists of British Columbia, 2003).

As a result there is broad understanding and acceptance within coastal British Columbia of the importance of landslide hazards in forested steeplands. Tied to the legislated requirements, there is a province-wide standardized hazard mapping methodology based on air photograph and ground-based expertise, that is largely based on qualitative or semi-quantitative interpretations tied to legislation. Clearly established relationships between terrain attributes and frequent landslides, such as very steep slopes and gullied terrain, have resulted in the development of professional guidlines aimed at reducing the impact of landslides. Recent reports suggest this reduction has been at least partially successful (Chatwin, 2005).

Significant gaps, however, remain. Qualitative landslide hazard mapping can and does result in considerable interpretive latitude or misinterpretation of actual landslide hazards. In addition, there is a dearth of scientific work that actually considers the distribution of landslide magnitudes and therefore potential impacts on the landscape. Without this consideration, risk cannot be accurately resolved because of questions remaining about hazard. Our ability to quantify landslide hazard has increased dramatically in the last several years. Around the beginning of the 21st century, magnitude-frequency relationships began to be developed for landslides elsewhere in the world and researchers realized that the results were fundamental to accurate characterization of landslide hazard (Hirano and Ohmori, 1989; Hovius *et al.*, 1997; Dai and Lee, 2001; Stark and Hovius,

2001; Guzzetti *et al.*, 2002a, 2002b, 2005; Malamud *et al.*, 2004a, 2004b). In coastal BC, similar research began with the analysis of landslides along transportation corridors (Hungr *et al.*, 1999) and finally for larger forested regions (Martin *et al.*, 2002; Guthrie and Evans, 2004a, 2004b; Hungr *et al.*, 2008). This research raised a host of questions concerning the distribution and behavior of landslides in time and space, many of which remain unresolved. For example, is the statistical distribution of magnitudes and frequencies observed by researchers a result of biases in their sampling methods? Is there a universal distribution curve? Is the statistical distribution of landslide size governed by fundamental landscape controls? If there are fundamental controls, could we use that knowledge to model landslide occurrence across the landscape?

An important component of landslide hazard is the analysis of landslide mobility. Despite considerable use of analytical models in site-specific instances (e.g. Hungr, 1995; McDougall and Hungr, 2004), there is no predictive model of landslide runout that fits easily into the hazard mapping methods currently used in coastal BC or that is employed across larger regions. An examination of controls on landslide magnitude and frequency distributions implicitly considers landslide mobility.

Because there has not been a substantial regional quantification of landslide hazard, it has not been possible before now to adequately consider the direct role of different sized landslides in modifying and forming the landscape. Similarly, it has not previously been possible to consider how landslide occurrence rates have varied through time, for example since the last Pleistocene glaciation, and therefore allow us to consider the impact of man and the impact of changing climate over longer time scales.

Even the role of weather has been problematic. Rainfall is widely recognized as the primary triggering mechanism for landslides in both natural and altered terrain in coastal BC, but the science behind rainfall shutdown guidelines for the forest industry has not significantly advanced from Caine (1976) and Church and Miles (1987). One difficulty is that landslides frequently occur at precipitation levels below the so-called triggering thresholds defined by intensity and duration. Lowering the threshold to a level that captures all landslides is impractical. In addition it is unclear how different are the precipitation levels at actual landslide sites compared to a sparse hydrometric network in coastal BC. Jakob and Weatherly (2003) developed a relatively sophisticated method of

anticipating landslide occurrence from precipitation, but it required regular readings from nearby hydrometric stations to calculate meteorological antecedents and storm intensity. Unfortunately, this is again impractical for most of coastal BC where the impact of landslide storm tracks has been observed, but for which no nearby hydrometric data exist (Guthrie and Evans, 2004a, 2004b).

1.2 THESIS OBJECTIVES

This thesis is my attempt to analyze and explain the behavior and distribution of regional rain-caused shallow landslides; shallow debris flows and debris slides, in coastal British Columbia. It substantially extends previous work on landslide magnitude-frequency (M-F) distribution for coastal BC and considers the questions: Why are M-F curves important? What can they tell us about the relationship between landscape and landslide hazard? What controls the shape of the M-F curve, and ultimately the distribution of landslide magnitudes? If those controls are physical rather than statistical artifacts, to what extent can we define them and incorporate that information into hazard maps? Conversely, what magnitude of landslide is the most effective in contributing to landscape form in steep terrain? Is it possible that we can more precisely define the relationship between landslides and rainfall, cause and effect? What state of the art methods lend themselves to more precise analysis of landslide cause? And finally, what can these data tell us about the geomorphic impact landslides have over a much longer time frame? Can we use that information to adapt to climate change scenarios?

1.3 CHAPTER OBJECTIVES

Each chapter is written as a stand-alone paper that provides some of the answers to the questions above. The format means that a chapter may be read on its own and that each chapter can contain new science with its own results and conclusions. However, the format also necessarily results in repetition of some fundamental concepts and descriptions of data, definitions or study areas. To this end, the reader's indulgence is requested. Each chapter is outlined below:

- Chapter 2 provides a brief review of hazard mapping in BC and argues the importance of quantifying M-F relationships to accurately assess landslide hazard. The key questions that Chapter 2 addresses are: Why are M-F curves important? What can we do with them? How do they contribute to our understanding of hazard and risk?
- Magnitude-frequency curves show a standard form which includes an artifact known as the rollover; a significant change in the distribution curve that occurs in almost all known landslide inventories at smaller sizes. Chapter 3 seeks to answer the question, what controls the shape of M-F curves and ultimately the distribution of landslide magnitudes? This chapter reasons that for rain-caused landslides (and by implication other landslides types as well) the rollover is a result of physical controls in the landscape. It uses an innovative model based on cellular automata to test this contention. This is the first time a cellular automata type model has been used to predict regional landslide statistical distributions, and it is the first detailed explanation for the rollover in landslide distributions.
- Building on the results in Chapter 3 and based on a considerable component of field data, Chapter 4 examines the controls on landslide behavior in terms of deposition and scour. This chapter aims at better defining the role of slope and topographic barriers to the mobility of rain-caused landslides in a manner that may be incorporated into landslide hazard maps and models. It tries to address the question: What makes a debris flow or a debris slide stop? It also tries to address the related question: How far can we expect a rain-caused debris flow in coastal BC to travel?
- Chapter 5 takes an altogether different but equally important approach: Instead of looking at landscape level controls on landslide magnitude, it looks instead at the extent to which landslides change the landscape. Chapter 5 once again relies heavily on the knowledge gained from M-F studies, this time to examine the size of landslides doing the most geomorphological work. It provides a comprehensive answer to a 40 year old problem: Do many small landslides

contribute more to landscape erosion than fewer larger landslides? In the process, Chapter 5 also quantifies what makes a landslide catastrophic.

- Chapter 6 departs slightly from the general analysis of landslide magnitudes and frequencies to a specific examination of several hundred landslides that occurred during a region wide storm on Vancouver Island in 2006. This chapter more precisely examines the relationship between the occurrence of rain-caused landslides and rainfall. Using new technologies for mapping, including one of the first ever attempts at a regional change detection analysis for landslides, the spatial occurrence of landslides is linked to detailed near real-time weather predictive models that include the component of wind-driven rain. The analysis refines the relationship between increasing amounts of rain and the occurrence of landslides, and demonstrates a critical onset of landslide-triggering rainfall intensity. It also demonstrates the importance of rain-on-snow events crucial to landslide occurrence in coastal BC, but which are currently understudied. Chapter 6 results, in combination with the results reported in Chapter 2, are critical data to consider for adaptation measures in a warming climate, which for coastal BC is expected to mean more frequent and more intense rainstorms.
- Finally, relying heavily on data from previous chapters, Chapter 7 considers the role of landslides in landscape denudation over the last 10,000 years on Vancouver Island. It proposes a model of erosion in different climatic regimes, established through paleo-environmental studies and considers the effect of human activity in the same framework. The results are illuminating, and suggest that one of the single best ways that we can adapt to a future warming climate is to improve our land management.

1.3.1 Appendix A1

Coastal British Columbia is distinct from many other landslide-prone regions worldwide: Population densities are low, and direct consequences of landslides are often low as a result. Nevertheless, indirect landslide costs can be high, as can the ultimate cost to society. Expectations for accurate forecasting of landslides (e.g. how big, how often,

and under what conditions they will occur) remain high and provide much of the rationale for landslide research. However, as coastal BC moves toward risk-based land management, one of the difficult questions becomes one of tolerability. To what extent are we responsible for landslide prediction? Is a large magnitude or a high consequence landslide more important than a small event? Appendix A1 presents a professional paper that considers these questions. It is included because of its importance for hazard assessment and land management practice in relation to the results reported in this thesis. This appendix provides additional rationale for why it is necessary to quantify the frequency and magnitudes of landslides in a region, why it is crucial to understand both where rain-caused landslides are likely to occur, and how far they will run out. By establishing regional landslide behavior patterns, we improve our ability to predict them under present and future climatic conditions. The expectation is high, and it is my hope that this work will help move the profession towards answers.

Chapter 2: An introduction to the role of magnitude-frequency relations in regional landslide risk analysis

Based on: Guthrie, R.H. and Evans, S.G., 2005. The role of magnitude-frequency relations in regional landslide risk analysis. In: Landslide Risk Management (Hungr, O., Fell R., Couture, R., and Eberhardt, E., Eds.) A.A. Balkema Publishers, London, UK, 375-380.

OVERVIEW: Correct characterization of landslide magnitude and frequency is necessary to adequately resolve the hazard component of the risk equation. Recent work across several watersheds in coastal British Columbia has led to new insights into magnitude-frequency relationships. These insights include probabilistic data that support the notion that landslides in coastal British Columbia tend to a larger size until limited by the landscape (valley bottoms, streams other landslides). Beyond about 10,000 m^2, the probability of successively larger landslides decreases rapidly in a relation typically described as a power law. We examine the relative importance of reliable regional inventories, data robustness and resolution (in both space and time), and temporal variation including human activity and climate change. We argue that probabilistic regional hazard analysis is a logical outcome of magnitude-frequency analysis and related to the sensitivity of the landscape to the hazard. To this end have mapped the regional mass movement hazard for Vancouver Island and present the generalized probabilistic result across four major hazard zones.

2.1 INTRODUCTION

Risk is commonly used as both a scientific term and a colloquialism. In general it is philosophically easy to comprehend. Risk is typically defined as some variation of the hazard times the consequence of that hazard occurring (Lee and Jones, 2004) and in its simplest form takes the equation:

$$R = H \times C \tag{1}$$

where R = risk, H = hazard, and C = consequence.

It is perhaps obvious that the equation may be complicated by breaking down each of the variables to component parts such as magnitude, elements at risk, vulnerability, and exposure, and each of these can be further broken down to tertiary measures to suit the needs of the assessment.

In general, analysis of risk takes geoscientists and engineers away from simply determining whether a landslide will occur in a specific area and asks the pivotal questions: With what probability and with what consequence? While it is generally recognized that the probability of a hazard occurring is a critical component of the risk equation, there is perhaps the notion that already fully understand hazard analysis or that are at the very least competent in assessing hazard. To a certain extent this notion is probably true; quantitative hazard analysis is well documented, particularly for site specific hazards (see Turner and Schuster, 1996, for detailed examples of landslide hazard analysis techniques).

Significant recent progress has been made on the quantification of regional landslide hazard (see recent review by Malamud *et al.*, 2004). Specifically, there has been considerable progress in the quantification of landslide hazard through the use of a characteristic magnitude and frequency (M-F) relation. The M-F relation is a type of hazard model (Lee and Jones, 2004) that considers the probability distribution of landslides of different sizes occurring in a region. The application of landslide M-F relations to hazard and quantitative risk assessment has been most successfully demonstrated with respect to rockfall hazard along transportation corridors. Following Hungr *et al.* (1999), work by Guzzetti *et al.* (2003, 2004), and Singh and Vick (2003) has demonstrated the utility of the methodology.

However, this progress is based on a very limited number of landslide data sets. In addition, a dearth of natural landslide data sets, complete inventories, time series analysis and available terrain data, combined with qualitative and inconsistent classification of hazard, have resulted in, at best, inconsistent understanding of regional landslide hazard from one practitioner to another.

The objectives in this chapter are four-fold: (1) To show that the correct characterization of landslide magnitude and frequency is critical to adequately resolve the hazard component of the risk equation; (2) To show that useful magnitude-frequency

relationships have been established as a result of complete landslide inventories and to present a brief summary of these data from British Columbia; (3) To demonstrate that probabilistic regional hazard analysis is one logical outcome of magnitude-frequency analysis; and, (4) To discuss the implications for the general understanding of landslide hazard as it relates to the sensitivity of the landscape.

2.2 LANDSLIDE HAZARD MAPPING IN BRITISH COLUMBIA

2.2.1 Qualitative regional hazard analysis

In 1995 British Columbia (BC) introduced the Forest Practices Code to govern its largest resource sector: the forest industry. Terrain hazard mapping was required for all areas proposed for harvest or road construction (alternatively a conservative series of defaults were applied that led to detailed assessments of potentially unstable ground at the site level).

Knowledge of landslide processes and terrain features generally resulted in a 'traffic light' system of hazard rating for landscape units at a given scale. The rating scheme was typically qualitative, with predictive descriptors and/or harvest and construction limitations attached to it (Table 2.1). The result was typically a landslide hazard map (often at a scale of 1:20,000, however, hundreds of block-specific maps have also been produced) codified to represent the range in hazard (Figure 2.1).

Despite a relatively consistent methodology for determining hazard, there is, in practice, little consistency in the meaning of each of the categories. Second there is a somewhat inconsistent application of decisions based on the hazard score. Third, hazard may have historically included some measure of consequence where the practitioner would base the hazard score not only on the likelihood of occurrence, but the impact of a landslide. In effect, prior to formal risk analysis, risk was implicitly incorporated by practitioners based on incomplete understanding of the hazard and incomplete consideration of the consequences.

New legislation passed in 2004 obligates forest companies to "*...ensure that the primary forest activity does not cause a landslide that has a material adverse effect...*"

(Government of British Columbia, 2004). In British Columbia, consequence is now written into law.

Despite this, or rather because of it, accurate hazard analysis is more important than ever.

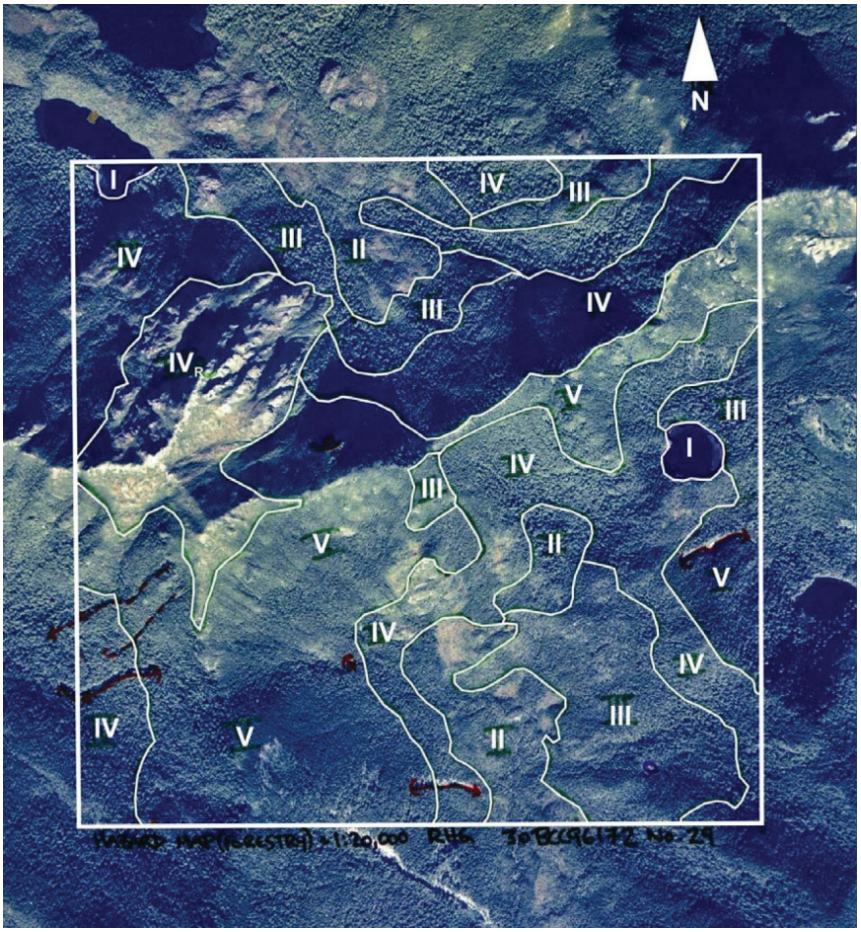

Figure 2.1 An example of a terrain hazard map in BC wherein the landscape is codified to hazard classes based on terrain attributes and landslide susceptibility. The original scale is 1:20 000 and high hazard portions of the map may be refined by field mapping. Qualitative definitions for each class are given in Table 2.1.

Table 2.1. Landslide hazard classification scheme adapted from the Mapping and Assessing Terrain Stability Guidebook (British Columbia Ministry of Forests and Ministry of Environment, 1999).

Terrain stability class	Interpretation
I	No significant stability problems Very Low likelihood of landslides following forestry activities; minor slumping at road cuts
II	Low likelihood of landslides following forestry activities; minor stability problems can develop
III	Moderate likelihood of landslides following road construction, low to very low following harvesting
IV	Moderate likelihood of landslides following forestry activities
V	High likelihod of landslides following forestry activities

2.2.2 Quantifying regional hazard analysis

In the regional context, quantifying the landslide hazard depends on an accurate and complete inventory. There are several types of landslide inventories including:

- Total count of landslides within an area from a point in time (air photograph analysis or a geomorphological map for example).
- Total count of landslides within an area through several points in time (time series analysis, including air photographs, archived maps, reports, dendrochronology and so forth)
- Total count of landslides within a sampled subset of the area of interest (through time or not)
- Partial or stratified count of landslides (by landslide type or size for example) through any of the above.
- Various incomplete inventories.

In each case, the power of the inventory is dictated by the constraints that bound it, and the completeness of the inventory within those constraints.

Landslides that are spatially constrained from a point in time give us an indication of landslide density rather than frequency; landslides per unit area rather than landslides per unit area per unit time; susceptibility rather than hazard. Such an inventory provides data that is amenable to probabilistic analyses; however, it incorporates several temporal biases that make comparisons between natural and altered landscapes difficult. Landslide inventories are by nature retrospective, and the natural conditions have existed for substantially longer than the conditions consequent of humans altering the landscape (in our previous examples, by logging and building roads). In general this serves to increase the natural landslide count as compared to, for example, the landslide count related to logging activity. Jakob (2000) recognized the problem in a complete inventory of landslides in Clayoquot Sound, British Columbia, and applied a correction factor to allow for an analysis of how landslides changed in time. The correction factor, while overemphasizing strong differences in landslide density and underemphasizing weak differences, gives reasonably comparable results to the more recent time series analyses (Guthrie and Evans, 2004a, Guthrie, 2005, 2002).

A landslide inventory taken at a single point in time, a spatial inventory, is by far the most common type, with several notable examples from coastal British Columbia (Rood, 1984, Sauder *et al.*, 1987, Thomson, 1987, Gimbarzevsky, 1988, Rollerson *et al.*, 1997, 1998, Jakob, 2000, Guthrie and Evans, 2004a).

Complete time-series inventories, while less common, actually record landslide hazard rather than just susceptibility (Guthrie 2002, Guthrie and Evans, 2004a) and can be used to predict the return interval of a particular hazard or series of hazards. Time series analysis can be further used to calibrate the spatial inventories, thereby increasing their analytical power (Guthrie, 2005).

Incomplete inventories (either spatial or time-series) are somewhat like case studies in that they may help to define, recognize and characterize landslide susceptibility and hazard; however, they hold limited predictive power and do not allow us to accurately assign risk. Unfortunately many decisions are made as the result of incomplete

inventories, beginning with our mental maps of landslide hazard through to analysis of only those landslides reported for a region and the biases inherent therein.

The inaccuracy of mental maps is demonstrated in the following example. In any given year, an employee takes (for example) two weeks off work for summer vacation. In year *x* 10 of 14 days he is on vacation are rainy and gray. In year *y* all 14 days are hot and sunny. Upon reflection the summer of year *x* is remembered as relatively cool and wet, while the summer of year *y* is remembered as hot and dry. In either case, the mental map may or may not be related to the actual conditions of a summer that occurs over 90 days. Similarly, an incomplete data set may or may not be a reflection of the whole. This is even more evident (in our example) if the vacation occurs in a place that is unfamiliar to the employee. His frame of reference is reduced further. In landslide-speak, this occurs when someone estimates landslide hazard in a watershed (or a given area) based on an incomplete inventory, and is compounded when that watershed is unfamiliar.

2.2.3 Magnitude and frequency

Complete inventories allow for the probabilistic analysis of landslide data, which in turn allows for the accurate characterization of the landslide hazard or landslide susceptibility. In this analysis, magnitude is addressed as a component of the hazard part of the risk equation. Specifically, M-F analysis seeks to answer, for landslide occurrences: How big, how likely and if calibrated against time, how often?

Guthrie and Evans (2004a, b) examined several complete inventories of shallow debris slides and debris flows for coastal British Columbia (Figure 2.2). Magnitude-frequency relations were compared between data sets that differed in location and study design. Clayoquot data (1109 landslides) was bound spatially while the Brooks Peninsula study incorporated a time series analysis (201 landslides), and the Loughborough Inlet study was the result of a single storm (92 landslides).

Cumulative M-F curves were generated for landslides from all three studies and each showed similar characteristics (Figure 2.3): The curves are relatively flat for landslides of lower magnitudes (measured as total area in m^2), and are defined by steep power law relations for landslides of larger magnitudes. The transition between the flat portion of

the curve and the portion defined by a power law is known as the rollover and occurs in these cases at approximately 10 000 m^2 total landslide area.

It would be convenient for hazard analysis if the majority of a landslide distribution fit a single equation such as a power law. The extent to which this is so has been discussed by several authors (Guzzetti *et al.*, 2002, Hovius *et al.*, 2000, Hungr *et al.*, 1999, Martin *et al.*, 2002, Stark and Hovius, 2001) and certainly, for the portion that does fall under a power law, exponents (the slope of the line) are similar from many data sets worldwide (often between -1.3 and -1.8). However, the power law typically only describes a portion of the data, and missed data may account for a considerable portion of the actual number of landslides. A rollover effect is typical of magnitude-frequency distributions, and describes the transition to data that falls below the power law line at smaller sizes. A more detailed discussion about the rollover and its implications follows in Chapter 3.

Insights gained from the analysis of coastal BC landslides included a renewed understanding of the rollover effect (see Chapter 3) and on the potential run-out distance (see Chapters 3 and 4) of coastal British Columbian debris slides and flows. Specifically, for coastal BC, landslides have a tendency to initiate on mid- and upper-slopes between about 31 and 45 degrees (generalized somewhat for this discussion), and travel to or beyond a topographic baseline of streams or the valley floor.

The inventories have also allowed us to begin to characterize the actual impact of human effects on the natural landslide rate. While there is substantial local variability, the regional impact that has resulted from logging and road building in coastal BC appears to be on the order of a 10 times increase in landslides per unit area per unit time (Jakob, 2000, Guthrie 2002, 2005, Guthrie and Evans, 2004a). A complete inventory and subsequent analysis for the Nelson forest region (interior British Columbia) yielded similar results (Jordan, 2003).

Additional analysis successfully applied from complete landslide inventories in coastal British Columbia include: relating landslide to terrain attributes and geology (Rollerson *et al.*, 1997, 1998, 2002, Sterling, 1997, Guthrie and Evans, 2004a, Guthrie, 2005), determination of landscape denudation (Martin *et al.*, 2002, Guthrie and Evans, 2004a, b), and establishing a relationship between high-intensity storm cells within regional precipitation events and landslide distribution patterns (Guthrie and Evans, 2004a, b).

In another example, complete inventories recently conducted by Weyerhaeuser suggest that there is a discernible improvement in road-related landslides following the Forest Practices Code in 1995 (Higman, pers. comm.).

In each case the analysis requires an understanding of the frequency characteristics of landslides for that region, and in all cases denoting impact (landscape denudation for example) magnitude is also critical.

2.2.4 A probabilistic regional hazard map: the next step

Landslide hazard maps are derived to a large extent on the fundamental assumption that the processes that made slopes unstable historically will do so again in the future. Existing landslides have long been used as indicators of future landslide potential. New landslides are predicted to occur under similar conditions (slope, material type, precipitation regime among other things) as landslides in adjacent terrain. In BC, terrain maps successfully lead to qualitative or semi-quantitative hazard maps based on this logic. However, as discussed previously, incomplete inventories of landslide magnitude and frequency (based for instance on limited local data) and mental maps frequently ignore the considerable variation across terrain or under different driving conditions. Communication and comparison of hazard from one region to another comes down to a best guess without M-F data, and is then insufficiently reliable to address risk. In contrast, landslide M-F distributions developed for a particular area have the advantage of being able to define landslide rates for the accumulated total distribution, or for any size class within it. The landscape can be parsed by any combination of driving factors including terrain, geology, climate, and slope and their role in landslide generation be quantified and importantly, predicted with some measure of reliability. These are the data that may then be incorporated into risk analysis. This crucial next step has begun on Vancouver Island, British Columbia, where a regional map showing mass movement potential was created at a scale of 1:100,000. The map was based on the compilation of the research of several authors referred to above, and on the digitally available data including slope, terrain and surficial geology, bedrock geology and climate. Guthrie (2005) subsequently developed an inventory based on stratified randomly sampled sites across the island to further establish the magnitude-frequency relationships.

Vancouver Island has been divided into four major zones:

- Zone I – The wet west coast; characterized by steep fjords, densely vegetated terrain and high precipitation falling as rain in winter months (>2.6 $m \cdot y^{-1}$). Landslides are typically debris slides and flows.
- Zone II – The moderately wet central island; characterized by steep terrain, densely vegetated with exposed small outcrops, precipitation between 1.6-2.6 $m \cdot y^{-1}$ falling mostly in winter months. Landslides are typically debris slides and flows with some rock falls.
- Zone III – The moderately dry east coast; characterized by more exposed bedrock, lower rainfall (<1.6 $m \cdot y^{-1}$), increased urbanization and rural development and shallower slope gradients. One quarter of landslides identified were rock falls.
- Zone IV – The alpine zone; characterized by high elevation, steep cliffs and plateaus, exposed bedrock, ponded water, steep gorges and sparse vegetation, most of the precipitation falling as snow in the winter months. Landslides commonly include rock falls, snow avalanches, debris slides and debris flows.

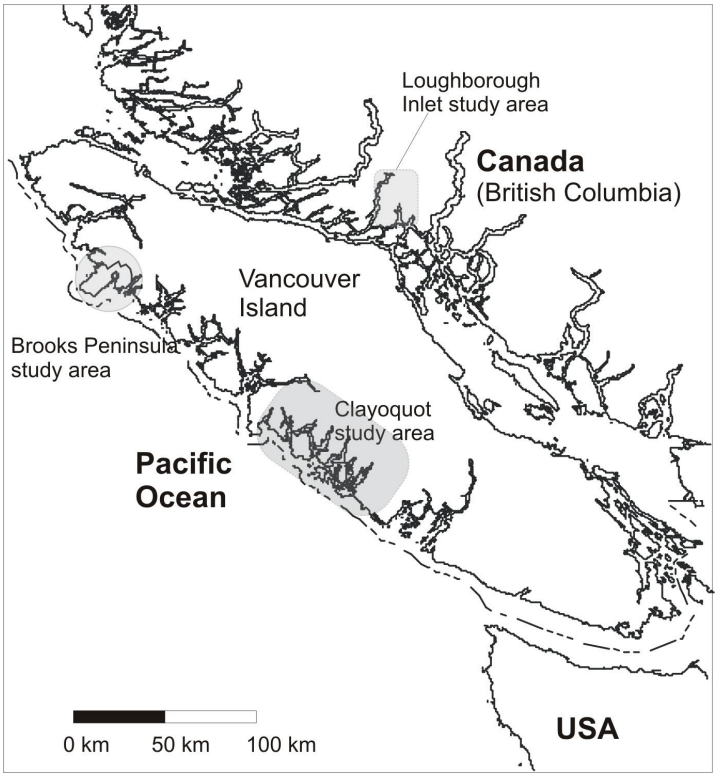

Figure 2.2 Locations of the inventories analyzed by Guthrie and Evans (2004a) for coastal BC. Recent inventories are available for the entire island (see Chapter 6).

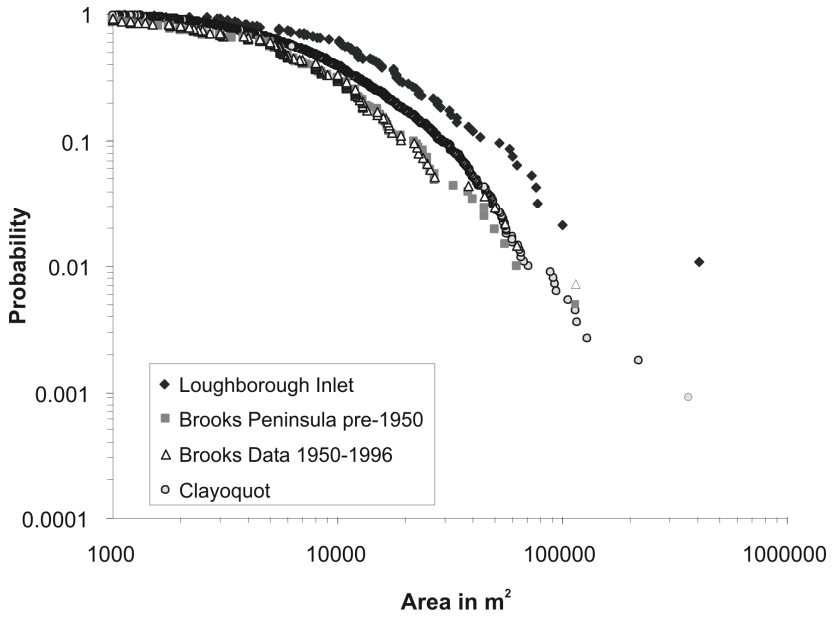

Figure 2.3 Cumulative magnitude-frequency curves for coastal BC watersheds shown in Figure 2.2 (from Guthrie and Evans, 2004a).

The approximate locations of three of the major zones are shown in Figure 2.4. The alpine zone spans the high elevation components of all three zones and was not included in the Figure. Please note that the Figure is simplified from its original for discussion purposes.

In the process of examining the data, primary, secondary and tertiary drivers to landslide distributions were determined. Primary drivers were slope and climatic regime, and these formed the basis of the regional hazard zones. Logging activity (forest harvesting and road building) increased landslide frequencies by an order of magnitude on average, considerably more than the regional variation caused by climate. However, logging was considered a secondary driver as it acted on a predefined landscape, was controllable, and behaved similarly in each zone (it increased the natural frequency and left the landslide size distribution unchanged). Other important secondary features included bedrock geology which resulted in the creation of several sub-zones. The reader is referred to Guthrie (2005) for a complete description of landslide distributions on Vancouver Island.

The natural and logging-related landslide frequencies were determined for zones I – III and compared to previous research. The results of natural landslides were mapped onto Figure 2.4 give a first ever approximation of the actual failure rates for those zones across Vancouver Island (Table 2.2).

While local variability is expected to be large, the map attempts to quantify the regional hazard and examines the difference in landscape sensitivity across the island. Differences in landscape sensitivity were already part of the mental maps for several slope specialists with local experience; however, the extent to which this is in fact the case is finally being explored.

One logical flaw that may arise in geomorphological mapping, using past conditions to predict future ones, is that the mapper is limited to a known static state and unable to incorporate the changing conditions (climate change for example). By quantifying the differing landscape vulnerabilities and the primary drivers behind those vulnerabilities, one can compare different conditions and make reliable predictions under different future scenarios that would impact those conditions (this approach is taken, for instance, in

Chapter 7 which examines climate over the Holocene and the affect on landslide generation across Vancouver Island).

Regional analysis can incorporate magnitude-frequency curves such as those in Figure 2.3 to predict over a defined period, not only how many, but how large the landslides will be. This leads to additional insights into overall landscape denudation and begins to contribute to the consequence component of risk analysis, again at a regional level.

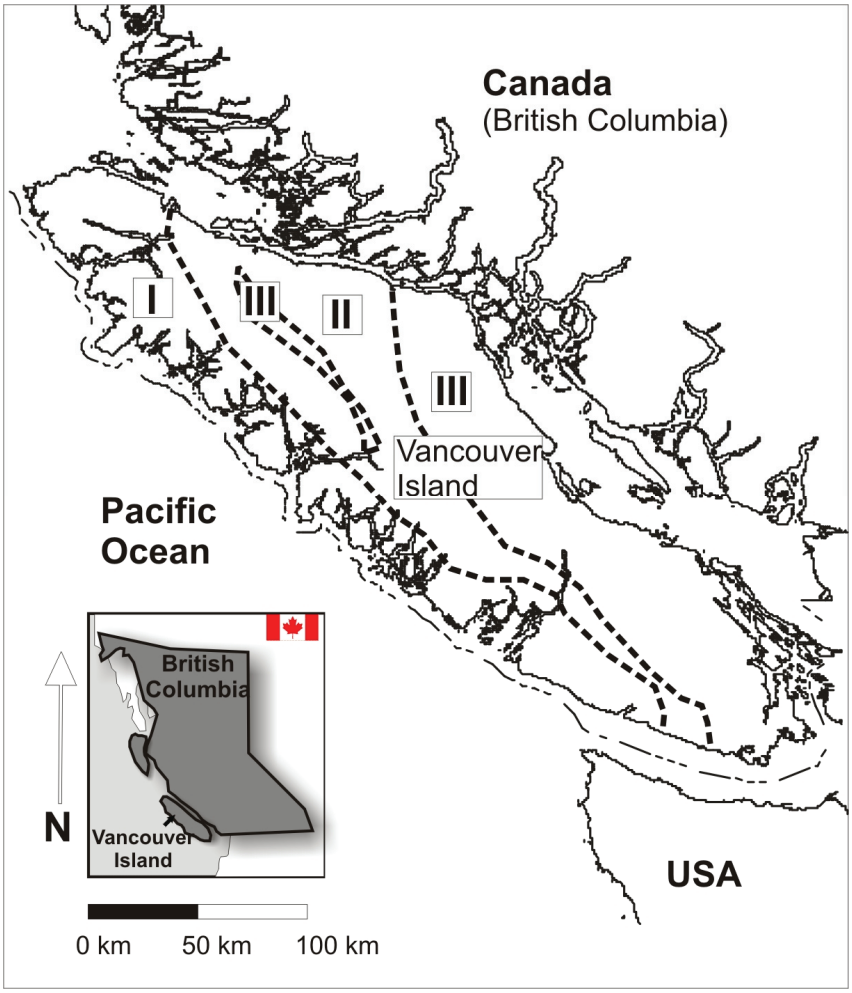

Figure 2.4. Simplified mass wasting potential zones for Vancouver Island, British Columbia. Zones I-III are described in Table 2.2. Note that the Alpine zone (IV) is not shown and spans the higher elevation portions of all three zones on this map (from Guthrie 2005).

Table 2.2. Natural landslide frequency tables for zones I-III. Logging-related landslide frequencies were also calculated and were about 10-13 times greater than the natural frequencies for all zones (Guthrie, 2005). Note that the frequency relates to a long term average, the actual failures are typically clustered in both time and space (Guthrie and Evans, 2004a, b).

Zone	Natural landslide frequency ($\#\cdot km^{-2}\cdot y^{-1}$)	Area required for 1 landslide per year (km^2)
I	0.012	83
II	0.007	143
III	0.004	250

2.3 CONCLUSIONS

Accurate landslide hazard assessment is a critical component of the risk equation. A dearth of natural landslide data sets, complete inventories, time series analysis and available terrain data, combined with qualitative and inconsistent classification of landslide hazard have resulted in, at best, inconsistent understanding of regional landslide hazard between practitioners. Complete inventories that allow the user to place hazard within a quantifiable regional context are becoming available, or can be acquired. Analysis of these inventories yields answers to the important questions: How big, how likely and how often? With sufficient data analyzed, differences in landscape sensitivity are revealed and can be handled accordingly.

Regional hazard mapping of Vancouver Island resulted in the generation of four major zones of mass movement potential, and subsequent magnitude-frequency characteristics. Differences in landslide type and frequency for each of the four zones are caused primarily by differences in climate. Natural landslides are three times more common on the wet west coast of Vancouver Island, than the eastern zone at, on average, one landslide per 83 km^2 per year. Distribution of landslide size can be derived from the magnitude-frequency relation for the west coast watersheds.

Once the landslide hazard is accurately characterized, the question of consequence takes on new relevance, and the risk assessment increases in value and accuracy.

Chapter 3: Exploring the Magnitude-Frequency Distribution: A cellular automata model for landslides

Based on: Guthrie, R.H., Deadman, P.J., Cabrera, A.R., and Evans, S.G. 2008. Exploring the Magnitude-frequency distribution: A cellular automata model for landslides. Landslides, 5, 151-159. http://www.springerlink.com/content/470443lh5457324x/?p=fba650c43fbe4610a226d03e7bcc018candpi=0

OVERVIEW: Landslide magnitude-frequency curves allow for the probabilistic characterization of regional landslide hazard. There is evidence that landslides exhibit self-organized criticality including the tendency to follow a power law over part of the magnitude-frequency distribution. Landslide distributions, however, also typically exhibit poor agreement with the power law at smaller sizes in a flattening of the slope known as rollover. Understanding the basis for this difference is critical if we are to accurately predict landslide hazard, risk or landscape denudation over large areas. One possible argument is that the magnitude-frequency distribution is dominated by physiographic controls whereby landslides tend to a larger size, and larger landslides are landscape-limited according to a power law. We explore the physiographic argument using first a simple deterministic model and then a cellular automata model for watersheds in coastal British Columbia. The results compare favorably to actual landslide data: modeled landslides bifurcate at local elevation highs, deposit mass preferentially where the local slopes decrease, find routes in confined valley or channel networks, and, when sufficiently large, overwhelm the local topography. The magnitude-frequency distribution of both the actual landslides and the cellular automata model follow a power law for magnitudes higher than 10,000 m^2 - 20,000 m^2 and show a flattening of the slope for smaller magnitudes. Based on the results of the both models argue that magnitude-frequency distributions, including both the rollover and the power law components, are a result of actual physiographic limitations related to slope, slope distance and the distribution of mass within landslides. The cellular automata model uses simple empirically-based rules that can be gathered for regions worldwide.

3.1 INTRODUCTION AND BACKGROUND

Landslide magnitude-frequency curves are necessary for the correct understanding and characterization of regional landslide hazard. They allow one to resolve the probabilistic nature of landslide size, occurrence, and when calibrated against time, frequency (Guthrie

and Evans, 2005). This in turn leads to increased understanding of landslide hazard, impact, risk, as well as hillslope denudation and the role of landslides in shaping the landscape. Unfortunately there are few complete landslide inventories worldwide (Guzzetti *et al.*, 2005) and few researchers dedicated to the task.

Landslide inventories that have been studied revealed for both experimental and actual data that landslides are log normally distributed and tend to follow an inverse power law over several orders of magnitude (Dai and Lee, 2001; Fujii, 1969; Guthrie and Evans, 2004a, 2004b, 2005; Guzzetti *et al.*, 2002a, 2002b, 2005; Hirano and Ohmori, 1989; Hovius *et al.*, 1997; Malamud *et al.*, 2004a, 2004b; Pelletier *et al.*, 1997; Reid and Page, 2002; Somfai *et al.*, 1994; Stark and Hovius, 2001).

Despite the aforementioned studies, there is evidence that landslide magnitude-frequencys follow a power law for only a truncated portion of the entire distribution (Figure 3.1) making them at best a weak inverse power law (Perline, 2005) and at worst a false inverse power law. Landslide inventories show a flattening of their respective distributions at smaller sizes in a cumulative probability plot and are therefore not predictable by a single simple equation. The departure of the data from a power law, a result of the flattening, is known as the rollover and has generated considerable discussion about probable cause.

There is, nevertheless, a case for landslides reaching self-organized critical states resulting in scale invariance or fractal landscapes (Bak, 1996; Bak *et al.*, 1988; Czirok *et al.*, 1994; Hall, 1992; Noever, 1993; Pelletier *et al.*, 1997; Malamud and Turcotte, 2000; Chen *et al.*, 2007). Several distributions have been considered to calculate the total hazard irrespective of cause, including the Double Pareto (Guthrie and Evans, 2004a, 2004b; Guzzetti *et al.*, 2002a, 2002b, 2005; Stark and Hovius, 2001) and an inverse gamma distribution (Guzzetti *et al.*, 2005; Malamud *et al.*, 2004a, 2004b). To date, however, the reasons for the rollover are insufficiently understood and total hazard characterization is limited by this lack of knowledge.

Data biasing is given as a common explanation for the rollover. This explanation suggests that, among other things, small landslides have been undercounted, artificially reducing the probability (Brardinoni *et al.*, 2003; Hungr *et al.*, 1999; Malamud *et al.*, 2004b; Stark and Hovius, 2001). Malamud *et al.* (2004b) proposed a universal curve

against which missing data can be extrapolated. The proposal of such a curve assumes that landslides have similar magnitude-frequency characteristics irrespective of physiographic constraints (for example, mean landslide size becomes universal), and its use implies that many inventories account for only a fraction (<1%) of the total landslide count. Whereas this is possible for historical events where a temporal lower bound is not defined, it disagrees with results of complete inventories from individual events such as storms (Guthrie and Evans, 2004b) or conducted through time series analysis (Guthrie and Evans, 2004a). The universal model is also a poor explanation for distributions where the rollover occurs at larger magnitudes in shallow soils. In shallow soils the persistence time of large and moderate sized events is similar but longer for successively larger events (Guthrie and Evans, 2007). As a result, historical inventories from a single set of images will show a limited bias whereby larger shallow landslides are over-counted. That bias, however, is insufficient to explain the overwhelming numbers of landslides that must be overlooked to match the universal model.

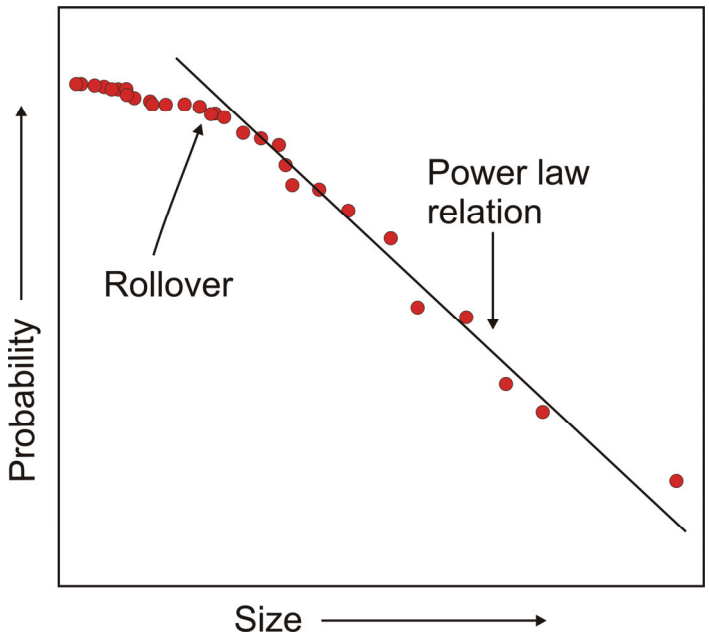

Figure 3.1. The conceptual relationship between landslide magnitude and frequency. Medium and large landslides tend to follow an inverse power law (the power law relation is a straight line on log-log scale axes); however, for smaller landslides, a flattening of actual data appears to be the norm. As a result, a power law only describes a truncated portion of the data, often larger than the most frequent smaller events.

Hungr *et al.* (2008), Guthrie and Evans (2004a, 2004b), Hovius *et al.* (2000), Pelletier *et al*. (1997), and Turcotte *et al.* (2002) considered that there may be a physical explanation for the rollover. In particular, Guthrie and Evans (2004a, 2004b), Pelletier *et al.* (1997) and Turcotte *et al.* (2002) all argued that the rollover occurred at sizes too large to be attributable to data biasing. These observations are corroborated by landslide data worldwide, where the rollover occurs at relatively large magnitudes (measured in area, and relative to consistently resolvable size): 10,000 m^2 – 30,000 m^2 for coastal British Columbia (Guthrie and Evans, 2004a, 2004b), 3,000 m^2 – 30,000 m^2 for Japan (Hirano and Ohmori, 1989) and 5,000 m^2 for the southern New Zealand Alps (Hovius *et al.*, 1997).

Pelletier *et al.* (1997) proposed physical explanations for the distribution related to soil moisture variability and its interaction with topography. Hungr *et al.* (2008) and Guthrie and Evans (2004a, 2004b) proposed that the overall physiographic variables of the landscape, and in particular slope geometry, controlled both portions of the magnitude-frequency (M-F) curve.

The physiographic argument states that for landslides over a given magnitude, the number of available locations in a landscape that could support successively larger failure events decays by a power law. The limit of this argument is intuitive in that a landslide cannot exceed, in size, the relief of the landscape on which it occurs; a size governed by incision rates and hillslope material strength (Schmidt and Montgomery, 1995). The portion of the distribution flatter than the power law is explained, at least for rain-triggered landslides of coastal British Columbia (BC), by the probability of landslides to tend to larger size based on their initiation point (in steep middle and upper slopes) and a tendency, once initiated, to flow to a lower slope position such as a stream or valley bottom. Figure 3.2 demonstrates graphically the portion of a slope on which landslides typically initiate in coastal BC. Lower slopes are depositional and the steepest upper slopes are exposed, limiting initiation opportunities for precipitation-triggered debris slides and debris flows to occur. Chung *et al.* (2001) showed, for example, that mid- and upper slopes in watersheds on Vancouver Island were most susceptible to landslide initiation. During a storm, we expect that several portions of a failing slope experience high water levels at approximately the same time, either from direct precipitation or rapid

runoff common to coastal BC. The saturated slopes are consequently less stable and a landslide that begins mid-slope will overload saturated slopes below it, entrain additional material and often travel to the valley floor (Figure 3.3). The consequence is fewer small landslides, limited by the physiography of the slope.

This paper explores in more detail the links between slope morphometrics and the distribution of landslide magnitudes and frequencies.

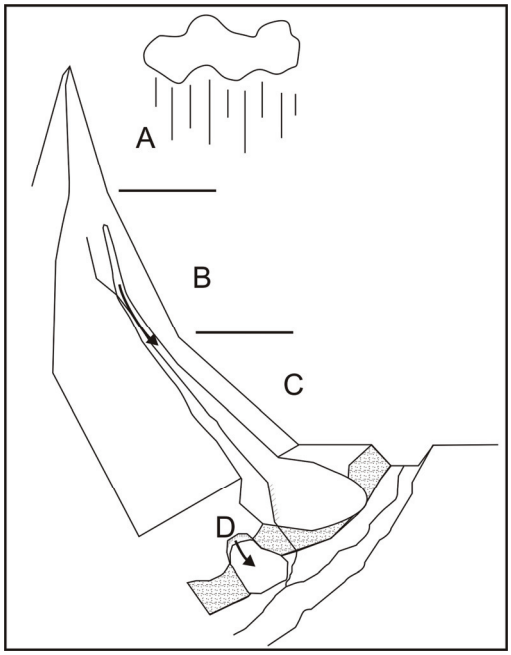

Figure 3.2. Cartoon schematic showing simplified hillslope morphology for coastal British Columbia. Section A represents steep upper slopes, typically bereft of sediment and consequently not particularly vulnerable to shallow debris slide or debris flow initiation. Section B represents the moderately steep (25^{o} – 45^{o}) middle and upper slopes, typically mantled in thin veneers of till and colluvium, and largely vulnerable to failure. Section C represents the depositional zone for material coming off the slope. It is typically comprised of coalescing colluvial aprons with debris flow fans at its base. A landslide that begins mid-slope will load saturated slopes below it, entrain more material and often travel to the valley floor. Opportunities for small landslides are thereby limited by the physiography of the slope. Small landslides occur at positions on the landscape where a long runout is improbable, however, those locations are limited (Section D).

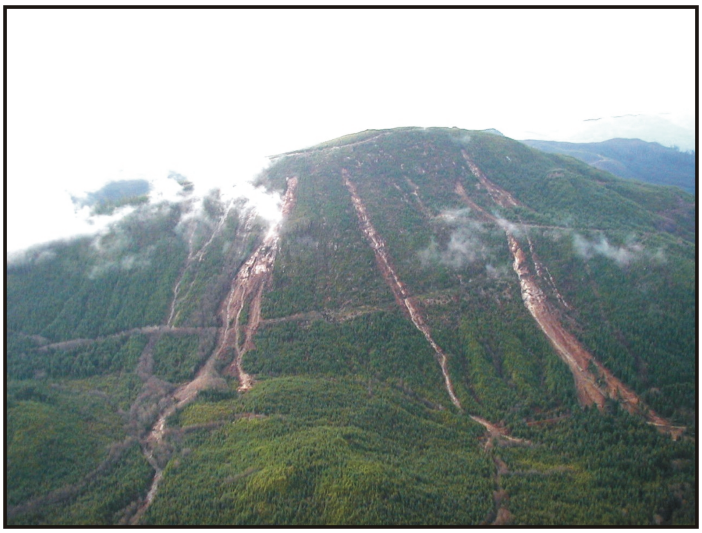

Figure 3.3. An example of landslides following the 2001 storm in Loughborough Inlet (Guthrie and Evans, 2004b)

3.2 STUDY AREA

Two sites were chosen to examine the physiographic controls on landslide Magnitude-Frequency (M-F) distributions: Loughborough Inlet, and the Klanawa watershed (Figure 3.4). Each is described briefly below.

The Loughborough Inlet study area is a 370 km^2 region on the west coast of the BC mainland. It was described in detail by Guthrie and Evans (2004b) and contains an inventory of 101 landslides that occurred as a result of a high-intensity storm cell within a larger regional event in November 2001. Landslide data was gathered from low level air photographs taken immediately following the event, landslide reports from local logging companies as well as reconnaissance field investigation. The Loughborough Inlet study area is comprised of glacially over-steepened fjordal inlets: broad U-shaped valleys bounded by rugged mountain peaks with 1769 m of total relief. Bedrock in the study area is predominantly comprised of undifferentiated diorites, gabbros, diabases and amphibolites, and a small band of competent volcanics (Guthrie and Evans, 2004b). Historical logging is extensive throughout the study area, as is the historical record of landslide activity. The area of each landslide in this chapter represents the total area including the runout.

Figure 3.4. Location map of Loughborough Inlet and Klanawa study areas.

The Klanawa River study area is a 242 km^2 watershed on the outer west coast of Vancouver Island, BC and contains an inventory of 381 landslides interpreted from aerial photographs, 331 of which are >500 m^2, a lower size cutoff to minimize data biasing and are included in the analysis herein. The Klanawa River study area is underlain by grano-dioritic and calc-alkaline volcanic rocks steepened and deepened by Pleistocene glaciations; the study area is rugged with approximately 41% of slopes steeper than 31^o and overall relief of about 960 m from sea level. Slopes and elevations were calculated from BC TRIM maps and digital elevation models. Landslides are common and the study area is located within a regional mass wasting zone described by Guthrie (2005) having annual precipitation in excess of 3,000 mm with most precipitation falling as rain between November and March, and natural landslide frequencies of about 0.024 $km^{-1}yr^{-1}$. Logging has occurred in 46% of the study area by 2001 and overall landslide rates are expected to be higher by at least an order of magnitude. Once again, landslide area in this inventory represents the total area including the runout.

3.3 MODELING LANDSLIDE MAGNITUDE-FREQUENCY DISTRIBUTIONS

3.3.1 A simple deterministic approach to understanding landslide magnitude-frequencies

We examine the argument, that landslide magnitudes and frequencies are dominated by physiographic controls by considering a strictly deterministic model for landslide generation (Figure 3.5). Physiographic constraints were considered by creating a series of possible landslides that initiated on steep slopes and traveled to the valley floor. In Loughborough Inlet, using a 25 m pixel size digital elevation model (DEM) based on Terrain Resource Information Management (TRIM) maps, about 85% of landslides initiated on slopes between 25^{o} and 45^{o} (the real percentage is expected to be higher), thereby providing reasonable limiting criteria for the initiation of most landslides. For the landslide coverage, terrain matching those criteria in Loughborough Inlet was divided into 5 m sized pixels and a centroid, representing a landslide initiation point, was placed in each pixel. In each instance, length L of the landslide is bounded by the slope (potential initiation locations) and the distance of a potential initiation site to the baseline. The down-slope travel path was determined in a geographic information system (GIS) by considering the steepest path at each pixel in the DEM to the baseline. For illustrative purposes, the landslide path is simplified in Figure 3.5 by straight lines; however, actual paths would resemble the path a drop of water would take down a slope. Length is related to area (A) in Loughborough Inlet by:

$$L=0.76A^{0.66} \quad (2)$$

Using this method, several hundred thousand imaginary landslides were created and the M-F data compared to the real events (Figure 3.5). The curve approximately parallels the actual data below magnitudes of about 20,000 m^2 and generally supports the physical argument that actual rain-triggered landslides, once initiated, will tend to flow down-slope until a physical barrier (including a substantial decrease in slope such as a valley bottom) is reached. It suggests that the M-F distribution for this range of landslides size is dependent on the distance between a potential initiation site and the bottom of the slope

and that as a rule, landslides are unlikely to stop mid-slope. However, this very simple model severely under predicts the likelihood of larger landslides and the error grows with increased magnitude. In addition, the curve decays exponentially and exhibits neither a definable break in slope, nor a power law over larger magnitudes.

The model run for the Loughborough data explains why, for rain-triggered landslides, the rollover might exist. However, it does not adequately account for the potential of landslides to continue further than a baseline, down a stream or gully for example, or for the increased spatial area of larger magnitude events, related not to length, but to the entrainment and deposition of mass.

If the physical explanation for landslide distributions holds, a cellular automata model with simple rules based largely on physiographic features might produce landslide distributions similar to those actually occurring in the landscape including both the rollover and power law portion at similar magnitudes to the actual data. The reciprocal is that a successful model would strongly corroborate the physical explanation. Finally, a successful model could aid in characterizing regional landslide hazard based on easily obtainable physiographic controls, reducing the requirement for complete inventories. This could be valuable in regions where air photographs are not easily obtained.

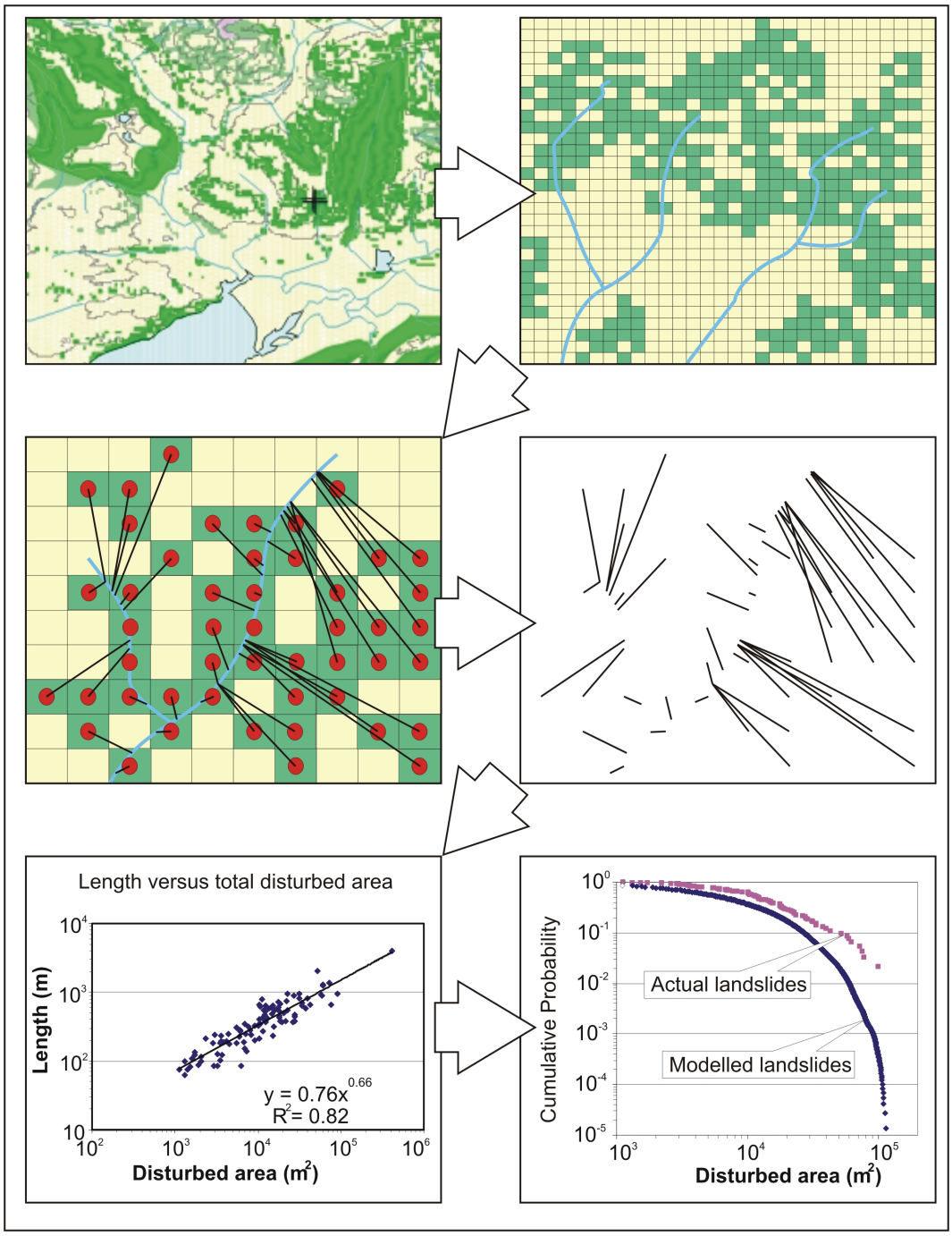

Figure 3.5. Schematic diagram showing a simple deterministic model of landslide magnitude-frequencies. Beginning in the upper left corner terrain is divided into units that are vulnerable to failure. Grids of cells (in this case 25 pixels) are given a value (1,0) for being either susceptible to landslide initiation or not. Centroids are placed in susceptible cells and they are determined to fail with the failure following the fall line and extending to the valley bottom or stream network (failures are simplified on this illustration as straight lines). The result is a range of possible landslide path lengths from every susceptible pixel. Length is related to area by an equation for actual landslides in the study area, and the M-F of the modeled landslides are plotted with the real data. See text for more discussion.

3.3.2 Exploring the landslide magnitude-frequency distribution using a cellular automata model

Cellular automata models were first constructed 40 years ago (von Neumann, 1966) and may be understood as mathematical models involving a grid or lattice of cells in which each cell evolves through a series of discrete time steps based on the value of neighboring cells, each similarly evolving. The evolution of each cell is based on the same set of rules and the values of the local neighborhood of cells (Wolfram, 1984). Although the underlying rules are relatively simple, cellular automata models tend to exhibit complex, self-organized behavior.

Cellular automata have more recently been used to model landslide behavior, from sand piles (Bak *et al.*, 1988) to individual landslide case studies (Avolio *et al.*, 2000; Clerici and Perego, 2000; D'Ambrosio *et al.*, 2003; Iovine *et al.*, 2003). Turcotte *et al.* (2002) suggest that cellular automata would work well for regional landslide characterizations that exhibit self-organized critical states, though, to our knowledge, this has not yet been done.

A cellular automata model was developed for the Klanawa study area on Vancouver Island, BC. The model was created using the Java Development Kit (5.0) from Sun Microsystems and the Recursive Porous Agent Simulation Toolkit developed by the University of Chicago and maintained as open-source software. The model consists of an agent (autonomous sub-routine) based simulation where physical rules are applied to individual cells in a raster grid. The grid consists of a DEM with an original cell size of 25 m, interpolated to 5 m sized cells. This does not increase the resolution of the DEM, but simply allows finer application of the rules to the cells of the landslide layer. Each cell in the working grid contains basic information from the DEM including elevation, position, slope, and aspect. Landslides in the model consist of a set of agents that each occupy a single cell on the grid at a given time step, and represent a variable mass of material moving from cell to cell down a slope. Agents are spawned and terminated as necessary (described below) to simulate landslide spread and decay. Landslide initiation sites may be predetermined by selecting a specific cell to fail (by latitude and longitude) or randomly selected within the grid.

Each simulation begins by populating 1-10 adjacent cells with agents based on a probability distribution of landslide initiation widths of 5-50 m typical of coastal BC landslides (from Wise, 1997). In each successive time step, each agent simultaneously processes rules for scour, deposit, path selection and movement/spread.

Rules for scour and deposition depth follow independent probability distributions for each of five slope classes: <16°, 16°-<21°, 21°-<27°, 27°-33°, and >33° and are given in Table 3.1. Probabilities are based on experience in similar terrain and on coastal British Columbia, using field data in Wise (1997) and field data gathered by Guthrie (unpublished). For any given cell, scour depths do not exceed 2.5 m but are more typically in the range of 0.5 m to 1.5 m and deposition depths do not exceed 3 m. The net effect of agents acting on steeper slopes is likely to be scour and on flatter slopes is likely to be deposition. The mass (net of scour and deposition) and DEM are recalculated at every time step. When the mass reaches zero, the agent is terminated.

Table 3.1. Scour and deposition rules for the cellular automata model. Numbers represent probability of falling into each depth class.

Depth (m)	Slope°									
	< 16°		16° - < 21°		21° - < 27°		27° - 33°		> 33°	
	S[a]	D[b]	S	D	S	D	S	D	S	D
0	1.00	0.00	0.80	0.42	0.16	0.50	0.00	0.65	0.00	1.00
0.5	0.00	0.09	0.13	0.19	0.35	0.30	0.31	0.35	0.14	0.00
1	0.00	0.32	0.07	0.18	0.38	0.15	0.46	0.00	0.49	0.00
1.5	0.00	0.29	0.00	0.11	0.11	0.05	0.13	0.00	0.20	0.00
2	0.00	0.22	0.00	0.08	0.00	0.00	0.10	0.00	0.15	0.00
2.5	0.00	0.03	0.00	0.02	0.00	0.00	0.00	0.00	0.02	0.00
3	0.00	0.05	0.00	0.00	0.00	0.00	0.00	0.00	0.00	0.00

[a]S=Scour, [b]D=Deposit

Path selection for each agent with mass is determined by ranking the Moore neighbors, the eight neighbors surrounding a cell, based on their angular difference from the aspect of the current cell (Figure 3.6), thereby moving the majority of the agents mass down-slope. A continuous probability function is used to describe the spread of the landslide mass to neighbor cells based on a normal distribution centered on the down-slope aspect with a standard deviation of 30°. Each Moore neighbor represents a cardinal direction

from the active cell and the amount of mass moved into that section is calculated by the definite integral of the probability distribution centered on the aspect, and bound by the angle from the active cell center to the outer edges of the neighbor cell, and multiplied by the mass of the source cell:

$$M_n = \int_a^b PDF(\theta)d\theta \times M_s \tag{3}$$

Where M_n = the mass of the neighbor, M_s = the mass of the source cell, a and b are cardinal directions limiting the neighbor cell, PDF(θ) is the probability density function.

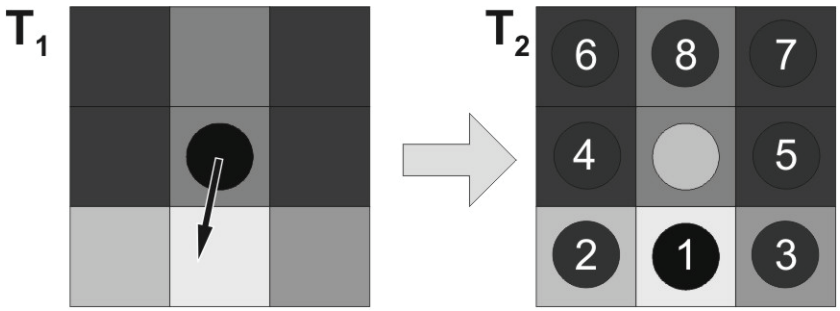

Figure 3.6. Aspect based ranking of Moore neighbors in a grid. In time step 1 (T_1) the black circle represents the original agent and the arrow indicates azimuth direction. The cell acted upon by the original agent is surrounded by eight neighbors. Potential spawned agents are ranked (T_2) based on the angular difference from azimuth.

The optimum standard deviation for landslide spread around the mean down-slope distribution can be found experimentally. In the BC case, 30^o produced the most realistic results compared to the shape and spread of actual landslides.

The mass of the landslide is distributed to neighboring cells, and new agents are spawned in each cell that contains landslide mass. New agents independently process the same sets of slope-based rules for scour and deposition. A lower threshold for initiation of an agent is used to limit unrealistic spreading of the mass where a very small fraction is moved to a particular cell. In cases where material is distributed to a cell already occupied by an agent, the agent terminates and the material is added to the existing agent.

If the mass reaches 0, the agent is terminated. In this way, a collection of agents, representing the moving mass of material, move from the starting point on the DEM, flow down-slope until all the moving material has been deposited. The lifespan of an agent is shown diagrammatically in Figure 3.7.

Using these simple empirically based rules for scour and deposition, the cellular automata model simulates landslides that initiate in similar locations as those in the deterministic approach, but that continue in each case until the mass of the landslide has reached 0.

The resulting cumulative M-F curves can be compared to actual data in Figure 3.8. Four sets of modeled data are included on the graph, each set containing several hundred randomly generated landslides within the Klanawa study area. The landslide M-F curves closely mirror the actual data over the majority of the distribution. Data spread increases for magnitudes larger than about 50,000 m^2 where fewer landslides are represented (only two landslides in the actual data base, both larger than those generated by the modeled distributions for similar probabilities). A power law may be derived for landslides > 10,000 m^2 with a slope that varies from about -1.8 to about -2.1. An argument could be made that a steeper line would fit several of the distributions beginning at greater sizes. Best fit lines were created using regression analysis through each distribution for landslides > 15,000 m^2, >20,000 m^2 and > 30,000 m^2. Fewer data points did indeed result in a better fit for some (not all) of the data sets and resulted in slightly steeper slopes in each case, the steepest being about -2.3.

Stark and Hovius (2001) defined the rollover, t, as the peak of the probability distribution curve, however, Guthrie and Evans (2004a) observed that the variability of t within 95% confidence limits could exceed an order of magnitude and argued that estimation of the rollover by eye was equally acceptable. We argue that for the real landslide data and at least one set of modeled landslide data in Figure 3.8, the rollover is reasonably estimated as occurring at approximately 10,000 m^2. This value may be higher for the other modeled datasets. Mean landslide size is about 5,200 m^2 - 5,700 m^2 for the modeled data, and about 6,600 m^2 for the actual data.

The rollover is not a result of a data bias, but of physiographic limitations related to slope, slope distance and the distribution of mass within the landslide. The landslide

magnitude and frequency distribution can be recreated using simple empirically derived rules in a cellular automata model.

3.3.3 A closer look at landslides in the cellular automata model

In addition to modeling the magnitude-frequency distribution of landslide sizes over a region, the simulation performed other functions well. Shallow rain-triggered landslides commonly split over high points in the landscape, and converge on and travel along the valley network. Landslides also tend to deposit substantial portions of their mass on benches (low-gradient topography), and behind physical topographic knobs. The model tended to do the same, bifurcating at local elevation highs, depositing mass preferentially where the local slope decreased, and generally finding confined gullies and streams in which to travel. Where the landslide became very large, it overwhelmed the local topography, again, similar to the actual case.

In the previous section, sets of landslides were considered that were located randomly on steep terrain in a watershed. Here, we generate a set of landslides beginning at single points, each related to the top of an actual landslide scar as interpreted on air photographs for the Klanawa watershed. Each simulation began by populating 1-10 adjacent cells with agents based on a probability distribution of landslide initiation widths of 5-50 m. Outside of the selection process, the rules for the model remained the same; that is to say, for each successive time step, agents simultaneously processed rules for scour, deposition, path selection and movement/spread until the landslide mass moving from each cell reached 0. Figure 3.9 shows an example of the results of the model (top) and compares the results to original data (bottom). Strengths of the model, including realistic path selection, size and shape of the landslides are evident; however, weaknesses are also revealed. For example, debris slides that transformed into long channelized debris flows were not modeled well. This is explained by the fact that scour and deposit rules were not designed for enclosed channel conditions with high water volumes. On the other hand, the model does a fairly good job of estimating when landslides will reach a channel, one of the major prerequisites for channelized debris flows. Another weakness in the model is that landslides appear to bifurcate too easily and split more frequently than their real life counterparts.

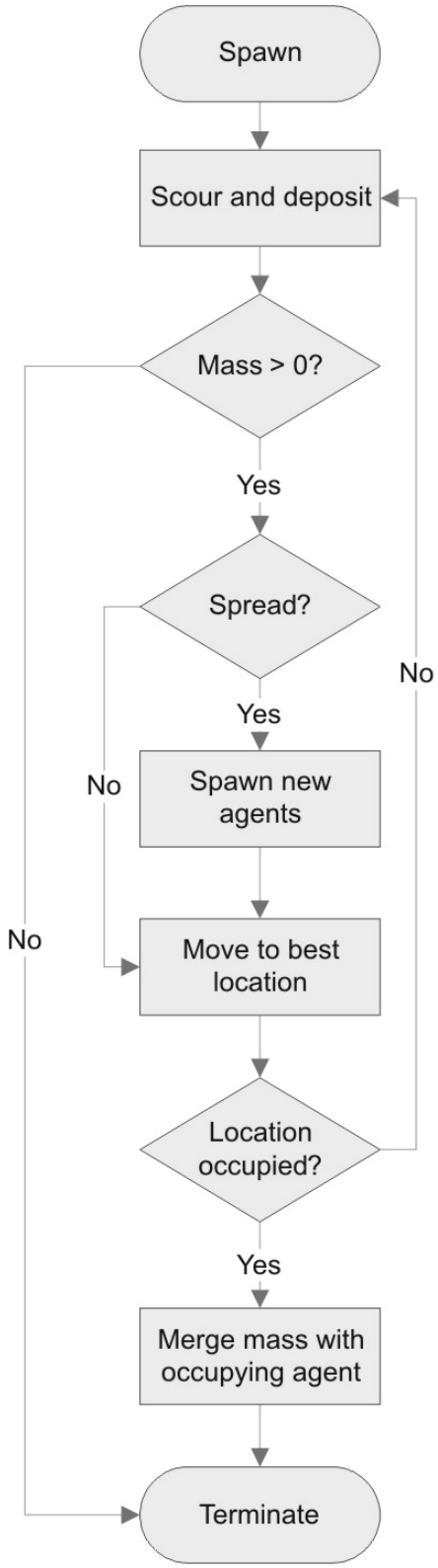

Figure 3.7. Flow diagram showing the steps in a landslide agent lifetime.

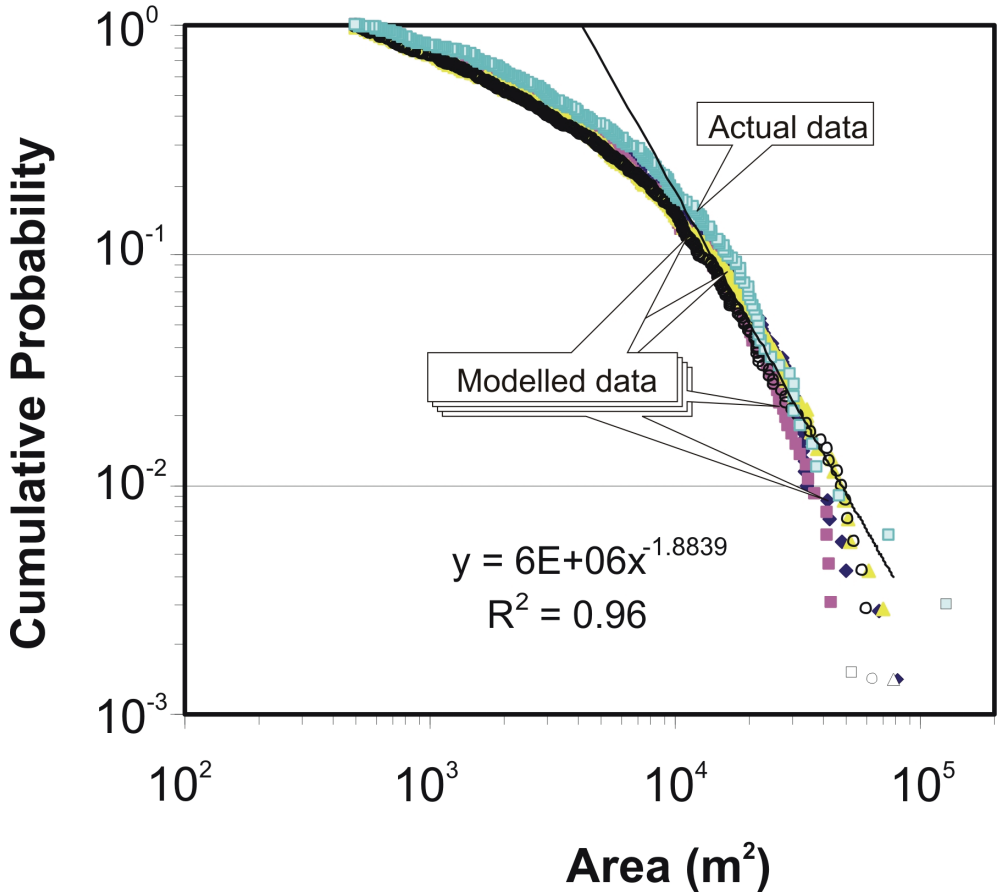

Figure 3.8. Cumulative M-F plot of four sets, each set of several hundred simulated landslides >500 m^2, in the Klanawa watershed on Vancouver Island, British Columbia, Canada. Landslides were modeled by cellular automata with simple empirically based rules for scour and deposition and path selection. Landslide spread was based on a probability density function around the aspect direction of movement. The results are compared favorably to the actual data from the same study area.

Figure 3.10 considers the landslides in more detail, including an apparently realistic fit with actual recorded data (landslides in the right half of the figure) and an example of a poorer fit with the actual recorded data (landslides in the left half of the figure). In both examples, the modeled landslides appear to respond to topographic limitations that were present in reality, converging in a gully on in the right half figure, and diverging around some barrier in the left half. Interestingly, the barrier that creates an island in the real data and a split in landslide mass in the modeled data isn't obvious from the contours alone.

Modeled landslide behavior, like real landslide behavior, exhibits variability between sets (in real life, landslides that begin in the same location often look substantially different). In the model, variability is based on its probabilistic and iterative nature including the initial conditions. For example, the widths of modeled landslides in Figure 3.10 are slightly different than those recorded on air photographs and initial width relates to initiating mass as the landslide develops. However, even with widths duplicated, modeled landslides would probably vary, in some cases substantially, from reality.

Limitations of the model are related to several things, including the DEM resolution, oversimplification of scour and deposition in the landside path, and other controls on landslide generation not accounted for in the model. Despite those limitations, the model produces reasonably realistic events.

Cellular automata models have been used to model individual landslides accurately after the events occurred, including for debris flows in Italy (Avolio *et al.*, 2000; Clerici and Perego, 2000; D'Ambrosio *et al.*, 2003), China (Segre and Deangeli, 1995) and Japan (Di Gregorio *et al.*, 1999). Previous simulations have incorporated varying levels of complexity to calculate some of the many geotechnical parameters representative of an actual landslide. Such parameters include, for instance, soil type and substrate size, rheological properties including water content, water loss and soil adherence, friction angle, cohesion, slope and elevation. Typically, the programs have been developed to model a specific landslide, and then to determine recurrent or adjacent hazards. While generally successful, the computational power and detailed geotechnical knowledge required for their success, in addition to real world heterogeneity, limit both the size of area assessed (Clerici and Perego, 2000) and the general use of the model. Interestingly, more complex rules don't necessarily give better results. For example, Clerici and Perego (2000) successfully modeled the Cornigliol landslide in Northern Italy using simple variables based on slope and surface topography.

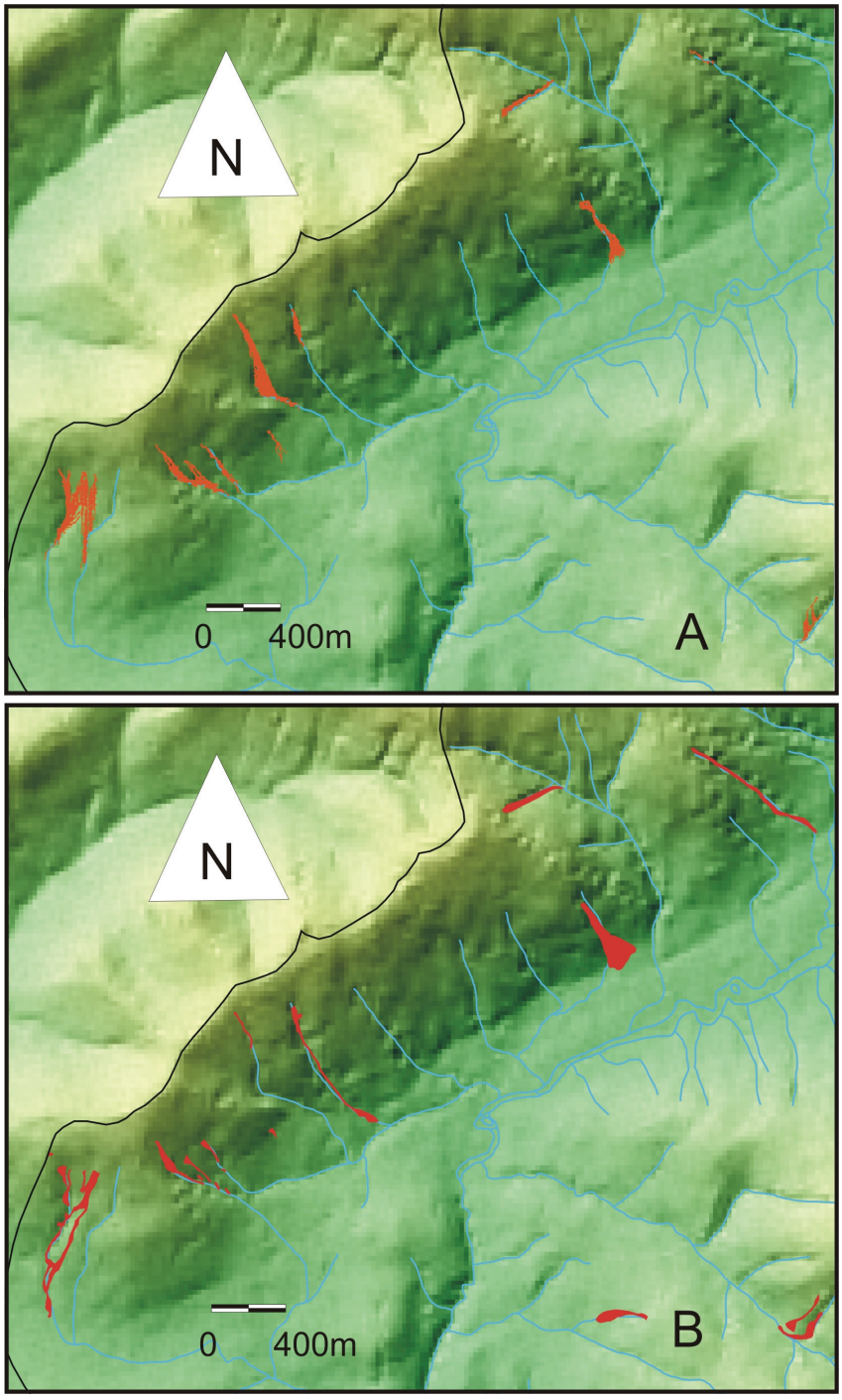

Figure 3.9. Comparison between modeled landslides (A) using the cellular automata model, and landslides identified on air photographs (B). Locations of landslides in (A) were predetermined by selecting a point at the top of the headscarp for actual events. The remainder is an output of the model, which like real landslides, exhibits variability between runs for each site. No attempt was made to run each landslide many times to get a 'best' match, and consequently the results displayed are considered typical of the range of variability for any particular run-set.

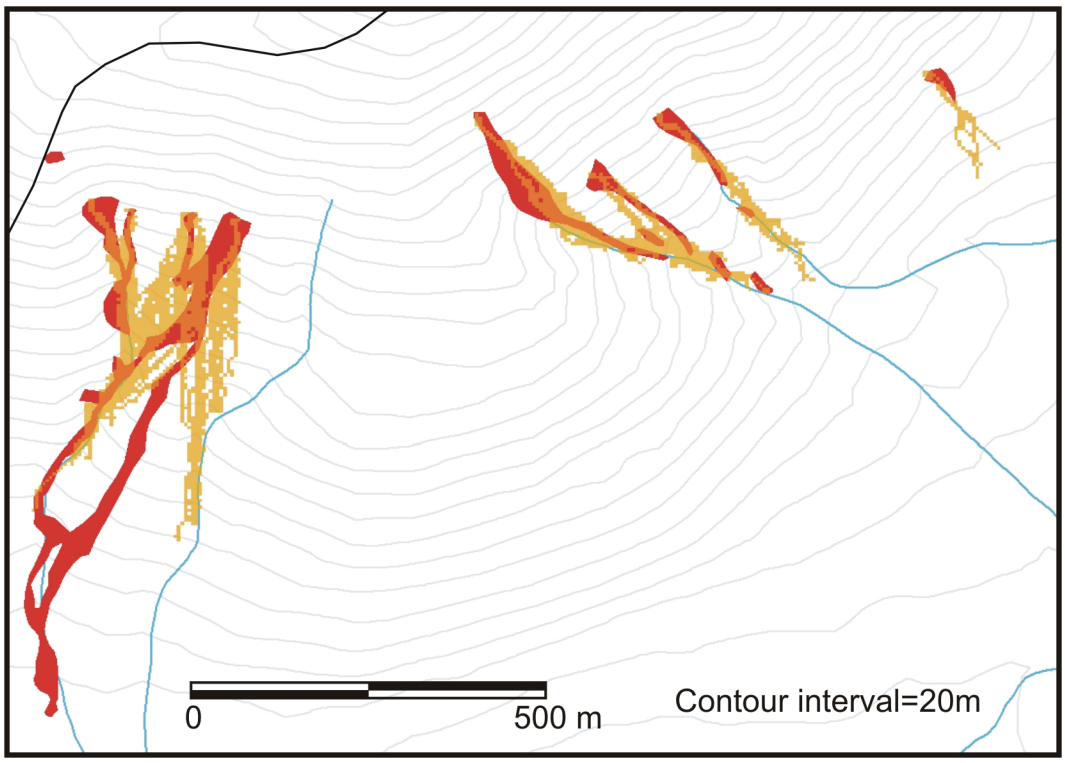

Figure 3.10. A detailed comparison between modeled (yellow) and actual (red) landslides from a single run-set shown in Fig 9. Note that the landslide modeled is affected by the initial width as well as variability between runs. The figure demonstrates some of the strengths of the model including realistic convergence in topographic lows, and divergence around topographic highs not immediately obvious from the contours alone.

Despite the site-specific geotechnical complexity of a landslide, the model used here incorporates simple empirically based parameters that are easily determined in a field program. Landslide scour and deposition, slope morphology, and landslide mass are amalgams of the geotechnical properties that produced them including water content, rheological properties, geology and slope. Consequently, very simple rules appear to give realistic results. Further, as scour and deposition (related to slope) are relatively easy to gather, we expect that the model would be portable to other regions. This in turn may assist in characterizing regional landslide hazard and reduce the requirement for complete landslide inventories.

3.4 CONCLUSIONS

Guthrie and Evans (2004a, 2004b) have argued that the power law alone inadequately describes the distribution of landslides in a watershed and that it ignores the effects of physiography on landslides at low magnitudes. A simple deterministic model and a cellular automata model were used to simulate landslides in the Loughborough Inlet and the Klanawa River study areas respectively in coastal British Columbia, and to examine the assertion that physiographic controls dominate the landslide M-F distribution.

The model run for the Loughborough data explains why, for rain-triggered landslides, the rollover might exist. However, the results also under-predicted the likelihood of larger landslides occurring and the error increased with magnitude. In addition, the curve did not exhibit a definable break in slope, nor a power law over larger magnitudes.

The cellular automata model run for the Klanawa watershed provides corroborative evidence that the main controls on landslide distribution, for both the power law component and the component below the rollover, are governed by the physical conditions related to slope, slope distance and the distribution of mass within landslides. Based on simple empirically based rules for scour, deposition, movement and mass spread, results compare favorably to actual landslide data: modeled landslides bifurcate at local elevation highs, deposit mass preferentially where the local slopes decrease, find routes in confined gullies and streams, and, when sufficiently large, overwhelm the local topography.

Empirically based rules for scour and deposition related to slope can be gathered for landslides in the field at any location worldwide, and represent the real world product of the major physiographic components of landslides, a simplified synthesis of geotechnical complexity. Landslide mobility, implicit in these rules, fundamentally influences both how large the landslides will be, and how far they will travel. Landslide spread may be visually compared to real landslides and adjusted easily by flattening or steepening the probability distribution function around the aspect of landslide direction.

Based on the results of the models, we conclude that the M-F distributions, including both the rollover and the power law components, are a result not of a data bias, but of actual physiographic limitations related to slope, slope distance and the distribution of mass within landslides.

Chapter 4: Controls on debris flow mobility: evidence from coastal British Columbia.

Based on: Guthrie, R.H., Hockin, A., Colquhoun, L., Nagy, T., Evans, S.G. and Ayles, C., 2009. An examination of controls on debris flow mobility: evidence from coastal British Columbia. Submitted to Geomorphology.

OVERVIEW: We characterize and consider fundamental controls to runout distance of debris slides and debris flows using 1700 field observations supplemented by air photograph interpretation from coastal British Columbia. We examine the role of slope on deposition and scour and determine that they occur on steeper and flatter slopes respectively than previously reported. Mean net deposition occurred on slopes between 18^o and 24^o for open slope failures and between 12^o and 15^o for channelized debris flows. We demonstrate a practical method for estimating both entrainment and runout in the field as well as in the GIS environment and provide an example entrainment map for Vancouver Island, British Columbia. We consider other controls to landslide mobility including the role of gullies and stream channels, roads and benches, and intact forests. Shallow landslides that hit streams and gullies at acute angles had a high probability of transforming into a channelized debris flow while landslides that hit streams and gullies at obtuse angles did not. Forests played a substantial role in landslide runout: Debris flows travelling through a logged slope deposited much of their load when hitting a forest boundary and stopped entirely within 50 m of that boundary in 72% of the cases examined. Roads also tended to stop or reduce the size of open slope debris flows in 52% of the cases. The results are expected to be useful to land management applications in regions with frequent shallow landsliding.

4.1 INTRODUCTION

The Canadian Cordillera is found almost entirely within the province of British Columbia (BC) and is comprised of approximately 800 000 km^2 of rugged mountains and, to a lesser extent, interior plateaus. Population density is low with approximately 4.3 million people living largely in urban centers, and affluence is high due in part to the

relative abundance of natural resources accessed through industries such as mining and forestry. Forestry has been the primary resource-based industry in BC over the last century, exploiting approximately 400 000 km^2 of merchantable timber. Unfortunately, forest operations are not without impact and the occurrence of landslides, naturally common on BC's steep terrain, has increased by about an order of magnitude in the last several decades (Schwab, 1983; Jakob, 2000; Guthrie, 2002; Guthrie and Brown, 2008). Guthrie and Brown (2008) report that human-induced landslides have approximately doubled landscape erosion over the next highest millennia during the Holocene. Environmental values such as clean running water, scenic vistas, clean air and abundant fish and wildlife, are part of the collective conscience in BC in spite of the physical cost of resource extraction, and as such there is considerable pressure to minimize the impact of landslides. Local geotechnical consultants and industry professionals are faced with the daunting task of building roads, harvesting forests and otherwise managing vast landscapes in some of the most rugged conditions in the world while minimizing impacts at a very low cost per unit area. Nowhere is this truer than for coastal BC, where high rainfall on remote rugged terrain produces both massive forests and frequent landslides.

4.1.1 Definitions

Landslides in coastal BC are predominantly debris slides, debris avalanches or debris flows according to Varnes (1978), Swanston and Howes (1994) and Cruden and Varnes (1996). They are rapidly-moving, shallow landslides from steep slopes, involving surficial rock, soil and debris. Sub-dominant landslide types represent only a small fraction of the total number of landslides and include: rock falls, rock avalanches, and earth slumps, (Guthrie 2005 for example).

Most coastal BC landslides begin as debris slides but typically evolve to debris flows or debris avalanches (the distinction being one of liquid content) as they break up with increased velocity downslope. Despite the recommendations of Cruden and Varnes (1996), complex terms often do not fully describe the range of variability in nature and run the risk of being split into ever more detailed categories. In regional studies at least there are analytical, descriptive and empirical reasons to generalize the landslide term.

One could make an excellent argument for using the mechanism at the time of failure as the primary descriptor (as used in Guthrie and Evans, 2004a, b for example). However, for shallow precipitation-induced landslides in coastal BC, runout is governed largely by the post-initiation behaviour downslope: most commonly non-plastic flows or avalanches. Volume and ultimately magnitude are determined by material entrainment rather than the size of the initial failure (Benda and Cundy, 1990; Dunne, 1998; Hungr *et al.*, 2008). Similarly limitations to size appear to be related to the deposition of material along the flow path. Consequently we have elected to use the term *debris flow* to describe the suite of shallow rapid unconsolidated mass movements on a steep hillslope (Figures 4.1 and 4.2). The term is meant to be inclusive of landslides that might otherwise be classified as debris slides or debris avalanches.

Debris flows tend to follow paths based on topographic expression (including swales, gullies and channels) except at the scale where that expression is overwhelmed by the volume. Where possible we have distinguished between open-slope debris flows and channelized debris flows (Figures 4.1 and 4.2); however, the reader is advised that despite distinct end members the transition between the two is gradational and not always distinguished clearly.

Unless otherwise specified, magnitude refers to the total area in m^2 of a debris flow. This includes all visible signs of source, entrainment and deposition. Total area has become the common measure for shallow debris slides and debris flows as it is consistently and reliably obtained from remote inventories (e.g. Hovius *et al.*, 1997; Guzzetti *et al.*, 2002; Guthrie and Evans 2004a; 2004b; Malamud *et al.* 2004).

Volume of shallow debris slides and debris flows is largely controlled by entrainment (Benda and Dunne, 1990; Dunne, 1998; Hungr *et al.*, 2008) rather than by initial failure (e.g. Corominas, 1996) and therefore volume refers to the total transported volume in m^3, including both the initial failure and the subsequent entrainment.

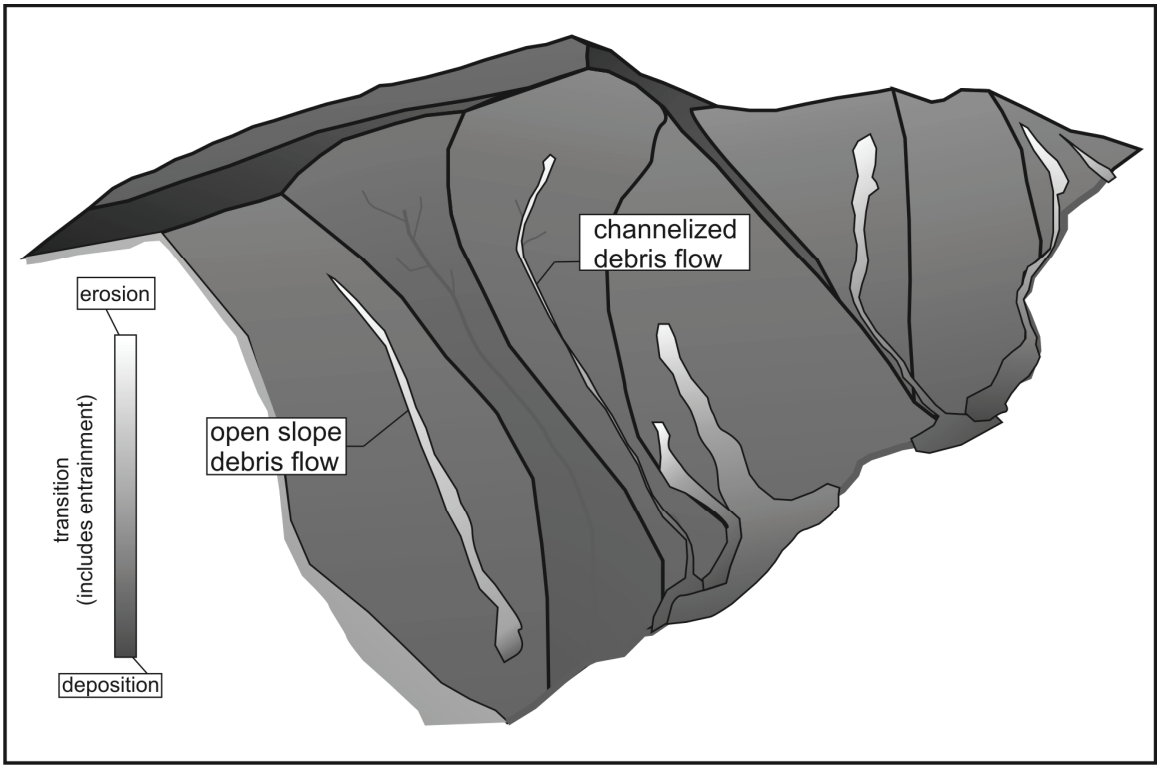

Figure 4.1. A conceptual diagram of coastal BC showing both open slope and channelized debris flows. Erosion of sediment, rock and debris is slope dependent, and entrainment occurs along the landslide path potentially increasing the volume by more than 10 times. Similarly, deposition is slope dependent and some deposition may begin even on steep slopes. Transitional reaches in the landslide path occur where the erosion and deposition are nearly equal.

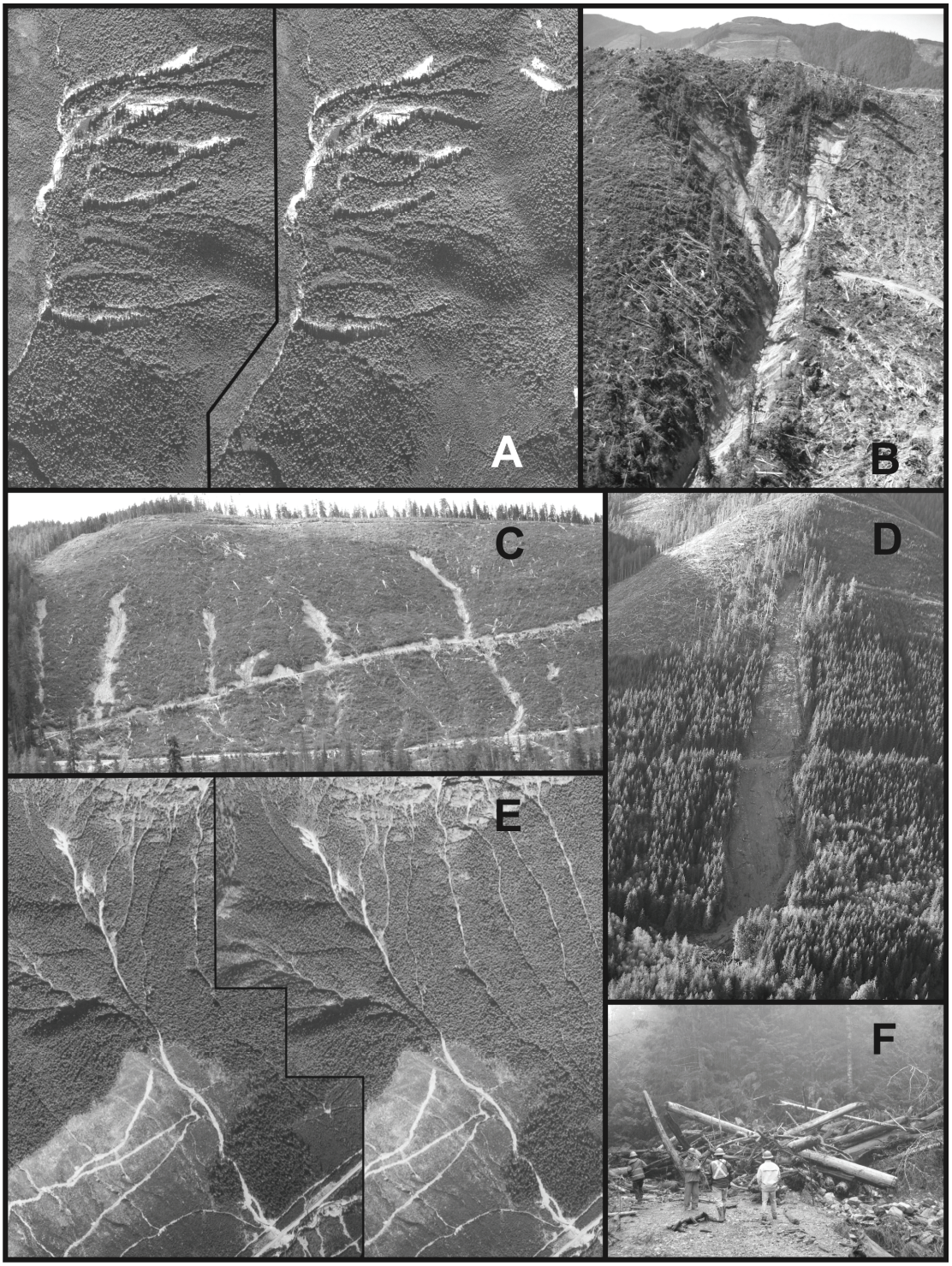

Figure 4.2. Examples of debris flows from coastal BC: A. Stereopair of several debris flows in a forested watershed. B. Three debris flows that coalesce to a single path, entraining considerable material along the way. C. Debris flows in a logging block. D. A debris flow initiated in second growth. E. Stereopair of a channelized debris flow. F. The impact of a debris flow at a road crossing.

Reaches are defined for landslide paths as they are for streams in hydrologic nomenclature: a length along the landslide path, uniform with repsect to discharge, depth, area and slope.

Erosion and entrainment are defined as the removal of rock, sediment and debris from a slope by a landslide; material that is then transported downslope. Entrainment is normally considered to be the volume added to the landslide following the initial failure. Deposition is defined as the placement of rock, sediment and debris along the path from an upslope source. Transition is the portion of the landslide path that contains both entrainment and deposition, but where the net balance of material lost or gained approaches zero. In BC and elsewhere, debris flows grade between zones of erosion, entrainment, transition and deposition.

4.1.2 Objectives

We employ, both field data and GIS analysis to consider the roles of slope, channel confinement, forest cover, and roads to landslide runout. Specifically:

(i) We examine the role of slope on erosion and deposition of material along the debris flow path, calculate net sediment balance and determine how changes in the topographic profile affect entrainment of rock, sediment and debris for confined and unconfined debris flows;

(ii) We examine, based on the same data, the likelihood that a debris flow entering a channel will continue as a channelized debris flow;

(iii) We examine the ability of roads and forests to increase, decrease or stop debris flows;

(iv) We develop a simple rule based methodology for estimating debris flow runout that can be used by practitioners in the field or in a GIS environment;

(v) Finally, we consider the broader implications of slope, confinement, roads and forests for runout prediction, and derive wherever possible practical

relationships between debris flows and their limiting factors in coastal British Columbia.

We intend for the results to be useable in direct hazard mapping techniques across similar settings, and suggest that they also enable calibration of modelled results.

4.2 REGIONAL SETTING

Data were acquired from two locations in coastal British Columbia: Vancouver Island and the Queen Charlotte Islands (Figure 4.3).

Vancouver Island (Figure 4.3) is comprised of 31 788 km^2 of predominantly steep rugged topography ranging from sea level to 2200 m. The central and largest part of the island consists of steep volcanic mountains intruded by granitic batholiths. Deep fjords and long inlets dissect a western coastline severely modified by Pleistocene glaciations that steepened and deepened the terrain and veneered the mid- and upper slopes of valleys with shallow surficial sediments (Guthrie, 2005).

Precipitation falls primarily as rain during the winter months with most locations on the west coast receiving more than 3000 mm y^{-1} at sea level (Environment Canada 1993). Landslides on Vancouver Island are commonly attributed to large storms (i.e. Guthrie and Evans 2004a; 2004b) though they may also be triggered by earthquakes (Mathews 1979; Evans 1989).

Vancouver Island lies approximately 100 km east of the surface trace of the Cascadia subduction zone. Consequently, the region is tectonically active and undergoing short-term elastic cycle uplift of 1–2 mm y^{-1} (Adams 1984; Dragert 1987), much of which is recovered by coseismic subsidence during great (larger than magnitude 9 on the Richter Scale) earthquakes that occur about every 500 years (Clague and Bobrowsky 1999; Hutchinson *et al.* 2000; Blais-Stevens *et al.* 2003), for a net gain of about 0.5 mm y^{-1} (Hutchinson *et al.* 2000).

Figure 4.3. The Queen Charlotte Islands (QCI) and Vancouver Island off the west coast of British Columbia Canada, combined represent a study area of > 40 000 km^2.

The Klanawa study area is a 3000 km^2 study area on the southwest portion of Vancouver Island (Figure 3; Guthrie *et al.* 2008).

The Queen Charlotte Islands (Figure 4.3) are comprised of 10 180 km^2 of terrain off the west coast of Canada, north of Vancouver Island and south of Alaska's Alexander Archipelago (Brown, 1968). Formed of seven major islands, Graham Island and Moresby Island dominate the set. With a total relief of approximately 1200 m, the physiography varies from dissected coastlines and fjords, coastal alpine ranges, to

plateaus and plains. The mountains along the west coast are steep and end abruptly at the western edge, essentially demarcating the continental shelf. Once again, geomorphic features relate largely to Pleistocene glaciations, including matterhorn peaks, U-shaped valleys, outwash plains and fjordal inlets.

The Queen Charlotte Islands are comprised largely of volcanics with interbedded fossiliferous sedimentary rocks, intruded in the Jurassic by granites contemporaneous with similar events on Vancouver Island.

Precipitation falls largely as rain in winter months and the west coast receives annual average amounts in excess of 4200 mm (Hogan and Schwab, 1990). Debris slides and debris flows are common, and typically related to precipitation events (Gimbarzevsky, 1988; Hogan and Schwab, 1991).

4.3 METHODS

Field data were acquired for 850 landslide reaches (Table 4.1): Seven hundred and seventy three landslide reaches were measured in the Queen Charlotte Islands (QCI) by T. Rollerson and employees of the MacMillan Bloedel Company in 1984 and 1985 (Rollerson, 1992; Fannin and Rollerson, 1993; Wise, 1997; Fannin and Wise, 2001). For each reach field measurements of erosion, deposition, slope, channel confinement (open slope or gullied), area and volume were taken. QCI data were analyzed in aggregate and separated into open slope and gullied data (515 and 258 landslide reaches respectively) for analysis.

On Vancouver Island, for this study, an additional 77 landslide reaches were measured by R. Guthrie between 2006 and 2007 (VI data) and again field measurements included erosion, deposition, slope, area and volume. Channel confinement was not explicitly recorded for the 77 landslide reaches measured on Vancouver Island. In both data sets, erosion and deposition were considered independently, resulting in a total database of 1700 field entries.

Table 4.1. Datasets used in current study

Where	Number of Events	Scale	Age	Reference
Queen Charlotte Islands	773 debris flow reach sections	Field	Historical	Wise, 1997
Vancouver Island	77 debris flow reach sections	Field	1995-2007	This study
Vancouver Island, Klanawa Range study area	331 debris flows > 500 m2 (total inventory of 381 debris flows)	1:15 000 – 1:20 000 air photographs	Historical – air photograph dates from 1994 – 2001	Guthrie *et al.*, 2008

Field data were compiled and analyzed on scatter plots and mean values were determined for 3^{o} slope classes. Net deposition was returned by subtracting mean erosion from mean deposition for each class.

Depth measurements in both data sets were rounded to the nearest 0.1 m perpendicular to slope, but show some measurement bias toward half meter depth breaks. The accuracy is nonetheless expected to be many times higher than observation by any remote means. Average depths less than 0.1 m were considered to be influenced by micro-topography not accurately measured in the field, and were reduced to 0 (actual 0 measurements were also recorded).

Analyses were further supplemented by an air photograph inventory of 331 debris flows acquired for the Klanawa study area on southwest Vancouver Island (Figure 4.4, Guthrie *et al.*, 2008). Using this dataset the transformation from open slope to channelized debris flows (thereby increasing debris flow mobility and ultimately runout) was considered by measuring the angle of entry of landslides that entered gullies. Azimuthal angles between the landslide direction and the stream direction were measured in degrees in a GIS and compared to runout characteristics.

A model of debris flow runout was created by estimating volumes along the landslide paths in a GIS for 331 debris flows in the Klanawa study area. Volume was calculated by measuring the width of landslides perpendicular to a centerline in 10 m intervals along the path (Figure 4.4), and multiplying by the average net deposition determined from field data. The debris flow ended if the sediment balance was zero. Based on sediment balance, a modelled debris flow could stop at the same location as the observed debris flow, or stop before or after the observed event. When modelled debris flow paths had positive volumes where the observed debris flow terminated, they were extended along an imaginary depositional surface of 6^{o}-9^{o} to predict total travel distance required to deposit the remainder of their load. The reverse was applied to modeled debris flows that had negative volumes where the observed debris flow terminated.

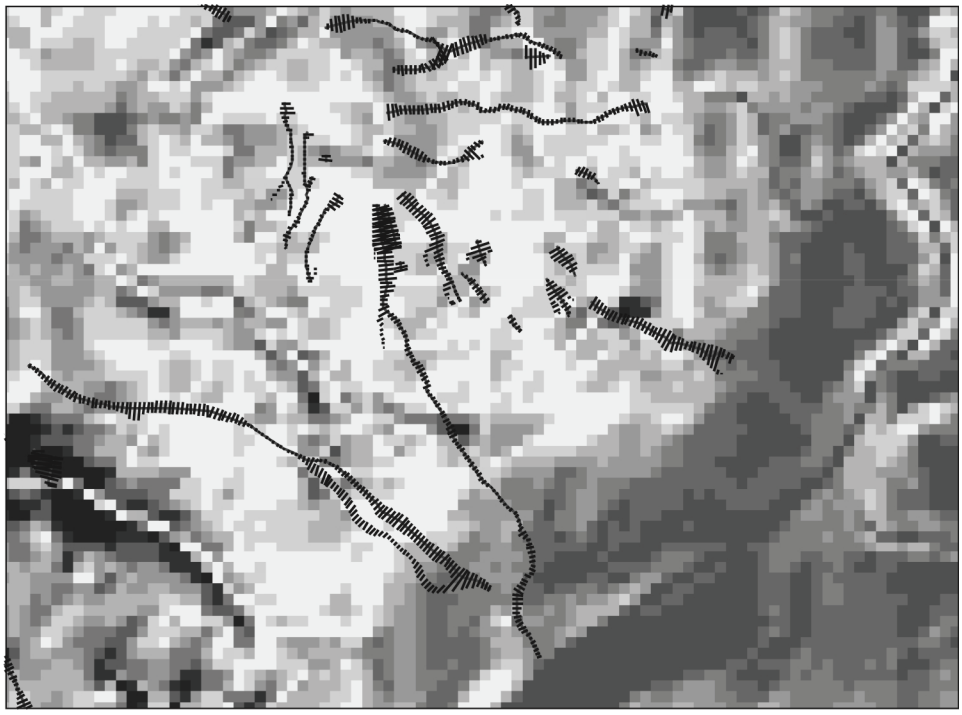

Figure 4.4. Widths were calculated along the landslide path by drawing a line perpendicular to the center line in 10 m increments downslope. The background pattern represents a slope map broken into 3^{o} categories.

To consider the role of forests on debris flow runout, a subset of 25 debris flows that each initiated as a single event in the Klanawa study area and crossed a forest boundary (from a clearcut into a forested slope) was examined to determine the role of forests as an energy dissipater. In a GIS environment, a 20 m buffer was placed on either side of the forest contact and mean widths were calculated above and below the buffer. Relative widths were calculated as a ratio:

$$\Delta w = \frac{fw}{hw}, \tag{4}$$

where Δw = the width ratio; fw = the forested width, hw = the harvested width.

Δw values equal to 1 indicate that the forest had no effect on debris flow width, $\Delta w > 1$ indicate an increase in debris flow width, $\Delta w < 1$ indicate a decrease in width, and Δw of 0 indicate that the debris flow stopped within the buffered zone.

Similarly, a subset of 60 debris flows that started as a single event in the Klanawa study area and that crossed a road were examined to determine the ability of roads to stop debris flows. A 25 m buffer was placed around known forestry road line drawings in a GIS, reflecting the conservative limit of the forestry road. Similar to the forest section above, mean widths were calculated above and below the buffer. Relative widths were determined as a ratio:

$$\Delta r = \frac{r_2}{r_1}, \tag{5}$$

where Δr = the road width ratio; r_2 = the width below the road, r_1 = the width above the road.

Δr values equal to 1 indicate that the road had no effect on debris flow width, $\Delta r > 1$ indicate an increase in debris flow width, $\Delta r < 1$ indicate a decrease in width, and Δr of 0 indicate that the debris flow stopped on the road.

4.4 LANDSLIDE HAZARD MAPPING

Relatively speaking, landslide initiation is fairly well understood in BC as it is worldwide. Hazard mapping may take several forms from qualitative to quantitative (e.g. Varnes, 1978; Swanston and Howes, 1994; Rollerson *et al.*, 1997; Corominas *et al.*,

2004; Nadim and Lacasse, 2004; Bonnard and Corominas, 2005; Guthrie 2005). In BC, computer-based models for landslide hazard mapping, runout and risk mapping have not replaced expert judgement and fundamental mapping techniques, nor are they generally considered practicable. The reasons are several: The finest digital elevation model (DEM) consistently available across BC is at 1:20,000 with 25 m maximum resolution. Detailed hazard maps, required for example for forest cutting permits, are typically at a finer scale than the DEM, but need to fit methodologically with the coarser scaled maps. Acquiring more detailed DEMs under dense forest cover in rugged conditions in remote areas is an expensive proposition. Hazard models at the scale of generally available DEMs (25 m) produce poor or impractical results and can effectively sterilize the landscape between mid and upper slopes in BC (i.e. Pack *et al.* 1998; Chung *et al.* 2002). In addition, models typically require considerable adjustment to determine sensitive input parameters that differentiate a stable slope from one that is unstable (Soeters and van Westen, 1996). As a result, computer based hazard models are more frequently used for site-specific cases or linear developments, where the investment reflects the precise nature of the problem, the consequence or the financial commitment.

British Columbia and many other jurisdictions worldwide use instead a terrain and hazard mapping system employing direct mapping methods: experience, expert judgement and empirical evidence that codify the landscape into morphologically consistent polygons that can in turn be rolled up into hazard classes (Figure 4.5). In BC those classes relate to management decisions through provincial guidelines and legislation. The methods are approximately similar at different scales, with the greatest difference being that coarser scales are more conservative thereby triggering detailed mapping where required. Attempts to better quantify the results occur in combination with statistical methods, and these results can feed into regional models, but the fundamental approach is still direct mapping. Soeters and van Weston (1996) observe that an ideal map of slope instability includes both spatial and temporal probability, landslide type and magnitude, as well as velocity and runout distance. Calculating runout distance remains problematic.

4.5 LANDSLIDE RUNOUT

For debris flows, there are several models that attempt to describe landslide travel distance or runout (Hungr, 1995; Corominas 1996; Finlay *et al.*, 1999; Fannin and Wise 2001; McDougall and Hungr, 2004; Kwan and Sun, 2006; Guthrie *et al.*, 2008; Miller and Burnett, 2008).

Numerical models estimate debris flow mobility by examining boundary conditions and constituent parts of the system to estimate where driving forces overwhelm resisting forces. These models require detailed knowledge of the component parts along the path including material properties, pore pressures, external loading and discontinuities and they have been more widely used for rock failures (Hungr *et al.*, 2005).

Analytical models are a special case of numerical models that solve for moving debris flows using physical rules of fluid dynamics, acting on the estimated rheological properties of the flow. These models, such as DAN (Hungr, 1995) are becoming increasingly useful to replicate site-specific landslide runout, or to back-analyze velocity and entrainment-deposition characteristics. However, they require simplification of key variables (material properties, rheological model, pore pressures) and calibration with field evidence.

New techniques for predicting runout include analysis by cellular automata methods (Turcotte *et al.* 2002; Guthrie *et al.* 2008) and early results suggest some promise for regional runout prediction. However, the use of cellular automata to estimate debris flow mobility remains relatively nascent at this time and further work will be necessary to determine its broader applicability.

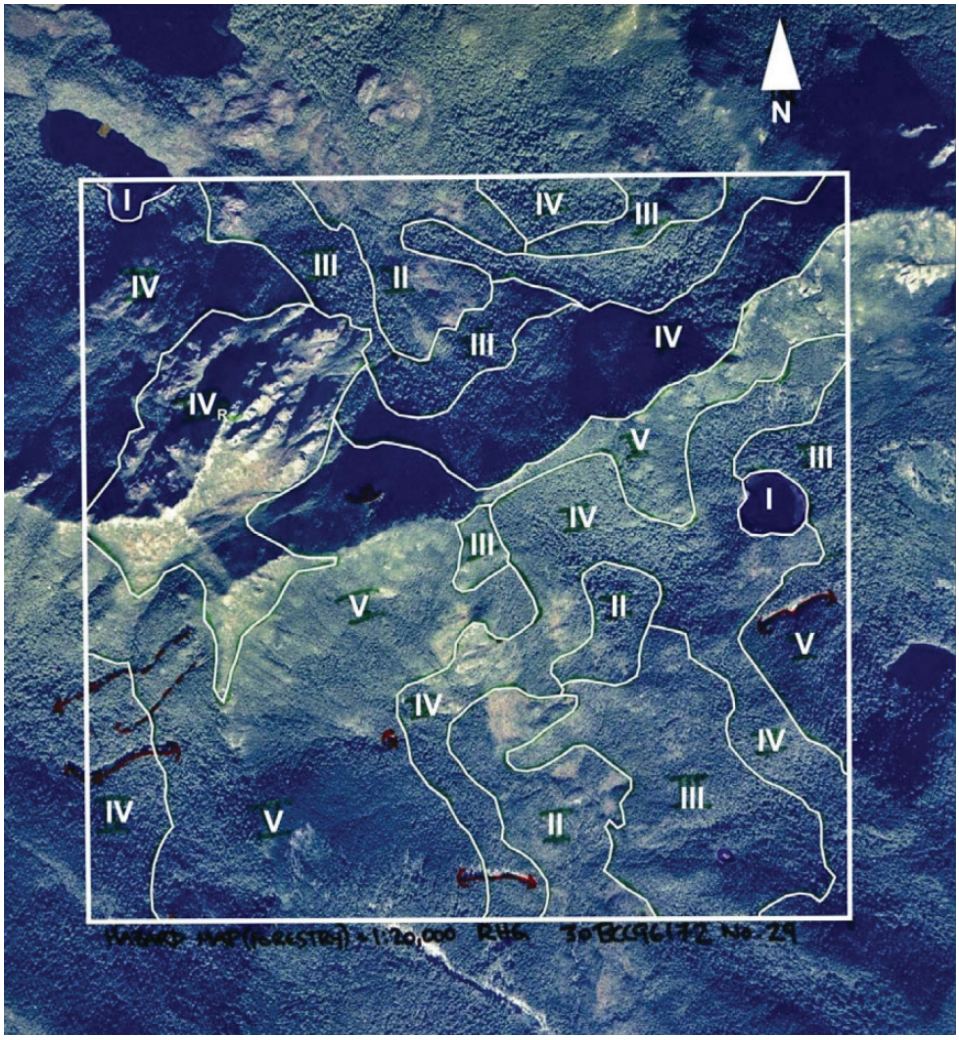

Figure 4.5. A five class terrain hazard map produced for forest harvesting and road construction in coastal BC. Original scale was 1:20 000. Red lines indicate previous debris flows. Areas designated as high hazard (IV and V) would require more detailed assessment before harvesting.

In all cases, many of the required parameters are calibrated or determined using empirical methods. In addition to increasing the accuracy of the numeric and analytical models, empirical methods have been developed that rely on established relationships between, for example, runout distance, volume, peak flow and slope geometry (Heim, 1932; Scheidegger, 1973; Hsu, 1975; Takahashi, 1981; Hungr *et al.*, 1984; Corominas, 1996; Fannin and Rollerson, 1996; Findlay *et al.*, 1999; Horel, 2007) and may therefore be used on their own to predict debris flow runout. These methods may also include changes to mobility as a result of major topographic controls, such as entering an adjacent

channel (Benda and Cundy, 1990; Millard, 1999; Miller and Burnett, 2008). In such instances, mobility may be decreased if the entry angle to the adjacent channel approaches the perpendicular, or increased if the entry angle is very low (Benda and Cundy, 1990; Millard, 1999; Miller and Burnett, 2008).

Empirical models are essentially of two types. The first type relies heavily on the initial or total volume component of a debris flow (ie. Corominas, 1996; Rickenmann, 1999; Hürlimann *et al.*, 2008). Rickenmann (1999), for instance, determined the relationship between maximum runout distance (L_{max}), debris flow total volume (V) and the vertical drop along the path (H):

$$L_{max} = 1.9V^{0.16}H^{0.83} \quad (6)$$

Several authors have observed that debris flow volume is dependent not only on the volume of initiation, but on the entrained material along the path (Benda and Cundy; 1990; Dunne, 1998; Guthrie *et al.*, 2008; Hungr *et al.*, 2008). Debris flows become increasingly destructive with increased entrainment and for those that extend beyond a first-order channel, the entrained volume may exceed the volume of the initial failure by an order of magnitude (Benda and Cundy, 1990). As a consequence, those empirical relationships that rely on volume as a key parameter are not adequate to predict the debris flow path *a priori*.

The second type of empirical model depends on the entrained component of volume and on volume balance along the flow path (Benda and Cundy, 1990; Cannon 1993; Fannin and Wise, 2001; Miller and Burnett, 2008). This sediment balance approach is based on the premise that a debris flow will continue to propagate until such time as the volume or mass of the event reaches zero. On flatter slopes, the tendency is to deposit sediment, and on steeper slopes the tendency is to erode. Consequently, the role of topography as a controlling mechanism to landslide runout is fundamentally reliant on slopes at all scales. Hürlimann *et al.* (2008) observe that the weakness of these methods is that they require detailed channel information. However, recent work by Miller and

Burnett (2008) for the state of Oregon suggests that volume balance can be used to predict regional debris flow runout characteristics.

4.5.1 The impact of forests, roads and benches on landslide runout

In the Pacific Northwest, the absence of mature timber appears to increase not only the frequency of debris flow activity (Schwab, 1983; Rood, 1984; Jakob, 2000; Guthrie, 2002; 2005; Guthrie and Brown, 2008), but also the magnitude and travel distance of individual events (Robison, 1999; Bunn and Montgomery, 2000; May and Gresswell, 2003; Lancaster *et al.*, 2003; Miller and Burnette, 2008). Landslide research from the Coast Range of Oregon demonstrates several ways in which forests can influence debris flow runout. Debris flows have lower mean runout lengths and shorter depositional zones in mature forests (Robison, 1999; May and Gresswell, 2003; Miller and Burnette, 2007) while landslides in younger stands (less than 9 years) have increased volumes of erosion compared to regenerating stands (9 – 100 years) (Robison,1999). In addition, wood entrained from forested slopes may reduce runout length by changing the behaviour of the leading edge of the debris flow (Lancaster *et al.*, 2003).

Johnson *et al.* (2000) reported that net deposition of debris flows in southeast Alaskan forested and clearcut slopes was 29˚ and 19˚respectively. In the same study, the mean gradient of terminal deposition for debris flows was 10˚ - 13˚ in forested terrain and 7˚ in clearcuts.

Roads are essentially human made benches in the landscape, typically too small to show up on the DEM (<25 in width). Roads are often the cause of landslides in coastal BC (e.g. Jakob, 2000; Wemple *et al.*, 2001; Guthrie, 2002, 2005); however, field experience shows that in some cases, roads play a mitigating role capturing sediment and reducing or even eliminating the impact of the debris flow on downslope resources. The role of roads in stopping landslides is similar to that of a range of topographically flat areas too small to detect remotely.

4.6 RESULTS AND DISCUSSION

4.6.1 The role of slope

Scatter plots of 1700 field entries are given in Figure 4.6 and compare erosion and deposition at each landslide reach to the measured slope for that reach. Figure 4.6 is divided into the QCI data (Figure 4.6A) and VI data (Figure 4.6B). In addition the QCI data are broken into open slope and gullied results (Figures 4.6B and 4.6C respectively).

Despite considerable data scatter, there are clear trends in each plot of decreasing deposition and increasing scour with increasing slope. In addition, some scour was measured on all but the flattest slopes in the study, and deposition was measured on all but the steepest. While this result is intuitive, the extent to which it is true exceeded what was reported from previous studies. For example, almost half a meter of deposition was recorded at slopes of 36^{o} on the Queen Charlotte Islands (QCI), substantially greater than 23^{o} previously reported for the QCI data (Fannin and Rollerson, 1996). Similarly, on Vancouver Island, the upper limit of deposition was almost 35^{o} (0.1 m), substantially higher than 15^{o} reported by Horel (2007), also for debris flows on Vancouver Island.

The deposition slope limits reported here are close to the angle of internal friction for gravel or wet sand (~35^{o}); therefore, while deposition on those slopes may be uncommon in shallow debris flows, there is a physical explanation for their occurrence and we would argue that similar conditions probably occurred unrecorded in previous studies. Our own field experience indicates that some basal deposition may occur on relatively steep slopes based on friction alone. In addition, topographic features and intact forests may influence deposition characteristics. In Alaska, for example, Johnson *et al.* (2000) reported that net deposition began in slopes as steep as 29^{o} in old-growth forests, and 19^{o} in clearcuts.

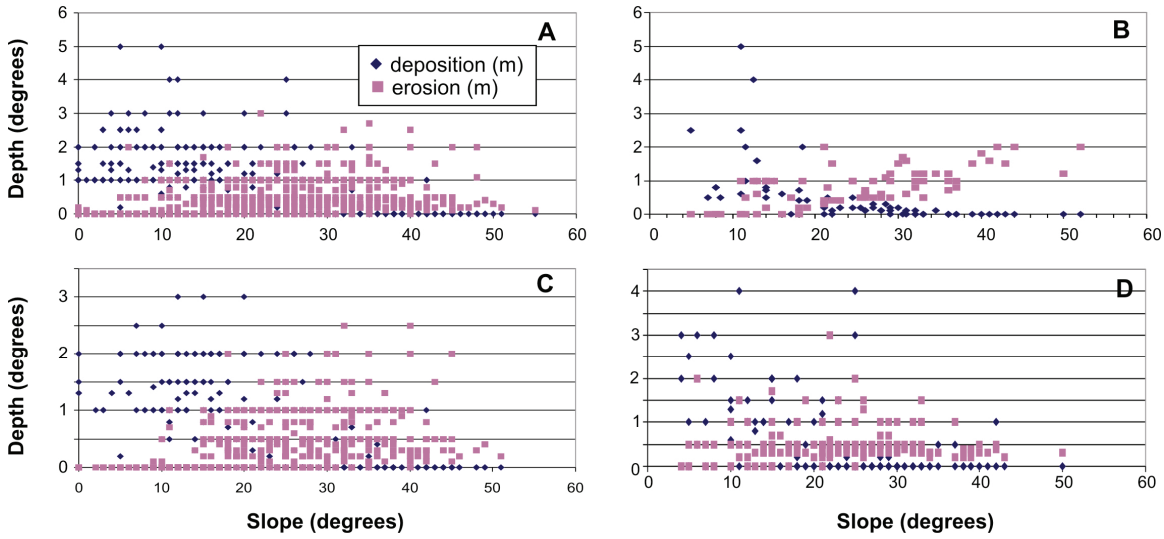

Figure 4.6. Scatter plots of deposition and erosion at 850 field stations compared to slope at each location. The QCI data is presented in aggregate in A, Vancouver Island data in B. QCI data is further broken into open slope (C) and gullied (D) data. QCI data published in Wise (1997).

A final consideration is that this study measured erosion and deposition independently in an attempt to better define the role of slope. Horel (2007), in contrast, was almost certainly describing net deposition at 15°. Fannin and Wise (2001) estimated that net erosion occurred on unconfined slopes above 19° and on confined slopes above 10° in the Queen Charolotte Islands. However, Fannin and Wise (2001) did observe erosion and deposition at a range of slopes. Hungr *et al.* (1984) reported the onset of net deposition took place between 10° and 16°, and suggested overall that 10°-14° was appropriate for unconfined debris flows, and 8°-12° was appropriate for channelized debris flows. Hungr *et al.* (1984) reported that similar results were found in Japan. We consider net deposition below.

Erosion in this study was measured on relatively flat slopes: 10° on both Vancouver Island and the Queen Charlotte Islands, and 5° for gullied debris flows on QCI. The erosion typically occurs in the center of the landslide track and may be difficult to distinguish from post-landslide fluvial reworking. Nonetheless, it is strikingly evident, particularly where the landslide is partially confined.

While the scatter plots show the variability in the data, the overall impact of slope is easier to understand if we consider the mean erosion and deposition of all measurements in 3^o classes (Figure 4.7A-C). Illustrated thus, further trends are evident: Erosion levels off at the steep end of the slope range to reflect the relatively thin post-glacial deposits that cover the majority of coastal BC slopes. This paucity of sediment also limits total failure volumes: debris flow erosion won't exceed the depth to bedrock, and in BC, bedrock is often within a meter of the surface. Deposition, on the other hand, is not so constrained, and terrain maps commonly reveal thicker colluvial and morainal deposits on flatter slopes approaching the valley bottom. In Figure 4.7, deposition increases rapidly with a drop in slope angle, peaking at almost twice the erosion depths. A crossover point between deposition and erosion, and related to slope reveals where net deposition is expected along the landslide path. That crossover point is between 18^o and 21^o for the Vancouver Island data (Figure 4.7C), and between 21^o and 24^o for the open slope QCI data (Figure 4.7A). This means that net deposition occurred on slopes steeper than previously reported for coastal BC (Hungr *et al.*, 1984; Fannin and Wise, 2001; Horel, 2007).

There is an anomalous drop in deposition for the VI data at the 9^o slope bin with no obvious reasonable physical explanation. It is likely an artefact of too few data entries in that bin; similar problems occur above the 39^o slope bin for erosion where depth of sediment seems anomalously high. Since sediment on steeper slopes is usually thinner, Vancouver Island results were expected to be similar to those from the QCI data (Figure 4.7A). However, it should be noted that field samples are inherently biased to steep slopes with sediment (the only kind on which debris flows occur), perhaps in greater proportions than on adjacent terrain. Depth of sediment may be symptomatic of failure prone slopes rather than indicative of a trend to deeper material on steeper slopes.

Net deposition is easily obtained by subtracting erosion from deposition and is shown in Figure 4.8. A line representing a best-fit third-order polynomial is drawn over the graphs for illustrative purposes. In addition to the crossover points (the onset of net deposition) being clearly defined, the present study reveals average entrainment and deposition along the landslide path related to slope. Using these measurements, one is

able to estimate, based on field measurements, the required runout distance for a given landslide. For the first time, practitioners can incorporate the predictions in a consistent way into direct mapping techniques already being utilized.

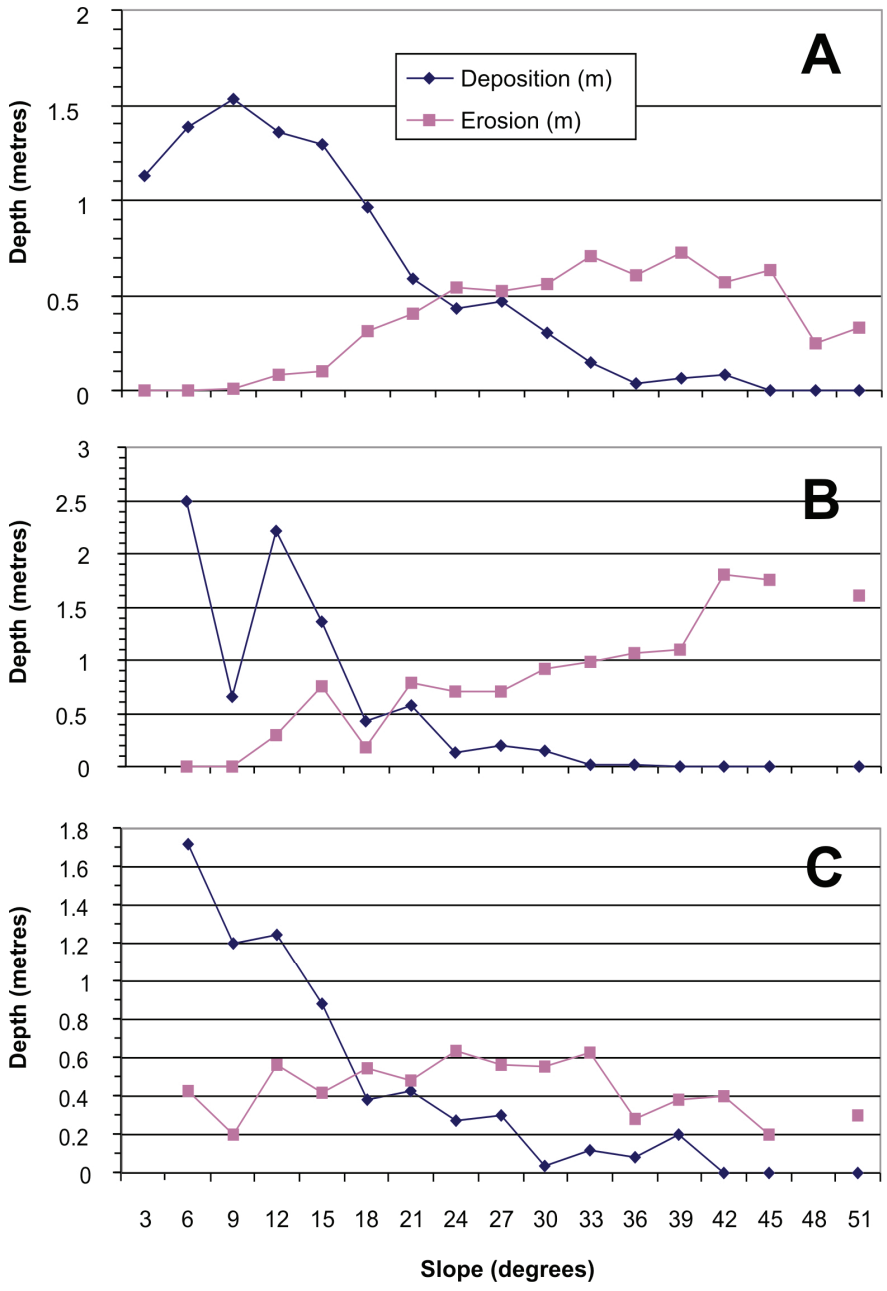

Figure 4.7. Mean erosion and deposition in 3° slope classes for QCI open slope debris flows (A), Vancouver Island open slope debris flows (B) and QCI gullied debris flows (C).

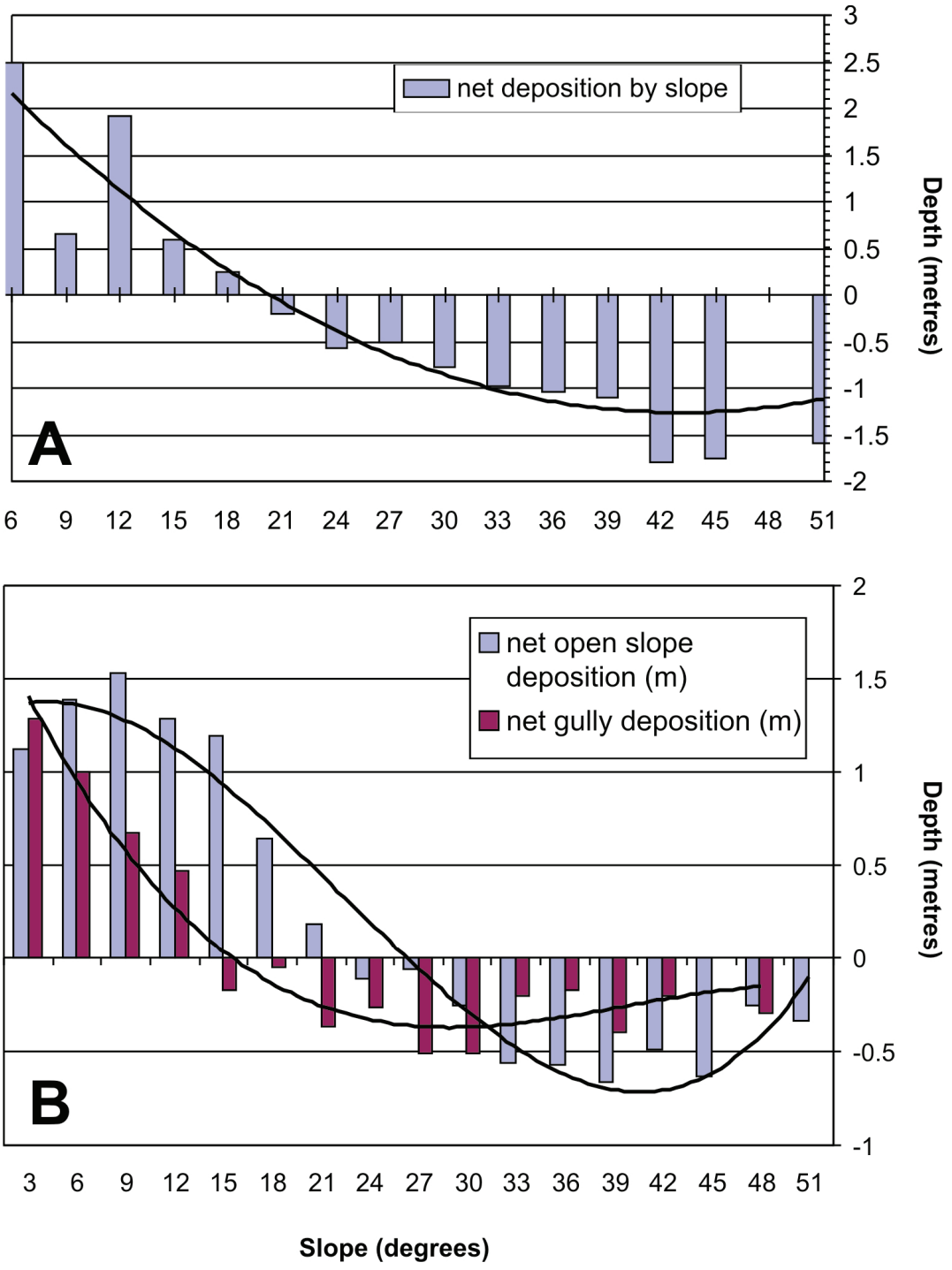

Figure 4.8. Net deposition in 3° slope classes for debris flows on Vancouver Island (A) and QCI (B). Based on 1700 field measurements, these graphs can be used to estimate runout distance requirements of shallow debris flows.

Table 4.2. A simplified example of a debris flow runout estimation based on observed mean net deposition characteristics for Vancouver Island. Net deposition was determined using actual observations rather than the given trendline except for the 12 degree slope where fewer data points are expected to bias results. Alternatively, the trendline could be used for all measurements.

Slope (degrees)	Distance (m)	Net Deposition from Figure (m)	Cumulative volume (m^3)
36	60	-1.1	-1320
27	30	-0.5	-1620
21	30	-0.2	-1740
12	50	+1.2 (using the line rather than the bar)	-540

Consider an example of an open slope landslide following a simple topographic profile: On Vancouver Island, a landslide initiates on a 36^o slope that extends 60 m to a slope break of 27^o for another 30 m, 21^o for 30 m and then flattens out to 12^o before reaching a stream 50 m away. Is the landslide likely to hit the stream? For simplicity assume a constant width of 20 m. The result is easily calculated (Table 4.2) and a credible scenario develops that results in 540 m^3 of material entering into the stream. In this scenario, avoiding the stream would require another 25 m of slope distance at or below 12^o, or the expectation that the landslide deposit would be deeper. If, for example, it was as deep as the observed average (1.9 m), it would have stopped just short of the stream. This method, based on repeated observations, gives a conservative approach to empirical landslide runout prediction for shallow open slope failures.

The impact of a change in slope on width, and therefore potential sediment balance, was considered herein: Over 13 000 width measurements taken at 10 m increments perpendicular to the landslide path revealed, for 331 landslides in the Klanawa, that the mean width was 22 m. Further, mean widths examined at each of the slope bins indicated that debris flows were widest on the steepest slopes, typically associated with initiation, and on the flattest slopes associated with deposition, but spent most of their length on transitional slopes, at a width just slightly less than the mean (Figure 4.9). While measured widths ranged up to about 300 m, fewer than 6% were greater than 50 m wide, indicating that the usual morphology of debris flows in coastal BC, even for open slopes, is more linear than previously thought. Hürlimann *et al.* (2008) noted that the primary

disadvantage to methods that used the concept of volume balance along the flow path was the detailed information necessary about the channel as well as knowing the initial volume. We argue, based on the observed relationships between slope and parameters of depth and width, that neither is absolutely necessary. On the other hand, the volume balance approach alleviates the need of the practitioner to explicitly include an assessment of rheology and associated parameters in debris flow predictions.

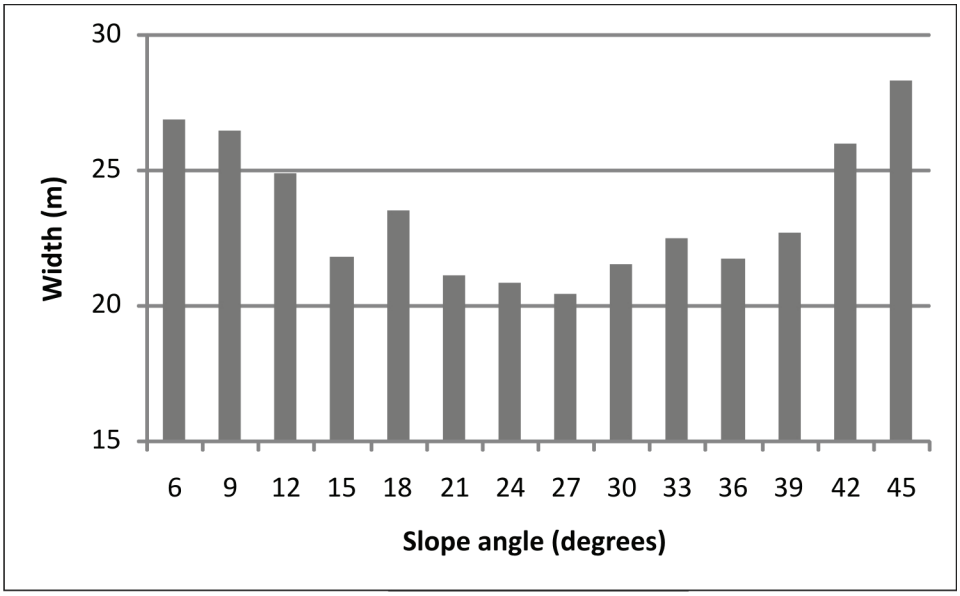

Figure 4.9. Mean debris flow widths related to slope for Vancouver Island. X-axis numbers represent the upper limit of each slope bin.

Generalizing the results, an entrainment map demarcating erosion and deposition zones based on the 3^{o} slope classes for all of Vancouver Island was created using a 25 m DEM (Figure 4.10). This gives a regional perspective of potential debris flow behaviour and reveals why the stream network provides a reasonable baseline to debris flow limits (Guthrie *et al.*, 2008). Erosional surfaces are in red, essentially transitional surfaces in white and depositional surfaces in brown. Lower-order streams tend to be tightly constrained between erosive surfaces where material is likely to be entrained. Large depositional surfaces, from a landslide perspective, are mostly contained by the lower slopes and valley floors of higher-order streams. Landslides reaching higher-order

streams are often larger, having avoided or overwhelmed smaller watershed features along their path and therefore need greater stopping room. Figure 4.11 shows an example of landslides superimposed on the entrainment map.

Debris flow runout, modelled using the methodology outlined in Section 3 above, compared favourably to observed runout (Figure 4.12). The trend line indicates that the methods slightly over-predict, on average, debris flow travel distance. Several explanations are proposed: (1) Estimates of erosion and deposition may be wrong, however, field estimations are likely to be more accurate than data acquired remotely. (2) Streams frequently remove part of material at the toe of actual debris flows (Figure 4.13). This was not calculated in the model. (3) The 25 m resolution of the DEM means that topography picked up in the field of a size sufficient to influence landslide behaviour, combined with the inherent variability of the results (Figure 6), is smoothed out considerably in the GIS. Consider the case for a 25 m staircase. The DEM would register such a staircase as having a 45^{o} slope, but in reality it would be several vertical falls, interposed with horizontal benches. Each bench has a significant role in the mobility of the debris flow. We observed the influence of benched topography on both large and small landslides. The discussion of roads below is an excellent case example of the role of topography too small to be observed in the DEM.

Three landslides extended much further than predicted (the shortest being > 2.7 km) as channelized debris flows where continued confinement limited opportunities for deposition. The influence of channel confinement on scour and deposition along the landslide path, and therefore mobility, may be discerned from Figures 6-8. The crossover to net deposition occurs at slopes about 10^{o} flatter than for open-slope events, corroborating previous observations by others (Hungr, 1984; Fannin and Rollerson, 1996; Horel, 2007) and indicating substantially increased mobility. However, the slope angle at which the onset of net deposition was observed was again steeper than previously thought.

Figure 4.10. An entrainment map of Vancouver Island with erosional surfaces in red, transitional surfaces in white and depositional surfaces in brown. Colors grade to one another based on 3° slope classes.

The relatively limited erosion depth of channelized debris flows is indicative of the active environment within the gully or channel. Essentially, the shallow erosion depth as indicated on Figures 4.7 and 4.8 is a product of highly efficient systems, repeated fluvial or colluvial erosion, that transport sediment to lower positions on the landscape. This is particularly evident in low-order streams which frequently get scoured to bedrock, but which fail repeatedly every several years. In the Klanawa study area, for example, more than 74 % of the debris flows ended in first and second-order streams of this nature.

Of the debris flows in the Klanawa study, 127 initiated from single points and hit a stream, thereby allowing discrete analysis in a GIS environment. Those landslides were divided into those that continued as a channelized debris flow (n=58) and those that ended at the stream (n=69). A comparison of the angles between the landslide path and

the stream for each type is shown on Figure 4.14. Open-slope debris flows had a median angle of entry of 70^{o} while those that became channelized had a median angle of entry of 26^{o}. Similarly, more than 75% of debris flows that stopped had angles of entry >45^{o} and more than 75% that continued had angles <45^{o}. The results corroborate previous results (Benda and Cundy, 1990; Millard, 1999; Miller an Burnett, 2008) and indicate, in terms of mobility, that headwall failures into a gully are much more likely to continue as a channelized debris flow than sidewall failures. Once again, this result is easily incorporated into direct mapping methods.

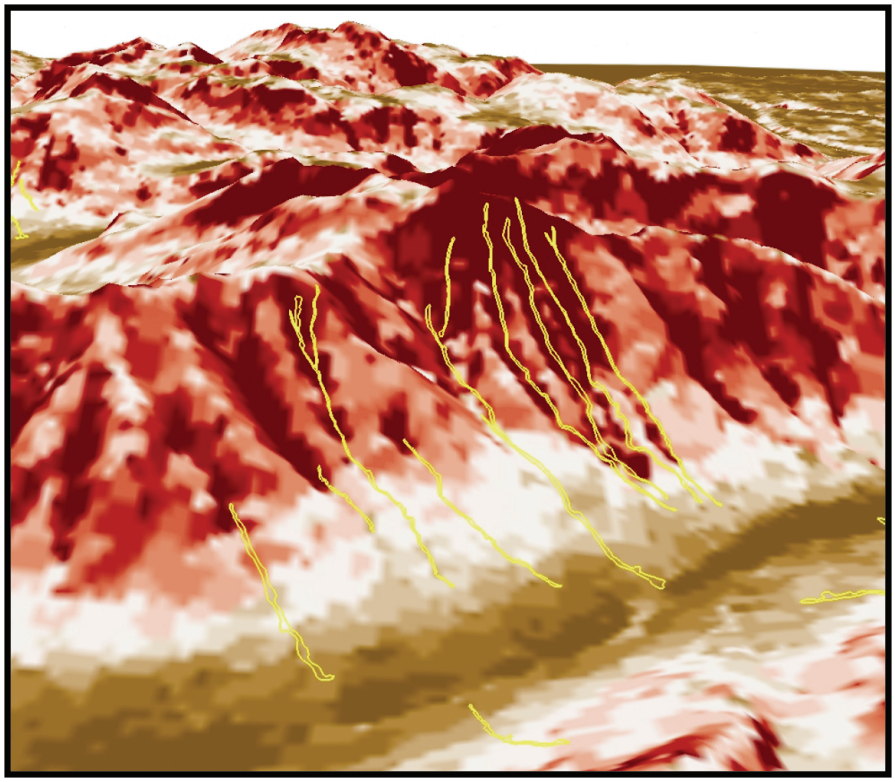

Figure 4.11. Landslide polygons superimposed in yellow on an oblique view of the entrainment map. The colour symbology is the same as in Figure 5, with erosional surfaces in red, transitional surfaces in white and depositional surfaces in brown.

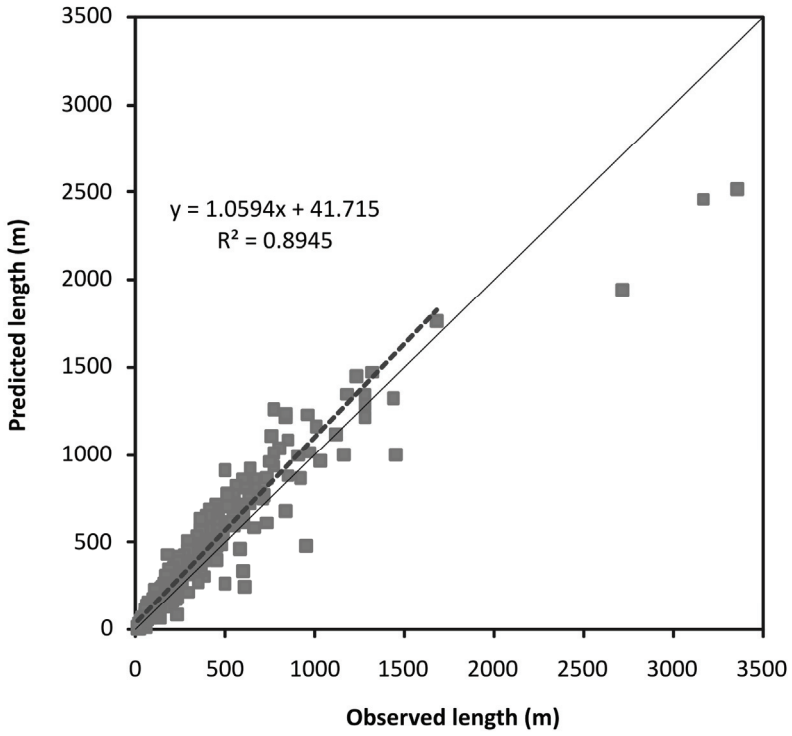

Figure 4.12. Predicted versus observed runout using the sediment balance approach for 331 landslides in the Klanawa study area. See text for discussion.

Figure 4.13. A dramatic example of a stream removing landslide deposits is shown here at the toe of a landslide on Vancouver Island.

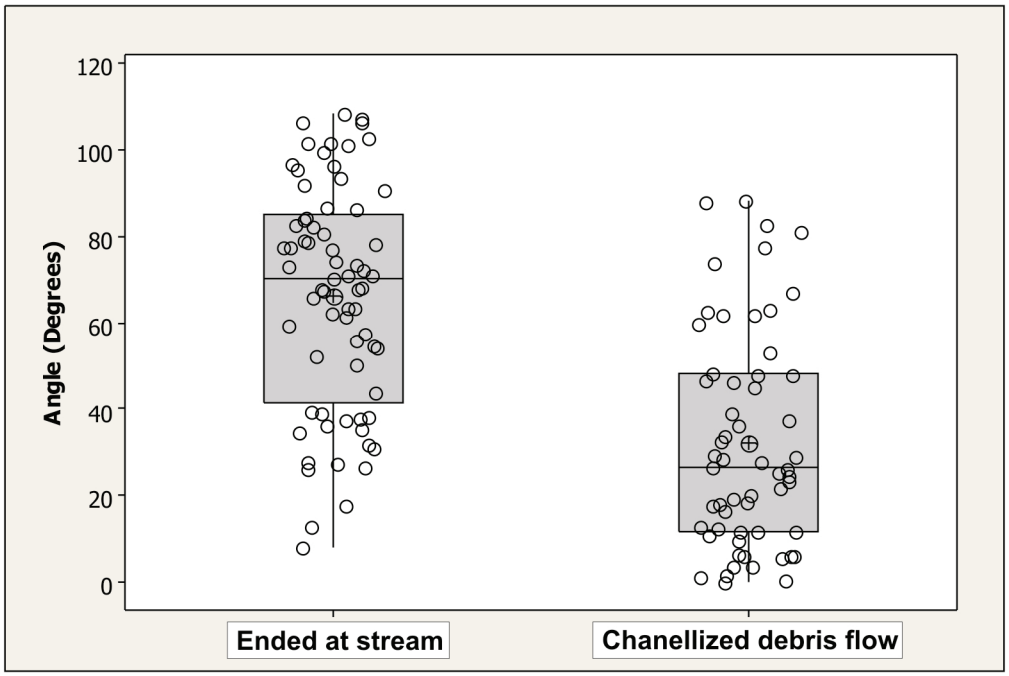

Figure 4.14. Box plots showing angle of entry to streams for 127 debris flows; 58 of which carried on as channelized debris flows. Median angles are shown by the crossed circle, means by a solid line.

4.6.2 The role of forests

As discussed, research indicates that the presence or absence of mature timber can influence the magnitude and travel distance of individual events (Robison, 1999; Bunn and Montgomery, 2000; May and Gresswell, 2003; Lancaster *et al.*, 2003; Miller and Burnette, 2008). Previous studies considered changes to mean runout length between landslides through clearcuts and landslides through intact timber (i.e. Robison, 1999; May and Gresswell, 2003; Miller and Burnette, 2007). However, causation may be difficult to ascribe to the results which are dependent on other factors such as slope and available sediment. Herein we attempt to understand what happens when a landslide travelling through an unvegetated slope hits an intact forest.

Twenty five landslides that travelled through a cutblock and crossed a forest edge were analyzed. Specifically we measured the change in width 20 m above and 20 m

below the boundary and the results are given in Table 4.3. Cutblock boundaries appeared to have a large effect in decreasing the momentum of open-slope debris flows (Figures 4.15 and 4.16). Debris flows that crossed boundaries between cutblocks and older forest crossed them at slopes ranging from 12˚ to 46˚ (based on a 25 m DEM) yet we observed no discernible effect from slope. In contrast, the Δw ratio ranged from 0 (the slide stopped at the forest boundary) to almost 2 (the slide doubled in width).

Table 4.3. The width ratio (Δw) showing the effects of forest on debris flow width and the road width ratio (Δr), or the change in debris flow width after crossing a road. Δw values equal to 1 indicate that the forest had no effect on debris flow width, $\Delta w > 1$ indicate an increase in debris flow width, $\Delta w < 1$ indicate a decrease in width, and Δw of 0 indicate that the debris flow stopped just inside the forest edge. Similarly, Δr values equal to 1 indicate that the road had no effect on debris flow width, $\Delta r > 1$ indicate an increase in debris flow width, $\Delta r < 1$ indicate a decrease in width, and Δr of 0 indicate that the debris flow stopped on the road prism. Count and % show the number and percent of total landslides respectively for each score.

Forest Boundary			Road		
Count	%	Δw	Count	%	Δr
12	48	0	31	52	0-0.15
8	32	0.25-0.65	6	10	0.25-0.5
2	8	0.75-0.8	6	10	0.65 – 0.85
2	8	0.9-1.2	7	12	0.9-1.2
1	4	1.9	10	17	1.25 – 1.75

Nearly half (48%) of the landslides examined stopped within the 40 m buffer against the forest boundary ($\Delta w = 0$) and another third (32%) were reduced by three-quarters to slightly more than one-half in width ($\Delta w = 0.25 – 0.65$). Over 60% of the second group stopped entirely within 50 m of the forest boundary. The remaining three debris flows were reduced in width but continued downslope otherwise unaffected. The largest of these failures continued 400 m further, eventually depositing onto a river terrace below.

Debris flows that showed no significant change in width ($\Delta w = 0.9 – 1.2$) were relatively large before they hit the forest boundary; one was the largest in the subset and stopped 170m downslope at a stream channel. The other was unaffected by the forest boundary continued 210m downslope and ended in the middle of the forest.

Only a single failure got significantly larger, in this case doubling in size. However, this relatively small slide deposited just 55m into the forest from the forest edge and the width ratio was in this case representative of a depositional phase.

While the sample size was small, we have shown that forests can provide a substantial barrier to shallow debris flows (Figures 4.15 and 4.16), impeding debris flow travel, shortening runout distance and reducing flow volumes. We propose based on field observations that forests can also serve to stop debris flows on steeper slopes. This corroborates previous studies and provides a strong argument for retaining mature forests as buffers between harvested areas in forestry management strategies. One could argue that 50 m forested buffers around major streams would dramatically reduce the potential for impact from upslope debris flows.

4.6.3 The role of roads

Roads are widely recognized as causing landslides in the Pacific Northwest (Jakob, 2000; Wemple *et al.*, 2001; Guthrie, 2002, 2005). Guthrie (2002) observed, for example, that when measured against the relative space that roads occupy, they may increase landslide frequencies by two orders of magnitude. However, roads behave as benches in the landscape and this in turn is expected to ameliorate landslide impacts. We considered the extent to which this was the case in much the same way we examined the role of forests, by examining the change in open slope debris flow width above and below the contact with the road for 60 events. The results are given in Table 4.3.

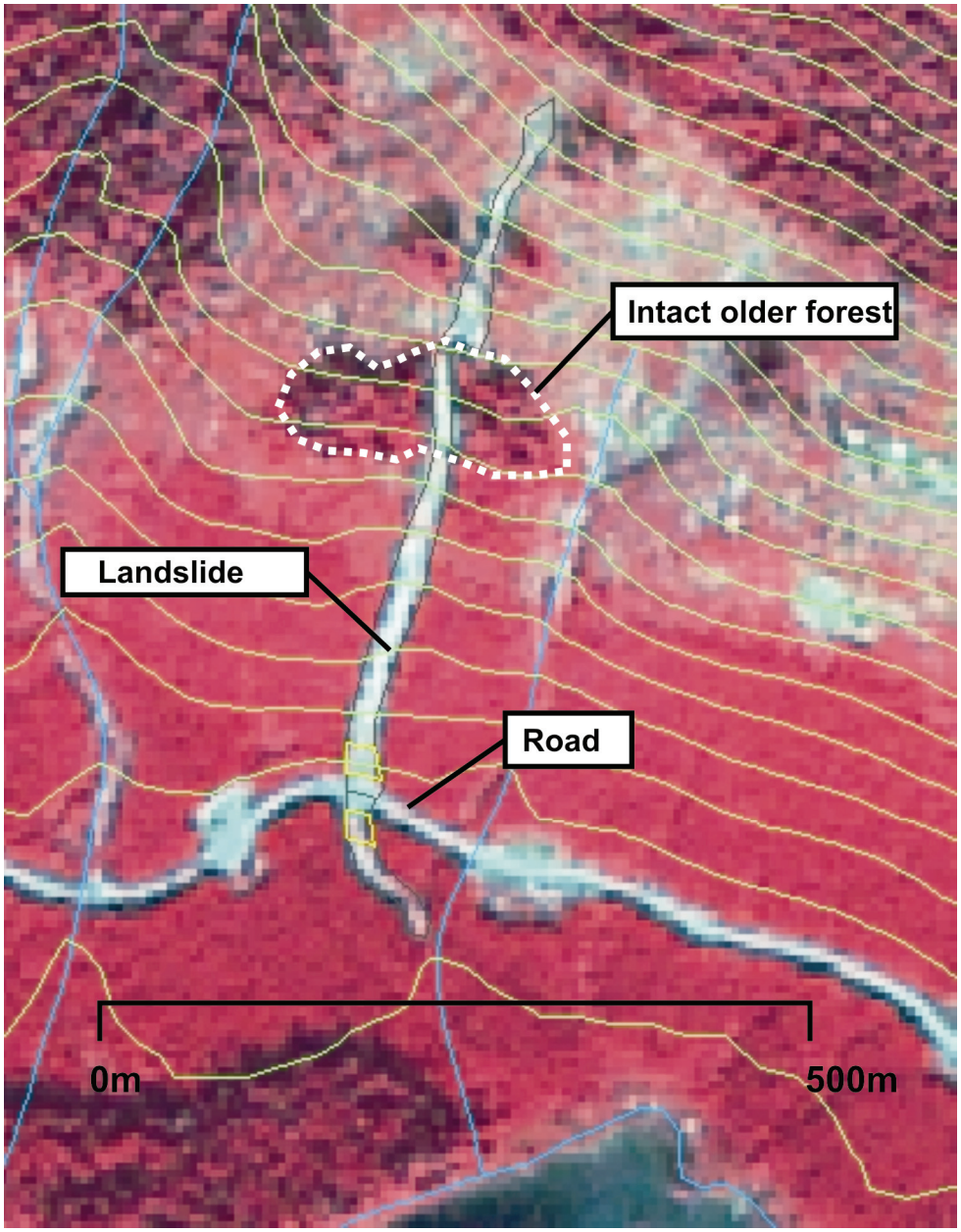

Figure 4.15. Debris flow overlain on a SPOT satellite image. An open slope debris flow travels from a clearcut, through a small block of older forest where it narrows considerably following the contact with the forest edge. The debris flow increases in width as it entrains more material below the intact forest. A reduction in width is measurable below the road contact, however, the landslide stops shortly as it reaches the valley floor and flatter slopes.

Figure 4.16. The role of mature forest in limiting landslide runout. This block was logged after the landslide, and the remains of the forest may be seen (arrows) as stumps with the landslide debris piled up against them over 4 m high (person for scale in circle).

As in the forest contact example, debris flows crossed roads at slopes ranging from 15˚ to 45˚ (based on a 25 m DEM). In terms of landslide mobility, the DEM slope alone was not a good indicator of stopping power at the road.

Overall, Δr ratios ranged from 0 (the debris flow stopped on the road) to 1.75 (the debris flow width increased by 75% after crossing road). Slightly more than half the population, had Δr values below 0.15 and the debris flows stopped on or within ten meters of the road. These slides ranged across all slope classes, however, and had a maximum size above the road of 5800 m^2.

Another 10% of the debris flows were reduced in width at the road by one-half to three-quarters. Of those, half stopped within a short distance of the road. In contrast, however, the reduction in width was temporary for the other half and continued down slope with the effect of the road diminishing rapidly with increased distance from the road along the landslide path. This is of critical importance when considering the role of any topographic benches: Essentially, a bench represents a single line of defence across

the landscape. If the bench is unable to contain the debris in a landslide, then the downslope rules of entrainment and deposition continue to apply. The bench in such a case has been of limited benefit, reducing only the immediate volume of the debris flow.

Six debris flows had a Δr ratio near 0.75 indicating a slight reduction in width after crossing a road. Of these, five continued down the slope reduced in width but otherwise unaffected. Once again, the road effect was to reduce the immediate volume of the debris flow. If the slopes below the road are largely transitional, entraining and depositing material in equal measure, then the benches and roads do serve a role in reducing the probable impact of debris flows that hit the valley floor or the stream network.

The remaining debris flows continued downslope apparently unaffected by roads, with widths remaining unchanged or even expanding. Of these, ten debris flows had ratios above 1.25 and all continued down slope apparently unaffected by the road crossings and eight entered higher order streams below. Morphologically, these debris flows were spreading rapidly in a teardrop shape, less typical of the debris flows in this study, but not unusual elsewhere. They appeared to overwhelm the road and continued to spread and travel downslope unabated. The largest of these was 67 000 m^2.

Roads were strikingly effective at stopping debris flows over half of the time. In addition, in several cases that the debris flows overran the road, they had persistent reduction in volumes as they moved to more transitional slopes. However, unlike forests which provide a constant frictional barrier, roads represent only a single line of defence. Multiple benches in the landscape are likely to be more effective than single benches. Finally, one needs to acknowledge that the stopping power of roads does not adequately account for the increase in landslide frequency as a result of road construction. Both, however, are served better by well-built roads with thoughtful application of geo-engineering.

4.7 CONCLUSIONS

Land managers in coastal British Columbia faces the constant challenge of mapping large remote areas inexpensively and efficiently. Direct mapping in the form of terrain and hazard mapping has been the historical solution and is the method most widely used as in other regions worldwide. Good hazard mapping incorporates runout and associated magnitude, both of which are historically difficult to predict in the field. We therefore examined topographic controls to shallow landslide runout and magnitude using datasets from coastal British Columbia and, based on 1700 field observations, general rules for slopes on which landslides entrain and deposit material were calculated. The field observations were supplemented by a dataset of 331 debris flows gathered through air photograph analysis and both sets of data were analyzed in a GIS environment. From these analyses we conclude that:

(1) Deposition and scour occur on steeper and flatter slopes respectively than previously reported. Importantly, mean net deposition was determined to occur on slopes between 18^{o} and 24^{o} for open slope failures and between 12^{o} and 15^{o} for gullied or channelized debris flows;

(2) Average net deposition or entrainment may be estimated on a variety of slopes in the field using the types of graphs provided (Figures 4.6-4.8), and runout can therefore be calculated in similar terrain (Figure 4.12). An example of an entrainment map for Vancouver Island is provided. An entrainment map may be used to quickly estimate erosion and deposition along a path and give a user a first-order approximation of expected debris flow mobility. Field estimates of mobility based on measured slopes should produce better runout predictions than those based on the 25 m DEM. However, both are useful;

(3) The simple rule-based methodology for estimating debris flow runout is based on real field examples from across Vancouver Island and the Queen Charlotte Islands. The methodology was tested in the Klanawa study on Vancouver Island and found to produce encouraging results where predicted runout matched very well the observed.

(4) More than 75% of debris flows that hit channels and transformed to channelized debris flows had angles of entry < 45^{o}. More than 75% of debris flows that stopped had angles of entry > 45^{o} to the channel. Landslide paths that lead to an acute angle with a stream or channel are significantly more likely to have long runout distances;

(5) Mature timber stopped debris flows within 40 m of the forest boundary almost 50% of the time, and within 50 m 72% of the time. Debris flow widths were reduced after passing through a mature timber boundary 88% of the time, indicating that forests can act as a substantial frictional topographic barrier. Forest managers are well advised to leave blocks of intact forest between clearcuts and around streams to buffer the potential effects of landslides; and

(6) Roads stopped debris flows in 52% of the cases and reduced the debris flow width almost 72% of the time. However, landslides that breached roads and continued onto steep slopes continued to entrain material and grow. The road itself can serve both as a point of erosion (steep fill slopes and drainage routing) and deposition. Thoughtful application of geo-engineering is an obvious solution to both aspects of the problem.

These results have significance to the management of steepland forested terrain in the Pacific Northwest.

Chapter 5: Work, persistence, and formative events: The geomorphic impact of landslides.

Based on: Guthrie, R.H. and Evans, S.G. 2007. Work, persistence, and formative events: The geomorphic impact of landslides. Geomorphology, 88, 266-275.

OVERVIEW: Understanding the scale and frequency of physical processes that act upon and form the surface of the Earth is a fundamental goal of earth science. Here we determine the magnitudes of landslides that impact the landscape in terms of work, persistence, and formative events. A systematic analysis of rapid landsliding (the analysis did not consider creep and other slow semi-continuous processes) indicate that moderate-sized landslides do the most work transporting material on hillslopes. The work peak defines the moderate magnitude, and that magnitude varies based on local physiography and climate. Landslides that form the work peak are distinct from catastrophic landslides that are themselves formative and system resetting. The persistence time for debris slides/debris flows (P_{DS}) and rock slides/rock avalanches (P_{RS}) is calculated over six orders of magnitude. We consider an event catastrophic when it persists in the landscape, as described by a persistence ratio (P_F), an order of magnitude longer than the population of landslides that form the work peak.

5.1 INTRODUCTION

In 1960, Wolman and Miller proposed to measure the relative work done by similar geomorphic events differing primarily in magnitude and to establish which of those event magnitudes were ultimately landscape forming. Based on observations that log-normal distributions are common representations of the frequency of several natural events, they determined that the moderate-sized events accounted for the largest portion of work done in a landscape.

It is perhaps a testament to the appeal of their early work that Wolman and Miller's 1960 publication remains the benchmark paper against which others continue to study the

concept of geomorphic effectiveness. It is one of the 10 most cited papers in *Geomorphology* (Doyle and Julian, 2005).

This paper examines the concept of geomorphic effectiveness as it applies to landslides. Effectiveness in river geomorphology as the conceptual framework in which Wolman and Miller (1960) first proposed their ideas is briefly reviewed; then the notion of what constitutes, in hydrology at least, moderate and extreme events is identified. The work done by landslides in the landscape is examined to establish whether or not the Wolman-Miller concept applies. The difference between work and formative events is distinguished for landslides, and landslide magnitude-frequency data are examined to determine likely magnitudes for each. In addition, the persistence of landslides over several orders of magnitude is characterized and related to landslides that are individually formative.

5.2 THE WOLMAN-MILLER CONCEPT

Wolman and Miller (1960) defined *geomorphic effectiveness* as work, an expression of the amount of material moved some distance by a geomorphic event. In the Wolman-Miller concept, the magnitude of the most geomorphically effective event was also the event magnitude responsible for landscape formation. They argued that high magnitude events, despite their visible impacts, occurred too infrequently to have effective influence on the geomorphic landscape and that smaller, more frequent events were similarly ineffective because they lacked power to sufficiently alter the terrain. Wolman and Miller (1960) suggested that the geomorphically effective event was one of moderate size, corresponding to the work peak seen in Figure 5.1. For alluvial rivers, the work peak occurred on average every 1-2 yr, corresponding to the bankfull flow. Leopold *et al.* (1964) refined the return interval for the geomorphically effective event for rivers at 1.5 yr. Both sets of authors call these the "moderate-sized" events.

Several authors have since considered various geomorphic events and found general agreement with Wolman and Miller's findings and largely corroborated the relationship between bankfull and geomorphically effective flows (Wolman and Gerson, 1978;

Andrews and Nankervis, 1995; Castro and Jackson, 2001; Emmett and Wolman, 2001). In contrast, however, others have suggested that extreme or high magnitude events are responsible for doing the most work in at least some landscapes (Dury, 1980; Ohmori and Hirano, 1988; Grant and Swanson, 1995; Trustrum *et al.*, 1999). Significantly, the processes that lend themselves most consistently to the Wolman-Miller concept are riverine in nature; river processes supply a continuous data set in a generally defined location and lend themselves well to analysis of the Wolman-Miller concept. In at least some cases, hillslope erosion and landslides appear to be different. As a consequence, the geomorphic effectiveness of landslides has not been formally established.

5.3 EVENT SIZE

The definition of a moderate- versus extreme-sized event is arbitrary and depends, among other things, on the time and spatial scales at which one examines the process. For example, in the case of rivers, if the reference scale is the maximum annual flow, then geomorphically effective flows are almost continuous (they occur with return intervals of about 1.5 yr). If instead the reference scale is daily stream flow, geomorphically effective flows appear to be infrequent. The timescale-dependent effect is shown in several studies; Andrews and Nakervis (1995) determined that effective discharges occur often, on average about 15 d/yr (~ 4% of the time). Hickin (1989) determined that the effective discharge was relatively rare and occurred only a few days per year on average. Hickin further observed that the largest 18.5% of the annual bedload was moved by "large-magnitude" floods occurring < 0.2% of the time. However, because the reference time used in the latter study is a day, 0.2% can be back calculated to an average return period of approximately 1.4 yr – remarkably close to the early Wolman and Miller (1960) and Leopold *et al.* (1964) estimates.

Even the largest events are dependent on the scale used to measure them. Hsu (1983) observed, for example, that rare events are only improbable in human terms, but a relative certainty in geological time. Dury (1980) similarly observed that if a sufficiently large area is considered there will be one or more examples of massive catastrophic events that

profoundly change the landscape. In this context, the role of catastrophic events appears contradictory to the Wolman-Miller model.

Geomorphic effectiveness lies somewhere over an undefined portion of the probability tail for log-normally distributed data. We are apparently unable to separate the notion of moderate size from our personal perception of event frequency. For rivers, the recurrence interval of bankfull flow (the geomorphically effective flow) is a convenient 1.5 yr. The probability, however, of any landslide event occurring in a specific location over short time durations (1.5 yr for example) is typically low irrespective of magnitude in a single location.

Provided that landslides can be shown to follow the conceptual model in Figure 5.1, one could argue that the landslides doing the most work (forming the work peak) are, by definition, moderate in magnitude.

5.4 WORK AND GEOMORPHIC EFFECTIVENESS IN LANDSLIDING

In contrast to river flows, landslide events are discontinuous in time and space, exceptional by nature, and arbitrary in magnitude (a similar trigger event, for example, can produce small to relatively massive landslides). They form discontinuous data sets and are therefore analyzed in aggregate.

We are reasonably able to describe the overall probabilistic character of landslide areas and therefore quantify landscape hazard, denudation, risk, and perhaps geomorphic effectiveness at a regional scale. Understanding the magnitude-frequency distribution is an integral part of this process.

Regional inventories of landslides have revealed that, for both experimental and actual data, landslides are log-normally distributed and appear to follow an inverse power law over several orders of magnitude (Fujii, 1969; Hirano and Ohmori, 1989; Somfai *et al.*, 1994; Hovius *et al.*, 1997; Pelletier *et al.*, 1997; Hungr *et al.*, 1999; Dai and Lee, 2001; Stark and Hovius, 2001; Guzzetti *et al.*, 2002a,b, 2005; Reid and Page, 2002; Guthrie and Evans, 2004a,b, 2005; Malamud *et al.*, 2004a,b). A case has been made for systems of landslides approaching self-ordered criticality resulting in scale invariance or fractal landscapes (Bak *et al.*, 1988; Hall, 1992; Noever, 1993; Czirok, *et al.*, 1994; Bak, 1996;

Pelletier *et al.*, 1997). Figure 5.2 shows cumulative magnitude-frequency curves for landslides from coastal British Columbia (BC), Canada, and from the 1994 Northridge earthquake in California, United States (US), all of which exhibited power law relationships over a substantial portion of the data. However, landslide magnitude-frequencys data appear to follow a power law for only a truncated portion of the entire distribution, making them at best a weak inverse power law (Perline, 2005) and at worst a false inverse power law. In each example in Figure 5.2, the landslide inventories are considered complete, and the power law does not describe magnitudes smaller than ~ 10,000 m^2 for the coastal examples, and ~ 1000 to 3000 m^2 for the Northridge case. Several distributions have been considered to calculate the total hazard including the double Pareto (Stark and Hovius, 2001; Guzzetti *et al.*, 2002a,b, 2005; Guthrie and Evans, 2004a,b) and an inverse gamma distribution (Malamud *et al.*, 2004a, b; Guzzetti *et al.*, 2005). These are attempts to provide a universal curve that quantifies the total distribution of landslides, including the portion that does not follow the power law. The latter transformations are unnecessary to understand the geomorphic effectiveness of landslides and continue to use the log-normal distribution, both for ease of application and for consistency with the original concept (Wolman and Miller, 1960).

When considering geomorphic effectiveness, landslides smaller in magnitude than the *rollover* (that portion of the distribution that lies to the left of the power law segment in Figure 5.2) must be included as they occur most often. In several cases worldwide, the volume of the rollover may also be relatively large: 10,000–20,000 m^2 for coastal BC (Guthrie and Evans, 2004a,b), 3,000–30,000 m^2 for Japan (Hirano and Ohmori, 1989), and 5000 m^2 for the southern New Zealand Alps (Hovius *et al.*, 1997). Small landslides need to be compared to the rarer larger events to determine which does the most work.

Work is defined for landslides as it was for rivers: the product of frequency and magnitude (Figure 5.1). Work has several potential metrics, including destructiveness (Evans, 2003; Malamud *et al.*, 2004b), fragmentation energy (Locat *et al.*, 2006), runout (Hungr, 1995; Ayotte *et al.*, 1999; McClung, 1999; Hungr and Evans, 2004), volume (Innes, 1983, 1985; Guthrie, 1997; Hovius *et al.*, 2000; Martin *et al.*, 2002), or a combination of volume and expected velocity (Cardinali *et al.*, 2002; Reichenbach *et al.*,

2005). Fundamentally, however, work may be characterized as the change from potential to kinetic energy through time:

$$\Delta E = mg(\Delta h) \tag{7}$$

where E is energy in joules, m is the landslide mass, g is the gravitational constant, and Δh is the change in elevation in a given time interval.

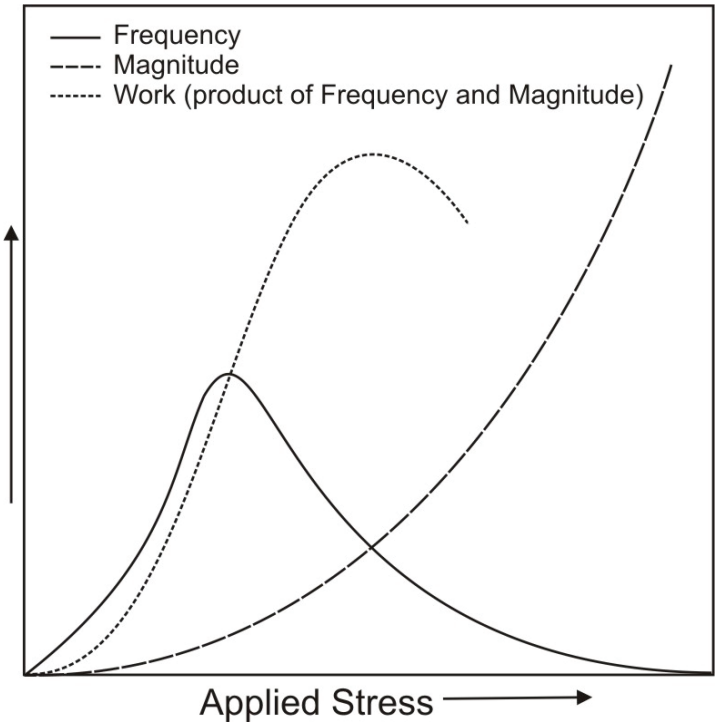

Figure 5.1. A simplified diagram of the Wolman-Miller (1960) concept. In continuous natural phenomena (e.g., river discharge, wind speeds), a stress is applied to a transportable medium (e.g., sediment). As the stress increases, the magnitude of material that may be transported increases. However, the frequency distribution of the event size is log-normally distributed and, consequently, the most work (a product of frequency and magnitude) is done by moderate-sized events given by the work peak on the graph.

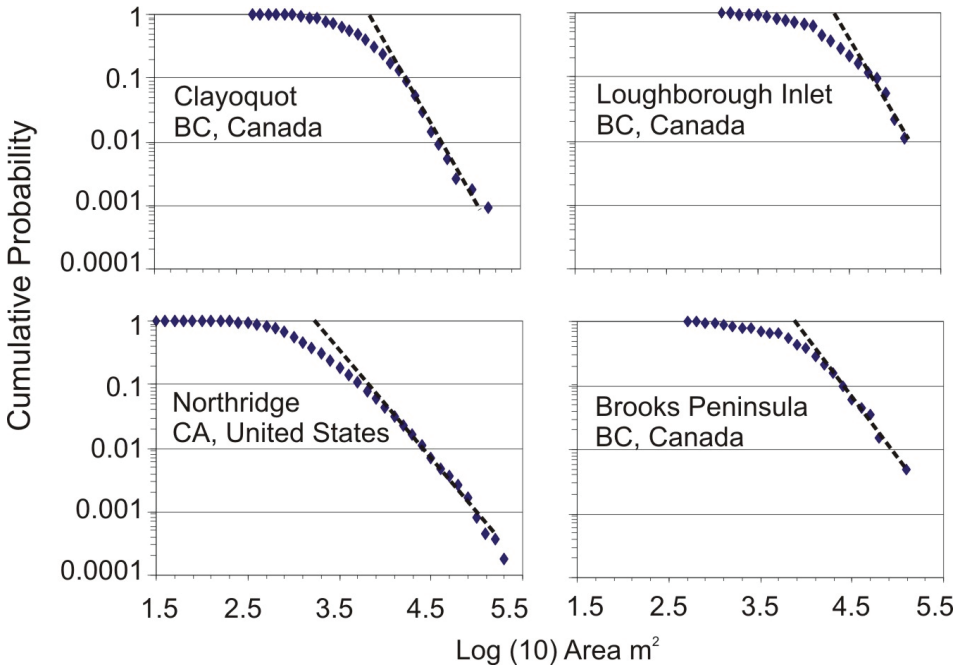

Figure 5.2. Cumulative magnitude-frequency curves for coastal BC (Guthrie and Evans, 2004a) and the Northridge earthquake in California (Harp and Jibson, 1995).

Landslide area is one measure of magnitude that can be accurately obtained from regional inventory maps (Guthrie and Evans, 2004a, 2005; Guzzetti *et al.*, 2005). Total landslide area can be shown to relate directly to both m (Guthrie and Evans, 2004a) and Δh (Caine, 1976). One can expect reasonable correspondence between variables within landslide types in similar material. For example, Guthrie and Evans (2004a) found that a linear relationship between debris slide mass and area in coastal British Columbia described about 95% of the variation. An unknown error may be introduced, however, by comparing different types of landslides. Where the difference in energy between events of various sizes is large, the magnitude of error is assumed inconsequential. Total area is henceforth used as a proxy for *work*.

There are relatively few landslide inventories available with sufficient detail to accurately examine magnitude-frequency statistics (Guzzetti, 2005). Two such landslide data sets were analyzed to examine the question of geomorphic effectiveness: (i) the Clayoquot data, which is a complete inventory of 1109 debris slides and debris flows from coastal BC covering about 50 yr of record (Guthrie and Evans, 2004a,b), and (ii) the Northridge data, which is a complete inventory of 11,036 landslides triggered by the 1994

Northridge earthquake in California (Harp and Jibson, 1995). Cumulative frequency distributions of these data sets are shown in Figure 5.2. The data were grouped into logarithmic bins, and probabilities were calculated for each bin. The probability of an event of size *x* was multiplied by the area of that same event to obtain the work done by each landslide size in the landscape. The results are given in Figures 5.3 and 5.4 to compare the probability distribution of landslide magnitudes for each of the data sets with the work done by the landslides. In both these figures, the y-axis shows the probability of a landslide of a given size class (the total probability approaches 1). Units of work are a function of the magnitude and frequency, and work on each graph is scaled back linearly to enable visual comparison to the probability of occurrence. The important component of the work portion of the figures is the magnitude for which it peaks rather than its actual metric. The intercept between the two graphs (approximately 1×10^4 m^2 in Figure 5.3 and 1×10^3 m^2 in Figure 5.4) is simply the mathematical product of the distribution. While one would expect that in general the intercept would fall near to the probability peak (as shown in Figure 5.1), it would depend to some extent on the skew or kurtosis of the data.

In both examples, the data strongly corroborate the original concept put forward for rivers in Figure 5.1 (Wolman and Miller, 1960). When each of these data sets is analyzed in aggregate, it appears that the magnitude of geomorphically effective landslides, those doing the most work, peaks slightly above that of landslides with the highest probability of occurrence.

The precise definition of "moderate" size remains thus far unresolved. The magnitudes of geomorphically effective landslides differ, for example, between coastal BC and California by 10 times. This may a response to different triggering events (precipitation versus an earthquake) or simply regional topographic variations. It is proposed, therefore, that moderate size be defined by the work peak (Figures 5.1, 5.3, 5.4). A range in magnitude of work peaks (as observed in the preceding examples) is expected based on the physiographic, climatic, and geotechnical properties of individual landscapes.

All landslides in both data sets are $< 0.5 \times 10^6 m^2$ in size. Analyzing the geomorphic impact of larger landslide events is problematic because they overwhelm the local system. Proper analysis requires a complete distribution of landslide areas leading up to and including individual large events.

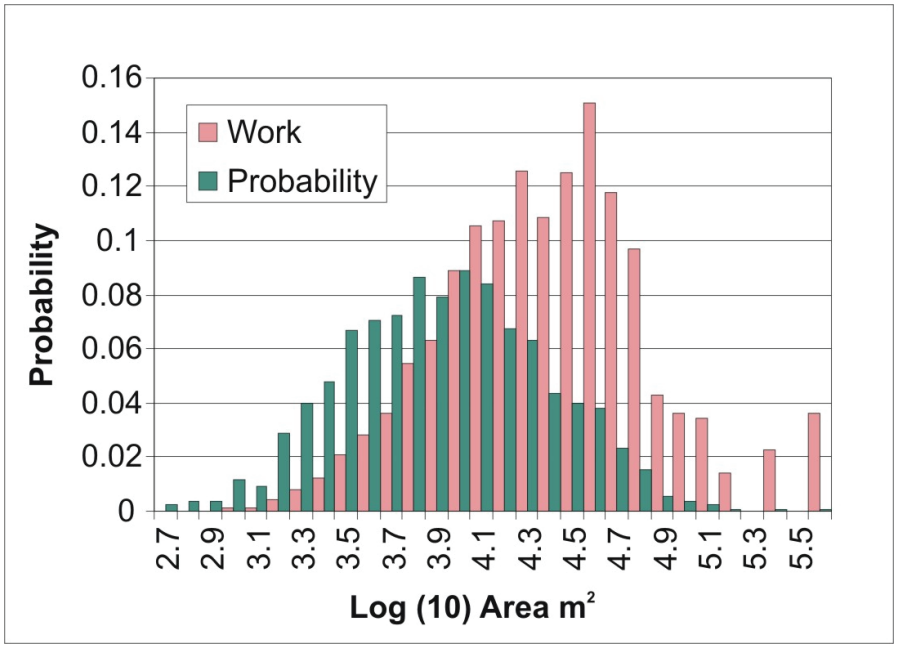

Figure 5.3. Probability distribution of landslides compared to work done by events of size *x* observed for landslides in the Clayoquot study area of coastal BC (n = 1109). Work is defined as Probability×Area and then scaled to fit the graph.

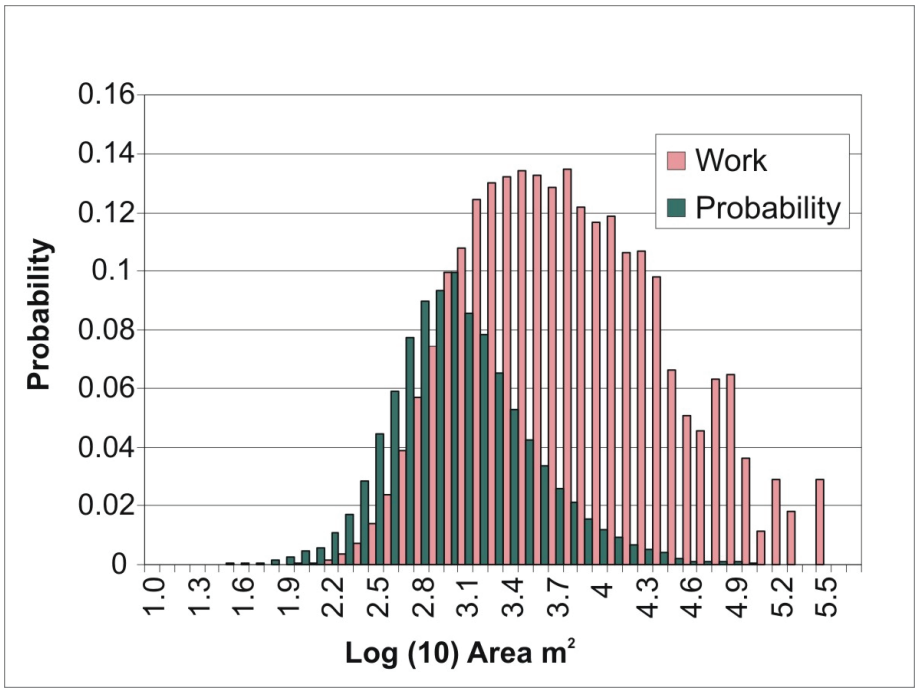

Figure 5.4. Probability distribution of landslides compared to work done by events of size *x* observed for landslides from the 1994 Northridge earthquake, California (n = 11,036). Work is defined as Probability×Area and then scaled to fit the graph.

One possible way to analyze the work done by larger landslides is to compare the global history of very large landslides (normalized to unit area) to local landslide distributions (also normalized for unit area). Evans (2006) recently compiled a detailed historical global study of massive rock failures for the period 1900–2000 (Table 5.1). Figure 5.5 shows the probability of occurrence of these very large rock failures per year per square kilometer of global mountainous terrain compared to the BC data.

Work (magnitude x frequency) is derived from Figure 5.5 and shown in Table 5.2. Landslide volume of the global dataset has been converted to area for comparison; however, the probabilities of occurrence were so low that the results are relatively insensitive to the correction. The results demonstrate that work done by the largest events worldwide is substantially less than the work done by the effective "moderate-sized" landslides over the same period. The Wolman-Miller hypothesis apparently still holds.

In view of this result, how does one now reconcile the fact that each of these massive landslides is, in its own right, a formative event?

5.5 WORK VERSUS PERSISTENCE IN THE LANDSCAPE

In 1978, Wolman and Gerson restated that *geomorphic work* is the quantity of material transported over a given distance and separately defined *formative events* as those ultimately responsible for shaping the landscape. New to the discussion was the concept of landform persistence, a measure of how long a particular landform is visible in the landscape. Wolman and Gerson (1978) argued that while any extreme event may persist longer than a moderate event, the work done by those of moderate size would ultimately return the landscape to its original form. Geomorphic effectiveness in this context would once again be dominated by events of moderate size.

For landslides, the work peak refers to a population of landslides doing the most work in a given landscape. We can reasonably project that they are also, therefore, collectively formative. However, broad experience also tells us that occasionally a single event

Table 5.2. List of the 37 largest known rock slope failures that occurred globally in the twentieth century (Evans, 2006)

Locality	Country	Estimated failure volume (x 10^6 m^3)	Year
Usoi	Tajikistan	2000	1911
Mayunmarca	Peru	1000	1974
Pufu Ravine, Luquan	China	450	1965
Yigong	China	300	2000
Vajont	Italy	292	1963
Bairaman	Papua New Guinea	180	1985
Hiedayama	Japan	150	1911
Diexi	China	150	1933
Tsao-Ling 4	Taiwan	125	1999
Zana	China	120	1943
Tsao-Ling 2	Taiwan	100	1942
Paatuut	Greenland	90	2000
Tsao-Ling 1	Taiwan	84	1941
Huascaran 2	Peru	75	1970
Khait	Tajikistan	75	1949
Tanggudong	China	68	1967
Falling Mountain	New Zealand	57	1929
Ok Tedi Mine	Papua New Guinea	50	1989
Chiu-Fen-Erh-Shan	Taiwan	50	1999
Hope	Canada	47	1965
Sale Mountain	China	45	1983
Gros Ventre	USA	40	1925
Mount Ontake	Japan	36	1984
Valtellina	Italy	35	1987
Frank	Canada	30	1903
Xintan	China	30	1985
Schwan	Alaska USA	27	1964
Fairweather	Alaska USA	26	1964
Tsao-Ling 3	Taiwan	26	1979
Ancash 2	Peru	25	1946
Allen 4	Alaska USA	23	1964
La Josefina	Ecuador	23	1993
Madison Canyon	USA	20	1959
Steller 1	Alaska USA	20	1964
Ancash	Peru	20	1946
Bualtar Glacier	Pakistan	20	1986
Costantino	Italy	20	1973

Table 5.2. A comparison of work done per unit area (km^2) of the 37 largest landslides in the twentieth century worldwide and from landslides in the Clayoquot study area in coastal British Columbia

Log (10) Magnitude (bin midpoints)[a]	Work done by 37 largest global landslides in the 20th century (per km^2)	Work done by landslides in coastal BC in the 20th century (per km^2)
2.5		0.000111
2.7		0.001060
2.9		0.004760
3.1		0.018637
3.3		0.068216
3.5		0.169418
3.7		0.310906
3.9		0.523550
4.1		0.745462
4.3		0.829847
4.5		0.958550
4.7		0.759599
4.9		0.279973
5.1		0.177491
5.3		0.070326
5.5		0.111459
6.1[b]	0.007118	
6.3	0.016922	
6.5	0.015645	
6.7	0.017711	
6.9	0.016842	
7.1	n/a	
7.3	0.014101	
7.5	0.022349	

[a] Magnitude is measured in m^2. Areas for the 37 largest global landslides in the 20th century was determined by the following formula: $30.3 \cdot V^{0.6377}$ where V is equal to landslide volume. Work is determined by multiplying magnitude by probability of occurrence (Figure 5).

[b] Landslide count is cut off at 20 Mm^3 and this bin is therefore under-represented. The real number would be higher.

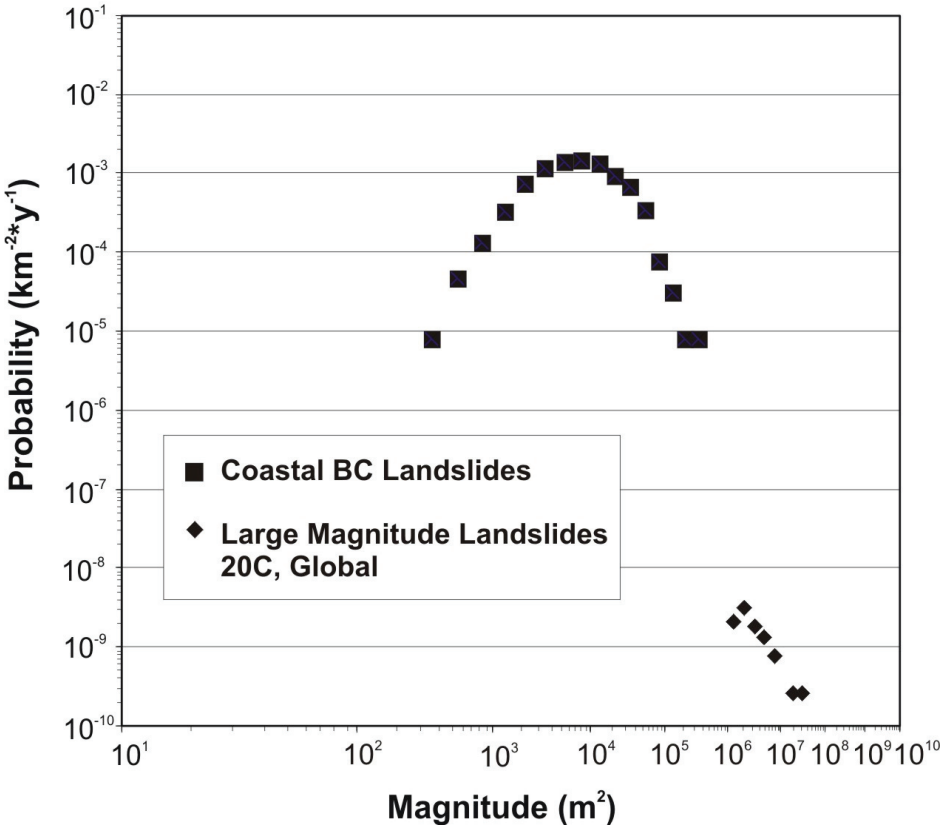

Figure 5.5. Probability magnitude distribution of landslides for coastal BC and the largest 37 landslides of the twentieth century worldwide, per year, per square kilometer of mountainous terrain. The magnitude of the global data set has been converted from cubic meters to square meters using $A = 30.3 \cdot V^{0.6377}$, where A is landslide area and V is landslide volume (Evans, 2003).

occurs that is sufficiently large as to overwhelm a geomorphic system and prevents the system from returning to its former characteristic state (Brunsden, 2001). Ultimately, this defines an extreme, often called catastrophic, event; it is catastrophic for both its rarity and its geomorphic impact.

Several authors have demonstrated examples of "large" landslides dominating the landscape. Sugai *et al.* (1994) and Sugai and Ohmori (2001) stated that small landslides dominate geomorphic effectiveness at lower elevations (<800 m a.s.l.) in Japan; however, large and rare landslides were more effective at higher altitudes (>1600 m a.s.l.). They argued that in mountainous regions or areas of significant uplift larger landslides would dominate (the Japanese Alps experience ~ 4 mm/yr of uplift). The results may be limited, however, as Sugai *et al.* (1994) only considered landslides larger than 10,000 m^2. Korup

(2005), in a New Zealand inventory of 778 landslides, determined that landslides > 1 km^2 accounted for 83% of the total landslide area. Sugai *et al.* (1994) also argued that there were significant differences in underlying geology that, in turn, affected the effective landslide size. In the Tsitika River on Vancouver Island, Guthrie (1997) documented 29 landslides from ~ 10,000–110,000 m^2 that occurred over a period of about 100 yr. Two large (0.5 x 10^6 m^2) landslides were documented in the same setting, having occurred over a period of about 600 yr. Scaled against frequency, the "moderate" events moved about four times the volume of the larger events while working on the landscape; however, the larger events fundamentally changed the local geomorphic setting and the subsequent forms will persist for years to come. One could argue that in sufficient time more frequent moderate events would prevail; however, this argument is of no practical current use. Geomorphic processes today can be shown to work on inherited landscapes (from prior formative and effective events) that may or may not be of similar magnitudes to the present condition (Brunsden, 1993, 2001; Crozier, 1999).

The question as to when an individual event may be regarded as catastrophic, exceeding the capacity of the geomorphic system within which it occurs, remains unanswered. At some point, a single event of sufficient magnitude would be resolvable above the background noise of the various processes active within a system and would persist in the landscape sufficiently long to be quantifiable as individually formative. The remainder of our discussion focuses on resolving this problem.

In order to determine when individual events became formative, a model of landslide persistence, determined using the time series landslide inventories, was constructed. Recovery was based on the number of new landslides in each time slice, the total number of landslides, and the number of landslides that were no longer visible. Larger landslides were estimated using known ages (e.g., Philip and Ritz, 1999; Wörner *et al.*, 2002) and geomorphic indicators of persistence.

The results (Figure 5.6) provide an estimation of landslide persistence over nearly six orders of magnitude. Two distinct groups are indicated: (i) debris slides and debris flows are shallow failures involving unconsolidated surficial material, and (ii) rock slides and rock avalanches are failures in bedrock. Persistence time for debris slides and debris flows is defined as:

$$P_{DS} = 2.5834A^{0.3248} \quad (8)$$

where P_{DS} is the expected persistence time of a debris slide or debris flow in years, and A is the magnitude (total area) of an event in square meters. The persistence equation for debris slides and debris flows suggests that a 1000 m^2 landslide is likely to persist in the landscape for approximately 25 yr, while a 100,000 m^2 landslide is likely to persist for approximately 100 yr. The findings are consistent with previous research on landslide recovery in British Columbia (Smith *et al.*, 1986; Jakob, 2000). Jakob (2000), for instance, estimated landslide persistence in Clayoquot of between 40 and 60 yr and used that estimate to compare natural landslides to logging-related landslides that would have occurred over a shorter period of development. If landslides between 3,000 m^2 and 20,000 m^2 (accounting for 72% of the probable size distribution) are considered, P_{DS} = 35 yr–64 yr, remarkably close to Jakob's earlier estimate.

The persistence time for rock slides and rock avalanches is greater than for debris slides and debris flows and is defined as:

$$P_{RS} = 6\times10^{-5}A^{1.2631} \quad (9)$$

where P_{RS} is the expected persistence time of a rock slide or rock avalanche in years, and A is the magnitude (total area) of an event in square meters. Note that the persistence time of rock slides and rock avalanches is estimated for events > 0.5×10^6 m^2.

Persistence, or residence time, of an extreme event can be estimated from this relationship. The Frank Slide (2.7 km^2) in Canada, for example, has a global probability of about 3.14×10^{-9}/yr/km^2 of mountainous terrain worldwide (Figure 5.5). On average, a landslide equivalent in magnitude to the Frank Slide occurs somewhere in the world every 8.6 yr. The persistence of such an event (Figure 5.6) is estimated at ~ 8000 yr.

There is global evidence that very large rock slides and rock avalanches have persisted through major erosion episodes including glaciations. North America's most recent Cordilleran glacial maximum was, for example, ~ 14,000 yr before present. The minimum required size for a rock slide or rock avalanche to persist for just 14,000 yr is

more than 4 km^2, and the probability of such a landslide occurring in any given area is very low (Figure 5.5). However, massive paleo-landslides have been identified (e.g. Philip and Ritz, 1999; Wörner *et al.*, 2002).

Beyond some threshold magnitude, the persistence of an individual event will exceed the ability of the more moderate processes active within the system to return the landscape to its former state. It will be catastrophic. The degree to which a large landslide overwhelms a system is dependent on the magnitude-frequency characteristics of the landslides associated with the work peak (Figures 5.3, 5.4) and their persistence in the same system (Figure 5.6).

A new term, the persistence ratio (P_F), is proposed to define the extent to which an event is individually formative (catastrophic):

$$P_F = P_E/P_{WP} \tag{10}$$

where P_E is the persistence of the extreme event in question and P_{WP} is the persistence of the magnitude corresponding to the work peak.

When $P_F \geq 10$, the extreme event is individually formative and can be considered catastrophic. At intermediate values of P_F between 5 and 10 the extreme event is probably individually formative. At P_F values < 5, an individual event begins to merge with the background noise of the system as it tends toward the magnitude of the work peak. It is important to recognize that the P_F ratio is a sliding scale that looks at the geomorphic conditions where a catastrophic event occurs, and the magnitude of such an event. The choice, for a catastrophic event, of an order of magnitude increase between the persistence of the extreme event and the persistence of landslides of a work peak magnitude is for convenience as much as it is based on empirical evidence. Despite that, field evidence suggests that it is a good fit with reality. In coastal British Columbia, for instance, rock avalanches of approximately 0.5 x 10^6 m^2 were recorded that, according to Figure 5.6, are expected to persist for ~ 1000 yr in the landscape. Landslide magnitudes that appear to be typical of the work peak persist ~ 80 yr. The geomorphic impact of the larger rock avalanches included the creation of lakes, the long term scarring of bedrock, and the creation of major slope features. Landslides of this size were clearly "formative";

however, a similar event of only 0.35 x 10^6 m^2, though major, was less clearly "formative" in the field. The geomorphic system was impacted, but it was easy to see how processes already at work would return the landscape to its former condition (in hundreds of years).

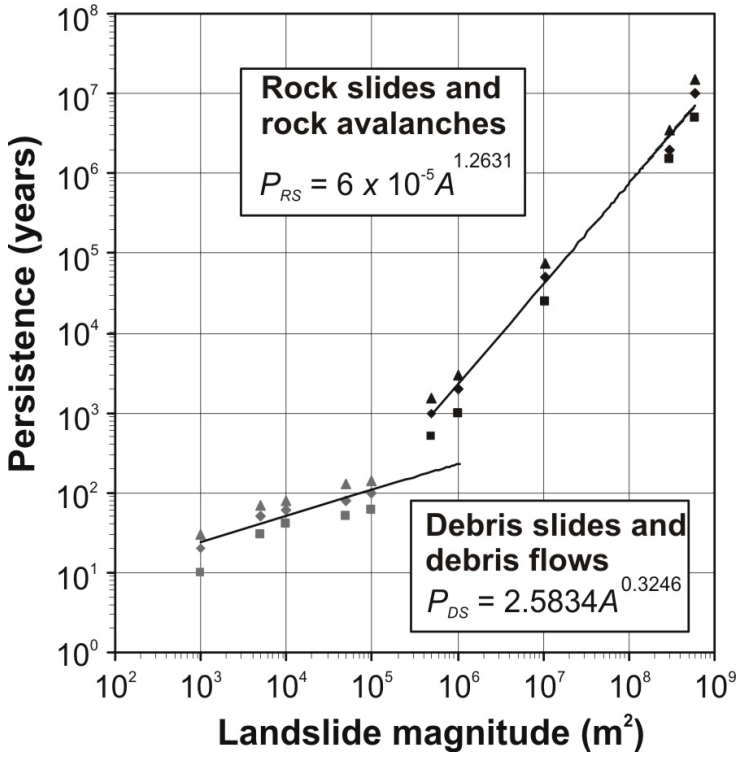

Figure 5.6. Landslide persistence for debris slides, debris flows, rock slides, and rock avalanches. The diamond symbols represent expected values; the squares and triangles represent estimated lower and upper bounds respectively (data from Guthrie, 1997, 2002, Philip and Ritz, 1999, Wörner *et al.*, 2002; Guthrie and Evans, 2004a; and unpublished inventories related to this work).

The work peak based on magnitude-frequency distributions from previous studies (Fujii, 1969; Hirano and Ohmori, 1989; Somfai *et al.*, 1994; Hovius *et al.*, 1997; Pelletier *et al.*, 1997; Hungr *et al.*, 1999; Dai and Lee, 2001; Stark and Hovius, 2001; Guzzetti *et al.*, 2002a,b, 2005; Reid and Page, 2002; Guthrie and Evans, 2004a,b, 2005; Malamud *et al.*, 2004a,b), is expected to be larger for coastal BC than most other areas around the world. The reality, therefore, is that catastrophic events that are typically recognized are likely to have $P_F >> 10$. This can be crudely estimated using Figures 5.3-5.6 for a known catastrophic landslide of interest.

5.6 CONCLUSIONS

A systematic analysis of landslide occurrence data was undertaken to determine the event magnitudes of landslides that are geomorphically effective in the landscape. Effectiveness was analyzed in terms of work (material transported a given distance), persistence (residence time), and formative events (effectiveness in shaping the landscape).

Most geomorphic work in the landscape is performed by "moderate-sized" landslide events in the manner originally conceived by Wolman and Miller (1960) for rivers. This concept holds despite difficulties comparing landslides, which are discontinuous temporally and spatially, to rivers.

A proposed work peak defines the moderate event and, therefore, the definition of moderate is located on a sliding scale with the magnitude determined largely by the physiographic, climatic, and geotechnical settings of the landscape.

Landslide persistence was estimated over nearly six orders of magnitude and is described by a power law. Persistence times are substantially different for rock slides and rock avalanches (P_{RS}) compared to debris slides and debris flows (P_{DS}).

A landslide is catastrophic when it is individually formative, that is, of sufficient magnitude to persist above the background noise of the work done by more moderate-sized events in the landscape. The degree to which an event is individually formative is given by the persistence ratio (P_F). Where $P_F \geq 10$, a catastrophic event has occurred and the geomorphic system has been overwhelmed.

Chapter 6: Extreme weather and landslide initiation in coastal British Columbia

Based on: Guthrie, R.H., Mitchell, S.J., Lanquaye-Opoku, N., and Evans, S.G. (accepted). Extreme weather and landslide initiation in coastal British Columbia. Quarterly Journal of Engineering Geology and Hydrogeology.

OVERVIEW: More frequent more intense storms predicted by climate models for the Pacific Northwest of North America could increase the regional landslide hazard. We examine the impacts of one such storm on Vancouver Island, British Columbia during which 626 mapped landslides occurred, encompassing > 5 km^2 total area and generating >1.5 $\times 10^6$ m^3 of sediment. We examined the relationship between rainfall intensity, air temperature and wind speed obtained from mesoscale numerical weather modeling with landslide incidence across steep terrain. We demonstrate a critical onset of rainfall intensity between 80 mm and 100 mm in 24 hours that results in a rapid increase in landslides with increasing precipitation. We argue that this response is more practical than a minimum threshold. We determined that wind concentrated rainfall and increased precipitation that caused landslides an average of 15.6 mm, with the greatest increases occurring above 120 mm. Approximately half the landslides studied were not related to rainfall alone, but to rain-on-snow and we argue that wind played a crucial role. This often neglected component of hydrological analysis remains a major challenge as we consider the role of snow transition zones and a warming climate in coastal mountain watersheds.

6.1 INTRODUCTION

The Intergovernmental Panel on Climate Change Fourth Assessment Report (IPCC 2007) summarized over 28 000 statistically significant data series and demonstrated that the evidence in support of climate change and global warming is overwhelming. Of 764 data series in which physical systems (hydrology, coastal processes and the cryosphere) were analyzed for a period longer than 20 years, 94% were consistent with a warming trend (IPCC 2007). In Western North America there has been considerable research on the physical aspects of climate change including, more recently, efforts to downscale or

regionalize the global climate models (e.g. Zhang *et al.* 2000; Salathé 2006; Rodenhuis *et al.* 2007; Salathé in press).

For British Columbia (BC), Canada's westernmost province with a land area of about 1×10^6 km^2, mean daily temperatures changed by about +1.2 ^{o}C over the last century, about +0.5 ^{o}C greater than the global average (Rodenhuis *et al.* 2007). Precipitation changes have been observed in BC (+22% per century on average so far) and are expected to continue since global climate models (GCMs) predict a poleward shift of storm tracks (Yin 2005; Tebaldi *et al.* 2006) and a general increase in the intensity and frequency of winter storms (Tebaldi *et al.* 2006). Regionalization and downscaling of GCMs suggest that the American Pacific Northwest is likely to get increased numbers of high-intensity winter storms (Yin 2005; Salathé 2006; Tebaldi *et al.* 2006), and local variability related to orographic and topographic effects is expected (Salathé in press). Increased temperatures in BC have favoured a decreased snowpack overall (Rodenhuis *et al.* 2007), however, warmer ambient temperatures may also make more snow available during a 'rain-on-snow' event on the coast. In these events, rain falls on ripening snow, thereby compounding the impact of a winter storm with added meltwater. When combined with model composites that show the highest precipitation levels in the Pacific Northwest will occur along the Canadian coast (Salathé 2006), it is likely that Vancouver Island and parts of coastal British Columbia will experience more intense winter storms.

In terms of landslides, the impact of high-intensity storms on the Canadian west coast is dramatic. Landslides in coastal BC are dominated by precipitation-caused shallow ($\leq$1 m) debris slides and debris flows with a mean size of about 12 000 m^2 (Guthrie 2005) and an upper size typically below 0.5×10^6 m^2 (Guthrie and Evans 2004a, 2004b; Guthrie 2005). Guthrie and Evans (2007) found that 72% of landslides in Coastal BC were between 3000 m^2 and 20 000 m^2, and the size of the geomorphologically effective landslide, the landslide size doing the most work denuding the landscape, was only 30 000 m^2. They observed that in all cases that landslides were rainfall-triggered.

That large storms frequently cause shallow landslides has been observed worldwide (Caine 1980; Page *et al.* 1999; Zhou *et al.* 2002; Crosta and Frattini 2003; 2008; Jakob and Wetherly 2003; Gabet *et al.* 2004; Guthrie and Evans 2004a, 2004b; Luino 2005; Guzzetti *et al.* 2008) and Crosta and Frattini (2008) observe that rainfall is both the most

relevant factor for triggering shallow landslides and the most frequently analyzed factor used for forecasting them. There is therefore a need for detailed spatial analysis of landslide triggering storms and their impact on the landscape. Improvements in the resolution of mesoscale numerical weather simulation models, and integration of model results with remote sensed images and other spatial layers within geographic systems enable this detailed spatial analysis.

In the winter of 2006-2007, a series of storms associated with Pacific low pressure systems crossed Vancouver Island. Vancouver Island is approximately 32 000 km^2 located off the southwest coast of British Columbia (Figure 6.1). One storm between November 14th and November 16th 2006, caused hundreds of landslides across Vancouver Island, most of which were subsequently reported to provincial government offices. Using innovative change detection analysis of remotely sensed imagery, we identified 739 landslides that occurred across the Island over that winter and herein analyze the regional characteristics of those events in the context of the storm.

6.2 STUDY AREA

Vancouver Island is comprised of 31 788 km^2 of predominantly steep rugged topography ranging from sea level to c. 2200 m. The central spine of the island is composed of the Vancouver Island Ranges: steep mountains of volcanic and sedimentary rocks intruded by granitic batholiths (Yorath and Nasmith 1995; Massey *et al.* 2003a, 2003b). The western coastline is dissected by deep fjords, and long inlets and lowlands frame the northern tip and the eastern coastline. Pleistocene glaciation severely modified the landscape, rounding and smoothing lowlands while carving steep U-shaped valleys into the fjords and mountainous regions. Broad valley floors are infilled with glaciofluvial and fluvial deposits, while tills and colluvium typically mantle slopes, extended upward until gradients are greater than about 45^o, whereupon exposed bedrock dominates.

The Island, positioned about 100 km east of the surface trace of the Cascadia subduction zone, is tectonically active (Adams 1984; Dragert 1987; Clague and James 2002) and at least two earthquakes of sufficient magnitude to cause landslides have

occurred in the last century (Mathews 1979; Rogers 1980; Keefer 1984; Cassidy *et al.* 1988). Despite the tectonic setting, precipitation, falling mainly as rain in the winter months, is the greatest trigger of landslides across Vancouver Island. Mean total annual precipitation varies longitudinally across the Island: areas beneath the eastern rain shadow receive as little as 700 mm per year, compared to > 3500 mm at sea level on the west coast (Environment Canada 1993; 2007).

Geologic, physiographic, climatic and tectonic regimes of Vancouver Island combine to produce a steep, youthful terrain that is generally prone to mass wasting. Landslide types vary, but the vast majority of landslides are debris slides and debris flows as defined by Varnes (1978). They are extremely rapid, shallow mass movements of unconsolidated material, often beginning as translational failures that break up as velocity or water content increases downslope. Debris slides and flows are almost 20 times more common than rock falls in forested areas on the Island (Guthrie 2005).

6.3 CHARACTERISTICS OF THE NOVEMBER 14-16 2006 STORM

Subtropical moisture feeds from the south Pacific arrived on the British Columbian coast at about 07:00 hours Greenwich Mean Time (GMT) on November 15th, 2006 (0:00 hours local time). This warm moist air was preceded by elevated temperatures, and produced high rainfall intensities and extreme winds that peaked over the next 12 hours. Debris flows and debris slides blocked roads, buried campgrounds, wiped out bridges, scoured and filled streams. In addition, high speeds wind blew down sections of forest, stripped trees of branches and severely disturbed transmission corridors. Total costs of the storm have not been officially calculated; however, despite a relatively low population density on Vancouver Island (c. 30 persons•km^{-2}), estimated costs were substantially in excess of one million dollars (US), largely borne by timber and utility companies.

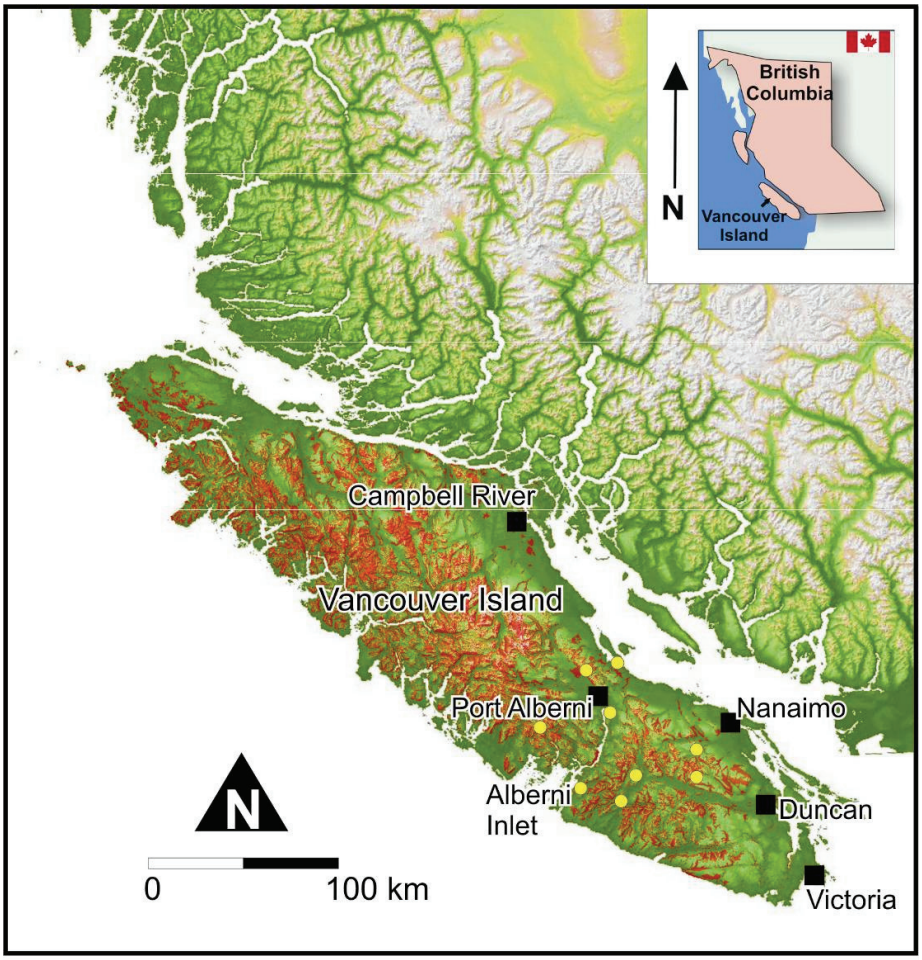

Figure 6.1. Study area showing Vancouver Island. Red shading indicates potentially unstable terrain (Guthrie 2005) and represents about 12 000 km^2. Yellow dots indicate hydrometric stations used in frequency analysis.

6.4 METHODS

6.4.1 Analyzing the storm

Miles *et al.* (2008) estimated the magnitude of the storm through conventional frequency analysis of data from hydrometric stations on southern Vancouver Island (SVI; yellow dots in Figure 6.1); however, insufficient hydrometric data precluded an accurate detailed analysis across Vancouver Island. Chang *et al.* (2008) and Chiang and Chang (2009) demonstrated that medium resolution (1km) Doppler radar rainfall estimates

performed better in the prediction of regional landslide occurrence than gauged weather stations that were infrequently distributed across the landscape. As part of an ensemble approach to weather forecasting, a research group at the University of British Columbia is running simulations using the model MM5 (Pennsylvania State University/National Center for Atmospheric Research Mesoscale Model Version 5; Dudhia, 2005) at 1.3 and 4 km grid resolutions for south western BC. Since the 1.3 km domain excludes northern Vancouver Island, hourly temperature, precipitation, wind speed and wind direction data was acquired for the full island using the MM5 weather model at a grid scale of 4 km. Wind outputs from the model are taken from the lowest model layers, and extrapolated or interpolated using surface-layer similarity theory to give the wind speed at a standard 10 m anemometer height above the local surface. These model-forecast winds are roughly equivalent to 10-min average measured winds, and there is no gust information explicitly forecast by the models. Temperature data are extrapolated to 2 m from the ground surface. Climate, terrain and landslide data was compiled in a geographic information system (GIS).

The effect of topography and the horizontal component of rainfall trajectories due to wind will change the actual impact of precipitation compared to a simple vertical model of rainfall (Sharon 1980; de Lima 1990; Pederson and Hasholt 1995; Erpul *et al.* 2002a, 2002b; Rulli *et al.* 2007; Erpul *et al.* 2008; Pike and Sobieszczyk 2008). Using the approach of Sharon (1980) and Pike and Sobieszczyk (2008), the effect of wind-driven rain (WDR) on uneven terrain was calculated using data from the MM5 weather model in the following calculation:

$$WDR_{24} = \sum P_V (1 + \tan a \tan b \cos(za - zb) \qquad (11)$$

where the index WDR_{24} is the wind-driven rain over 24 hours, P_V is the conventional vertical precipitation measured hourly, a is the terrain gradient (slope on the digital elevation model), za is the terrain aspect (from the digital elevation model), b is the angular departure of rainfall from vertical determined by wind speed experimentally by Sharon (1980), and Erpul *et al.* (2002a, 2002b; 2008) and zb is the hourly wind direction.

6.4.2 Landslide mapping and change detection analysis

Five meter resolution, colour SPOT satellite imagery was acquired and mosaiced into a single image that covered all of Vancouver Island for each of 2006 and 2007. Individual images were acquired between late May and September of each year, the season not normally associated with landslides. Change detection mapping was completed by combining the two images into a single change stack image, whereby the spectral signature of one image was identified pixel by pixel as being the same or different than the spectral signature of the other image at the same location. The change stack image created a coloured filter through which either of the original images could be subsequently viewed. Areas with no detected change appeared blue in this filter, while areas with change appeared red. There are some potential sources of error in this automated change detection, particularly in steep terrain. These include alignment errors and positional shifts, shadows and cloud cover. Therefore, the change stack image was used to guide an interpreter through a manual assessment of new (e.g. changed) terrain features on Vancouver Island. These new terrain features included recently built roads, new areas of timber harvest, wind damaged trees (windthrow) and landslides (Figure 6.2).

The November 2006 storm caused most of the reported damage on Vancouver Island. To simplify the analysis, it was assumed that all new landslides had initiated during this event. The new landslide layer was overlaid on storm data layers in the GIS to enable visual inspection. A regional map of potentially unstable terrain (Guthrie 2005) is shown in red in Figure 6.1 and was incorporated into the GIS. Data points gridded at 4 km resolution that had no overlap with unstable terrain were removed from the analysis and those that remained are described as potentially unstable. Landslide initiation points were extracted for all new landslide polygons. These data points were analyzed using Chi Square tests to compare the distribution of landslides with rainfall intensity. Separate analyses were run for Southern Vancouver Island (SVI), and Northern Vancouver Island (NVI) since landslides formed separate clusters in each of these geographic regions, and these two regions experienced different weather conditions during the November 2006 storm.

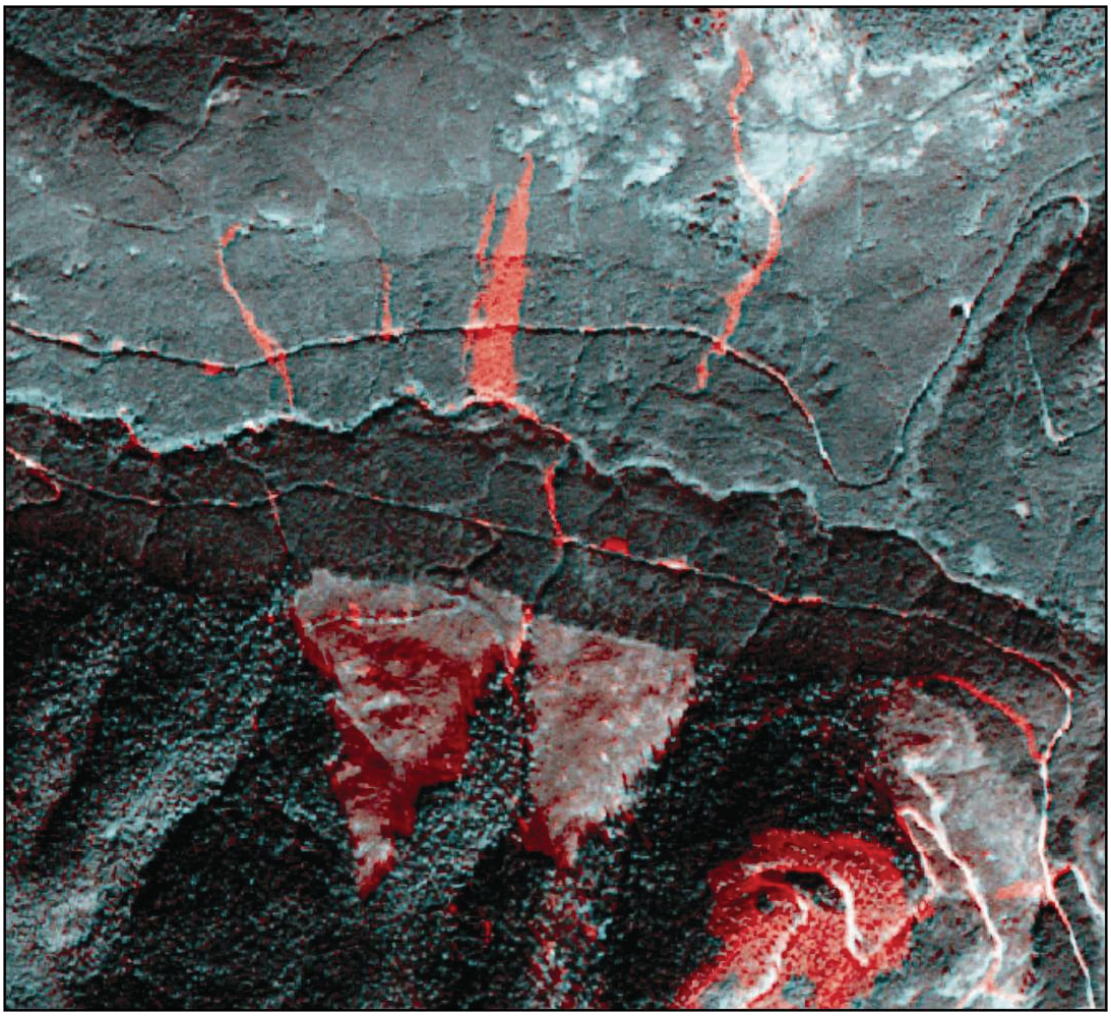

Figure 6.2. Change detection using 2005 and 2007 SPOT 5 colour images. Pixels with a change in the spectral signature between the two images are indicated by a red colour. No change is indicated by a blue colour. This red/blue layer is shown superimposed over the 2005 image. Changes can occur as a result of shadows, image shift and interference, as well as by actual events such as the landslides seen in the upper third of the image, or the cutblock in the lower right.

6.5 RESULTS AND DISCUSSION

In total, 739 landslides were recorded across Vancouver Island for the winter of 2006-2007. Of these landslides, 626 debris flows and debris slides >500 m^2 were identified and analyzed spatially. Smaller landslides were excluded from analysis to retain consistency with other coastal BC studies (see Brardinoni *et al.* 2003; Guthrie 2005; for a

discussion of this issue). Similarly, landslides that were only partially detected in the change detection (the deposition could be seen, however the event was sufficiently separated from the initiation zone by a canyon or small channel as to create uncertainty in the interpretation) were excluded unless confirmed by inspection in the field. Channelized debris flows were largely undetected in this analysis. This is typical in remotely acquired datasets (including those from air photograph interpretation) since channelized debris flows often occur within deep canyons or bedrock gullies, too narrow and hidden within terrain or tree shadows to accurately identify. Consequently, the reader is reminded that there are additional landslide impacts to those analyzed here.

Change detection for the previous two winters reveals that almost 3 times as many landslides occurred during the 2006-2007 storm season as during the preceding two years. Landslide reports from local resource managers and field checks by government officials confirm that the majority of landslides that occurred in the winter of 2006-2007 occurred during the November 15th storm. However, a small but unknown percentage of landslides will have occurred during other storms over the remainder of the 2006-2007 winter.

The landslide population had similar magnitude-frequency characteristics as observed in previous landslide inventories in coastal BC (Figure 6.3). Descriptive statistics are given in Table 6.1. The mean total area of individual landslides in the 2006-2007 inventory, 7930 m^2, is slightly smaller than previously recorded for Vancouver Island; however, within the range recorded by Guthrie and Evans (2004a) and Guthrie and Brown (2008), the landslides are representative of the size and nature of coastal BC landslides. The average landslide density for Vancouver Island over the 2006-2007 period is $0.023 \cdot km^{-2} \cdot a^{-1}$ compared with $0.008 \cdot km^{-2} \cdot a^{-1}$ the previous two years. Combined, the results indicate a landslide density of $0.013 \cdot km^{-2} \cdot a^{-1}$ between 2004 and 2007. In total > 5 km^2 of terrain was denuded by landslides over the 2006-2007 winter season. Applying the volume estimation equation of Guthrie and Evans (2004a) to each landslide and summing yields $>1.5 \times 10^6 m^3$ of sediment reworked in the landscape. Averaged over the whole island, this represents 0.05 $mm \cdot a^{-1}$ of total lowering. If one considers the denudation against the c. 12 000 km^2 of steep landslide-prone terrain, then the total lowering from that event exceeds 0.12 $mm \cdot a^{-1}$. The results are high but are

comparable to other studies for coastal BC (0.1 $mm \cdot a^{-1}$ - Martin *et al.* 2002; 0.06 $mm \cdot a^{-1}$ including flat ground in Brooks Peninsula - Guthrie and Evans 2004a; 0.07 $mm \cdot a^{-1}$ over the Holocene and 0.1 $mm \cdot a^{-1}$ over the last 100 years across Vancouver Island - Guthrie and Brown 2008) and are low when compared results focussed just around the area of impact (42 mm lowering in a 32 km^2 watershed in New Zealand – Page *et al.*, 1994; 2 mm lowering due to a storm in 370 km^2 area of coastal BC – Guthrie and Evans 2004b).

Guthrie and Brown (2008) examined denudation rates on Vancouver Island over the Holocene and determined that natural rates, based on total eroded area ranged from $0.003 \cdot km^{-2} \cdot a^{-1}$ to $0.008 \cdot km^{-2} \cdot a^{-1}$ but that rates over the last 100 years were markedly increased due to human influence to between $0.011 \cdot km^{-2} \cdot a^{-1}$ and $0.015 \cdot km^{-2} \cdot a^{-1}$. Guthrie and Brown (2008) stated that the impact of logging outpaced the impact of climate change and proposed that improved logging practices could offset potential increase caused by climate change. However, climate change is superimposed on an altered landscape that is more sensitive than it was previously. An increase in the number of high-intensity storms without an improvement in practices could substantially increase the long-term impact to the system.

Spatially, landslides were clustered in two general locations on the Island (Figure 6.4). Two major clusters on either side of the Alberni Inlet totalling 197 separate events dominate activity on southern Vancouver Island (SVI). Northern Vancouver Island (NVI) is dominated by two higher density landslide clusters, peaking at 0.34 $landslides \cdot km^{-2}$, compared with a maximum of 0.17 $landslides \cdot km^{-2}$ for SVI (using a 12 km radius kernel) and totalling 187 landslides. The remainder (242 landslides) are spread across the island, sometimes forming smaller clusters of their own. Both pairs of high density landslide clusters represent a focus of meteorological activity on steep unstable terrain. Other influences such as geology, logging and road building, and surficial materials, for example, will almost certainly affect the occurrence of individual landslides; however, none of the clusters are in and of themselves unique from adjacent terrain. Landslide clusters associated with storm activity have been identified in previous studies (Zhou *et al.* 2002; Guthrie and Evans 2004a, 2004b).

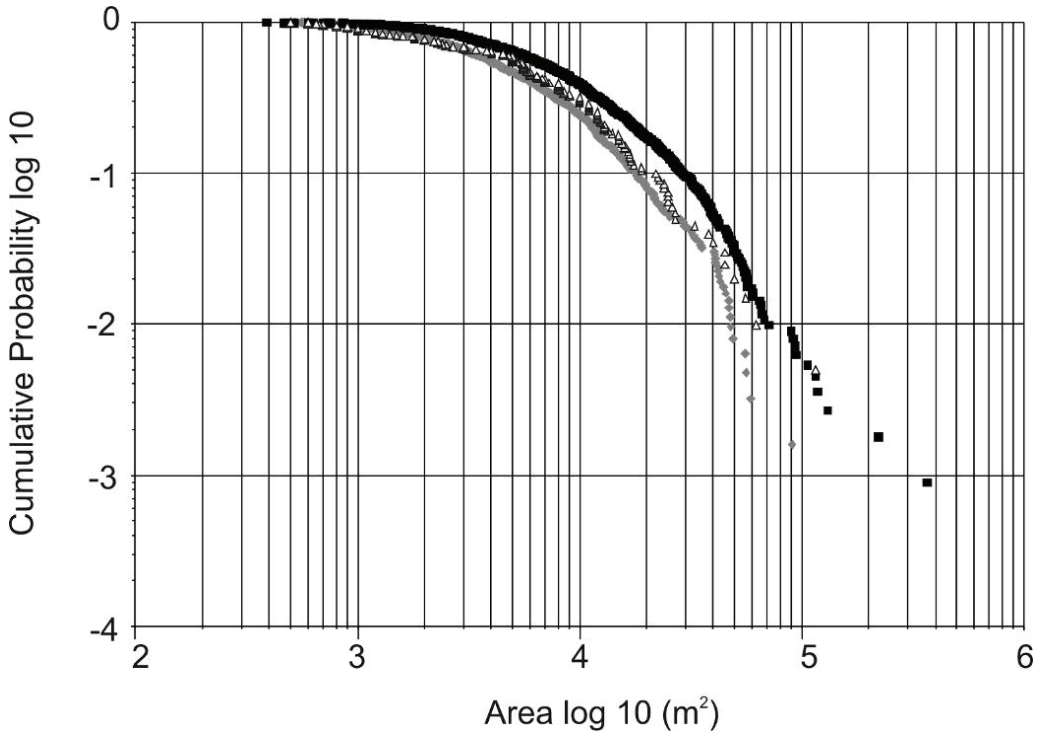

Figure 6.3. Magnitude-frequency characteristics of landslides in this study (open triangles) compared to previous studies (black squares = Clayoquot Sound and grey diamonds = Brooks Peninsula; see Guthrie and Evans 2004a for details) reveal that the size distribution is typical of landslides on Vancouver Island.

Table 6.1. Descriptive statistics of the 2006-2007 landslide inventory. Elevation is in meters above sea level. The winter rain-on-snow zone is typically considered to be 300-800 m, below 300 m is considered rain dominated throughout the year, and above 800 m is considered snow dominated in the winter months. The majority of landslides were identified as occurring during the November 15th storm.

Number	626	Year	Winter 2006/2007
Mean size	7930 m^2	Mean elevation	609 m
Standard deviation	9773 m^2	Standard deviation	271 m
Minimum size	500 m^2	Minimum elevation	19 m
Maximum size	90 476 m^2	Maximum elevation	1636 m

Landslides were relatively infrequent over the central portion of Vancouver Island. Two reasons are proposed. First, within the central portion of Vancouver Island lie the highest mountains. Though steep and geomorphologically active, they contain relatively large areas of exposed bedrock that consequently lack the material necessary for shallow,

precipitation-triggered landslides. Second, the entire central portion of the island also represents British Columbia's oldest provincial park, Strathcona Park, established in 1911 and encompassing more than 2500 km^2 of land (Figure 6.4). The park boundary cuts arbitrarily across topographic and geologic units, but marks the boundary between landscapes with and without logging and the landslide clusters begin immediately at the boundary edge. Previous work on Vancouver Island has indicated that logging increases landslide frequencies by at least an order of magnitude (Jakob 2000; Guthrie 2002; 2005) and the results of this study are consistent with that finding.

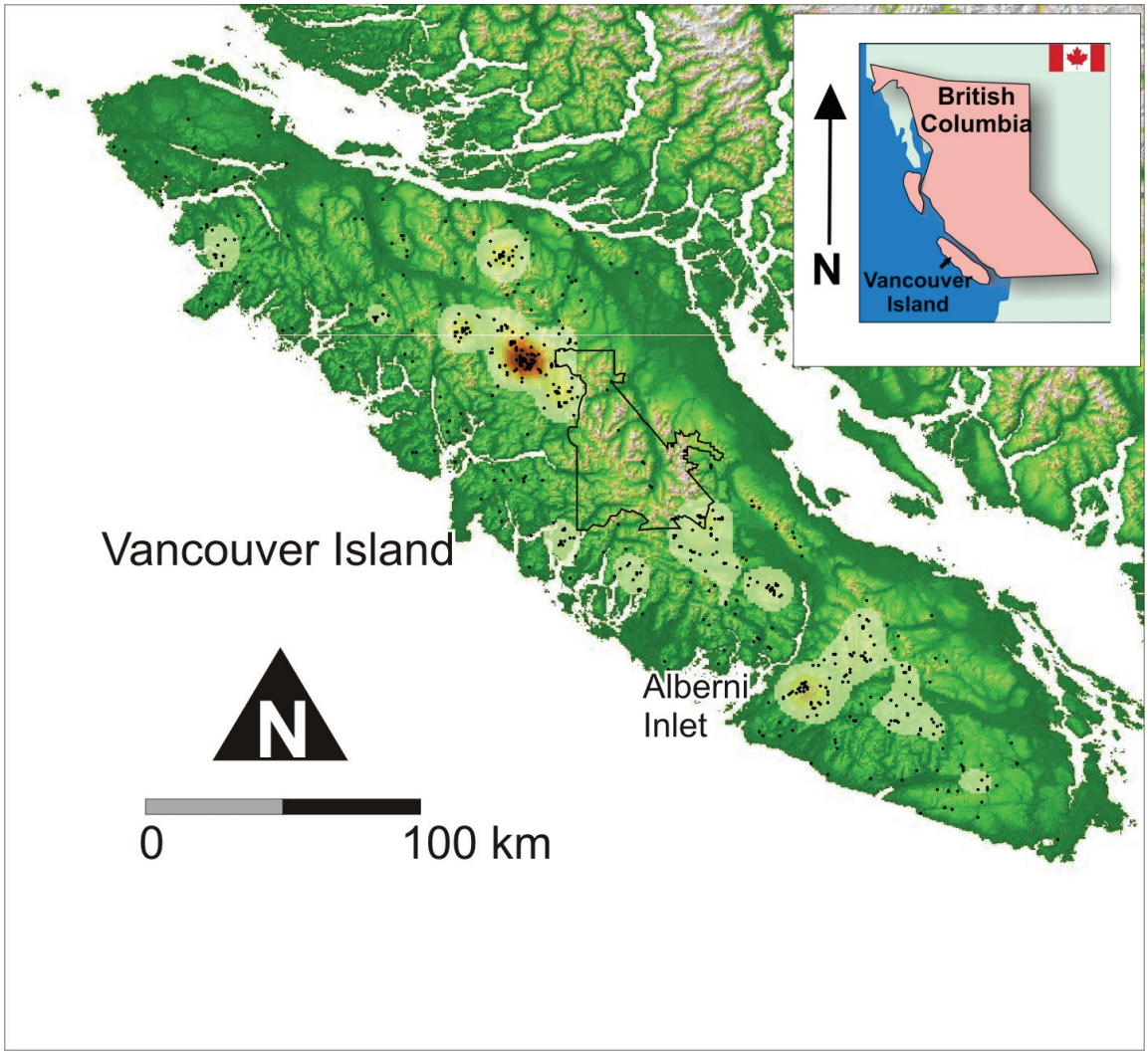

Figure 6.4. Landslide density plots using a 12 km moving kernel. Four major clusters are evident, two on either side of the Alberni Inlet on southern Vancouver Island, and two on northern Vancouver Island. Strathcona Park is outlined in the center of the Island and represents a 2500 km^2 piece of land that has been exempt from large-scale human disturbance.

6.5.1 November 15 2006

Subtropical moisture feeds from the south Pacific arrived on the British Columbian coast at about 07:00 hours Greenwich Mean Time (GMT) on November 15th, 2006 (0:00 hours local time). This warm moist air was preceded by increased temperatures on November 14th across the northern two thirds of the island. Temperatures on the southern third of the island increased on November 15th (Figure 6.5B and 6.5C). Average temperatures rose several degrees across the entire island (Figure 6.5A and 6.5D), shifting from near freezing to several degrees above freezing at sea level to mid-elevations, and from below to above freezing at higher elevations. The system also brought intense rains (Figure 6.6) and extreme winds (Figure 6.7). Each of these factors contributed to the occurrence of landslides.

6.5.2 The impact of intense rainfall

The highest intensity rainfall fell on southern Vancouver Island. Using visual estimation we separated southern Vancouver Island from the remainder and analyzed the 268 landslides that fell within this zone separately (Figure 6.8). We compared the pattern of landslides to rainfall intensity in all potentially unstable cells (Figure 6.1) for both SVI and NVI. Using rainfall intensity classes of < 60 mm, 60-80 mm, 80-100mm, 100-120 mm, 120-140 mm and >140mm, Chi Square (χ^2) analysis determined that the likelihood of the landslide pattern being achieved in SVI by chance alone was less than 0.001 (χ^2 = 41.3, χ^2 crit.= 20.5 for a significance level of 0.001, with 5 degrees of freedom). In the same analysis for NVI, in contrast, the χ^2 value did not exceed the critical value at a significance level of 0.01 (χ^2 = 12.9, χ^2 crit. = 15.1 for a significance level of 0.01 with 5 degrees freedom). On SVI, landslides associated with precipitation > 100 mm occurred

more frequently than expected in the χ^2 test, and landslides associated with precipitation < 80 mm occurred much less frequently than expected by chance alone.

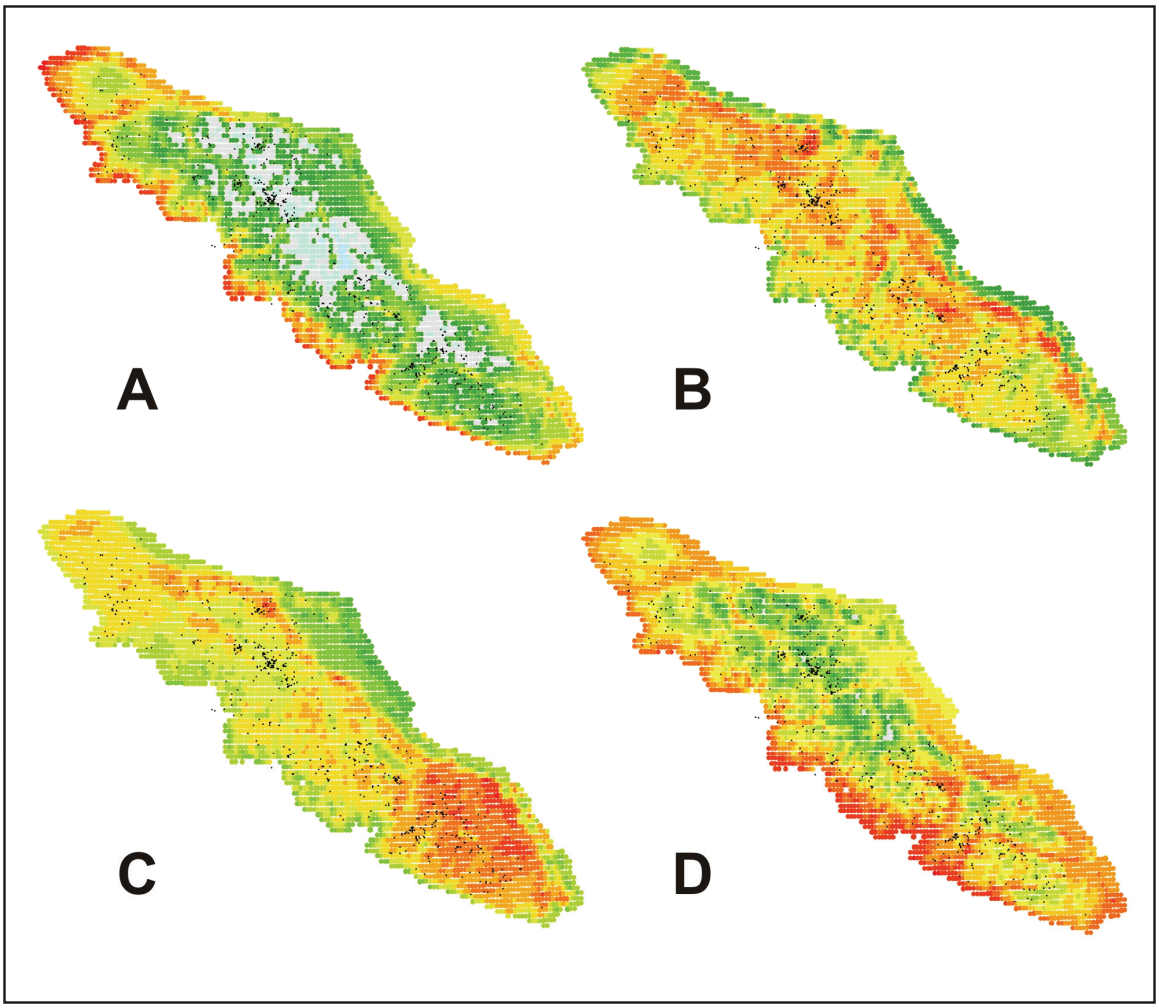

Figure 6.5. Surface temperature plots for Vancouver Island from the MM5 numerical weather prediction model. A: Average temperature for November 14th. Grey to blue indicates temperatures < 0 in 2°C increments, green to red indicates temperatures >0 in 1°C increments. B and C: Temperature increases on November 14th and 15th respectively. Colours grade from green to red (1°C – 10°C) in 1°C increments. D: Average temperature for November 15th, as in B, with red >10°C. In all plots, black dots represent landslide locations.

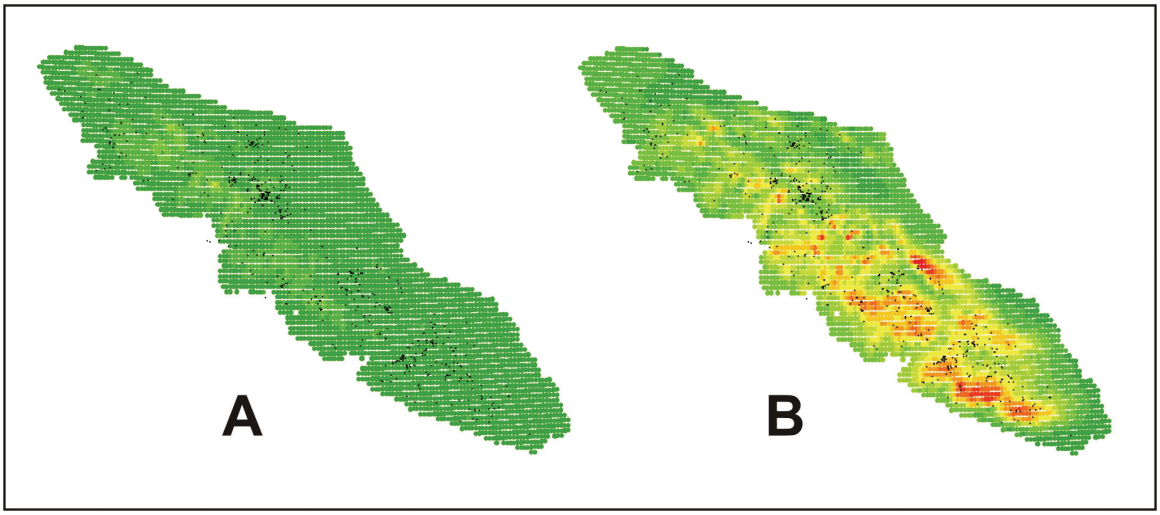

Figure 6.6. Surface rainfall plots for Vancouver Island from the MM5 numerical weather prediction model. A: Precipitation November 14th, B: Precipitation November 15th; dark green = <20mm of rain, and increases to >200 mm (red) in 20 mm increments.

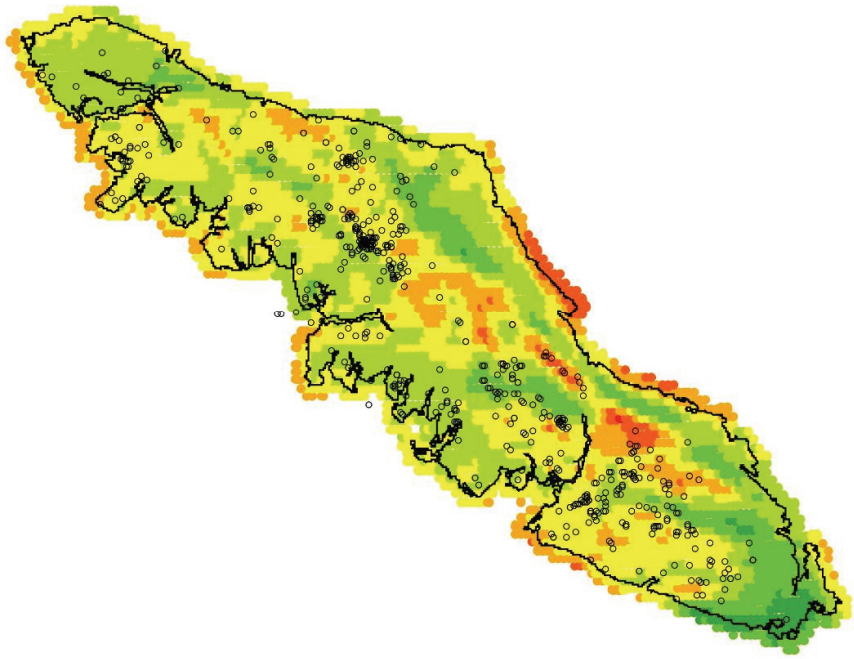

Figure 6.7. Average wind speed between 0700 and 1900 hours GMT (midnight to noon local) on November 15th, 2006. Values increase from dark green through yellow to red in 10 $m \cdot s^{-1}$ increments. Black circles represent landslide locations.

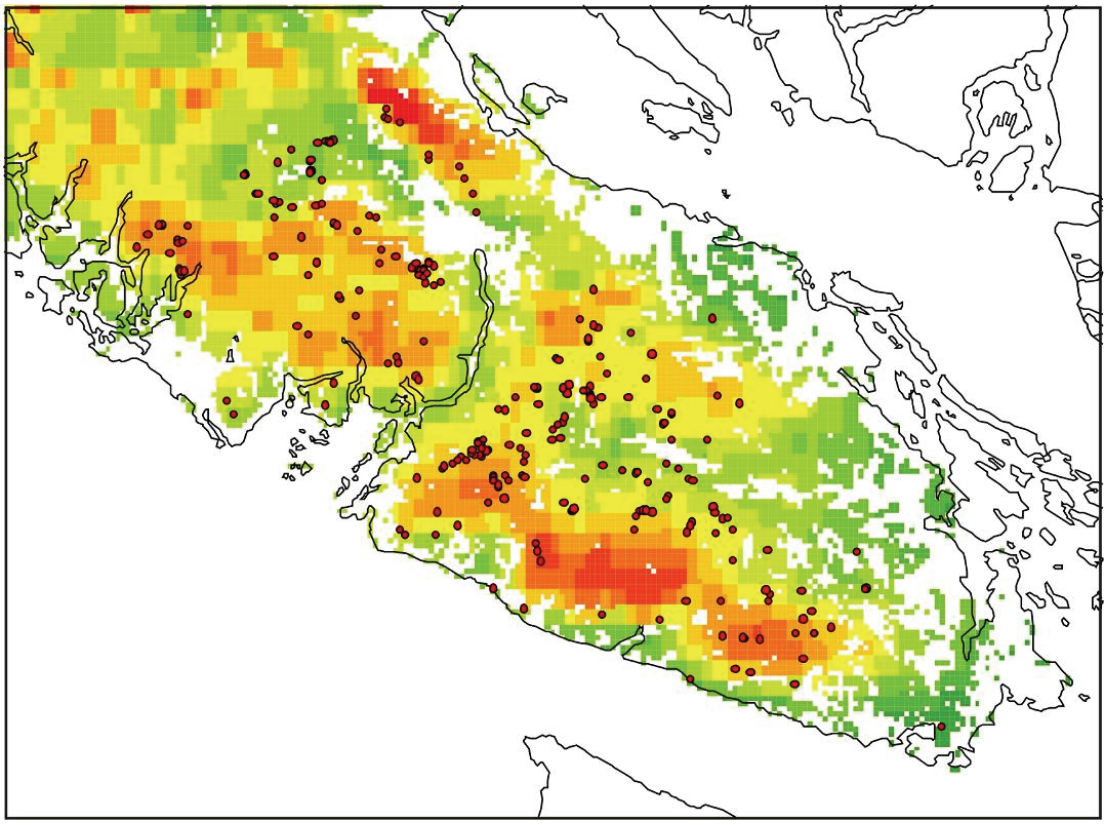

Figure 6.8. November 15th 2006 map of cumulative 24 hour rainfall over areas of potentially unstable terrain. Precipitation grades from green to red in 20 mm increments with red representing anything greater than 200 mm. Dark red dots represent landslides.

Guzzetti *et al.* (2008) reviewed minimum precipitation thresholds for shallow landslides and debris flows worldwide, and observed that landslides occurred associated with precipitation levels approaching $1mm \cdot hour^{-1}$ over 24 hours. Several reasons could account for the appearance of landslides initiating at low minimum thresholds in a database, thereby complicating their usefulness. These include localization effects such as high-intensity storm cells within regional events (Zhou *et al.* 2002; Guthrie and Evans 2004a, 2004b), antecedent conditions (Jacob and Weatherly 2003; Aleotti 2004), orographic precipitation and topography including upslope drainage area (Montgomery and Dietrich 1994; Salathé in press). Further, using rainfall estimates obtained from hydrometric station data can be problematic. There are a limited number of these stations and conditions local to the hydrometric station may be substantially different than those where the landslide occurs. In addition, missing records are a common feature in hydrometric datasets. For wet climates such as coastal British Columbia, using very low

minimum precipitation thresholds such as those given by Guzzetti *et al.* (2008) is impractical for hazard preparation and land management. The west coast of Vancouver Island, for example, receives measurable precipitation more than 200 days a year on average.

Establishing a local threshold that reflects the precipitation intensity at which landslides occur is an important component of hazard management. New tools such as medium-scale radar imaging of actual precipitation and high-resolution numerically modelled weather forecasts are now routinely available and offer sufficient detail for producing probabilistic estimates of precipitation linked to landslide occurrence (Chiang and Chang 2009). While generalization errors are expected to remain (spatial resolution currently varies between 1 and 4 km depending on location) the data are typically continuous both spatially and temporally.

Applying MM5 forecast 24 hour precipitation for our southern Vancouver Island study area, we obtained the following results: Landslides are observed at low levels of rainfall, however, the cumulative landslide probability curve becomes dramatically steeper between 80 and 100 mm of precipitation. Of 268 landslides measured, 88% were associated with > 80 mm of rain (Figure 6.9), and 70% were associated with precipitation > 100 mm. The sudden steepening of the curve in Figure 6.9 can be interpreted as representing a critical range or onset of landslide-generating precipitation intensity. This critical onset indicates a landscape response to rainfall, and is therefore expected to differ between physiographic regions. Conceptually it differs from a minimum threshold in that it separates the manageable hazard from the residual. To this end, numerical weather prediction models not only enable a probabilistic assessment of landslide occurrence against rainfall intensity, but they may be used to predict the timing and spatial pattern of landslides as weather fronts cross a region.

Since numerical weather predictions also contain wind direction and speed data, it is possible to evaluate the role of this factor, both direct and indirect, in landslide initiation.

Direct impacts from high wind speeds associated with the storm (Figure 6.7) were observed in the field, including trees blown down in the initiation zone. Windthrow has been identified as a contributing factor in landslides in the Pacific Northwest (Johnson *et al.* 2000), and numerically forecast wind speeds are useful in predicting windthrow

occurrence at the landscape scale (Mitchell *et al.* 2008). However, our initial inspection of large scale mapping of areas windthrown during the winter 2006 storms did not reveal any systematic association with landslide occurrence within the study area.

Indirectly, in areas with complex terrain, high winds may concentrate precipitation onto portions of the landscape (Figures 6.9 and 6.10). We calculated an index of wind-driven rain (WDR_{24}) and compared the distribution of landslides to this index of rain intensity in all potentially unstable cells (from Figure 6.1). Once again, χ^2 analysis of SVI revealed that the likelihood of the distribution being achieved by chance alone was less than 0.001 ($\chi^2 = 25.9$, χ^2 crit.= 20.52 for a significance level of 0.001 with 5 degrees of freedom) and again, for NVI, the relationship did not hold ($\chi^2 = 4.9$, χ^2 crit.= 15.1 for a significance level of 0.01 with 5 degrees of freedom).

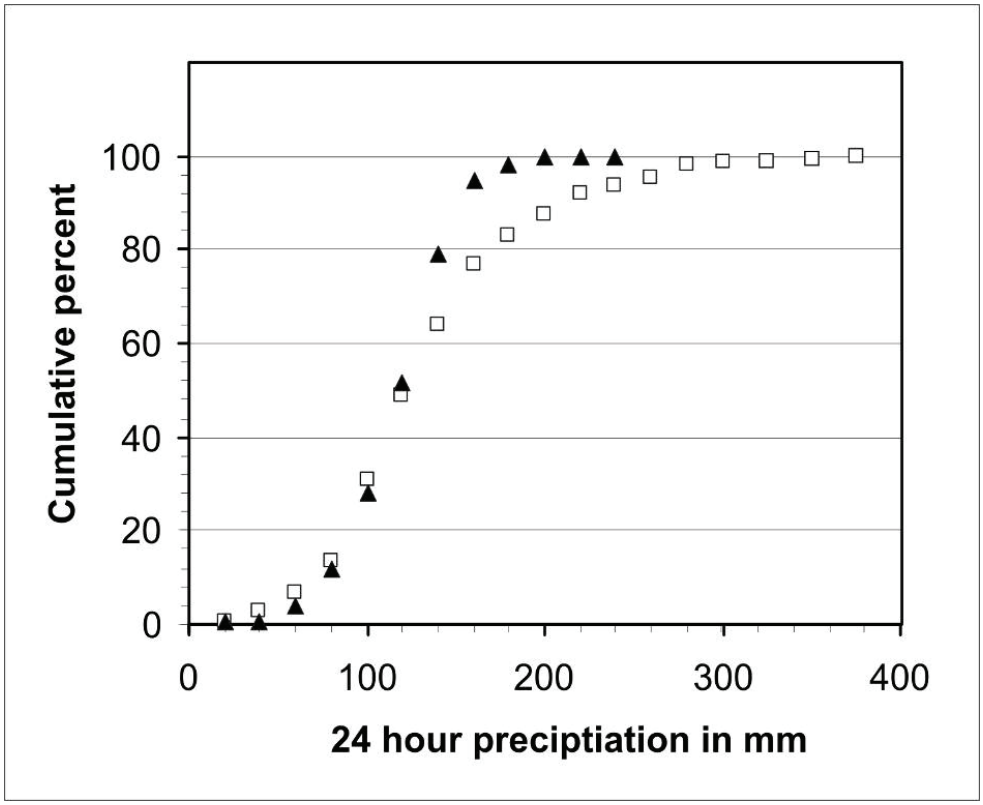

Figure 6.9. Cumulative percent distribution of landslides versus 24 hour rainfall amounts for 268 landslides on southern Vancouver Island. Black triangles represent the distribution using the precipitation model alone; the open squares represent the distribution using the wind-driven rain index. Note the steep increase in cumulative percent of landslides over the precipitation range between 80 and 140 mm.

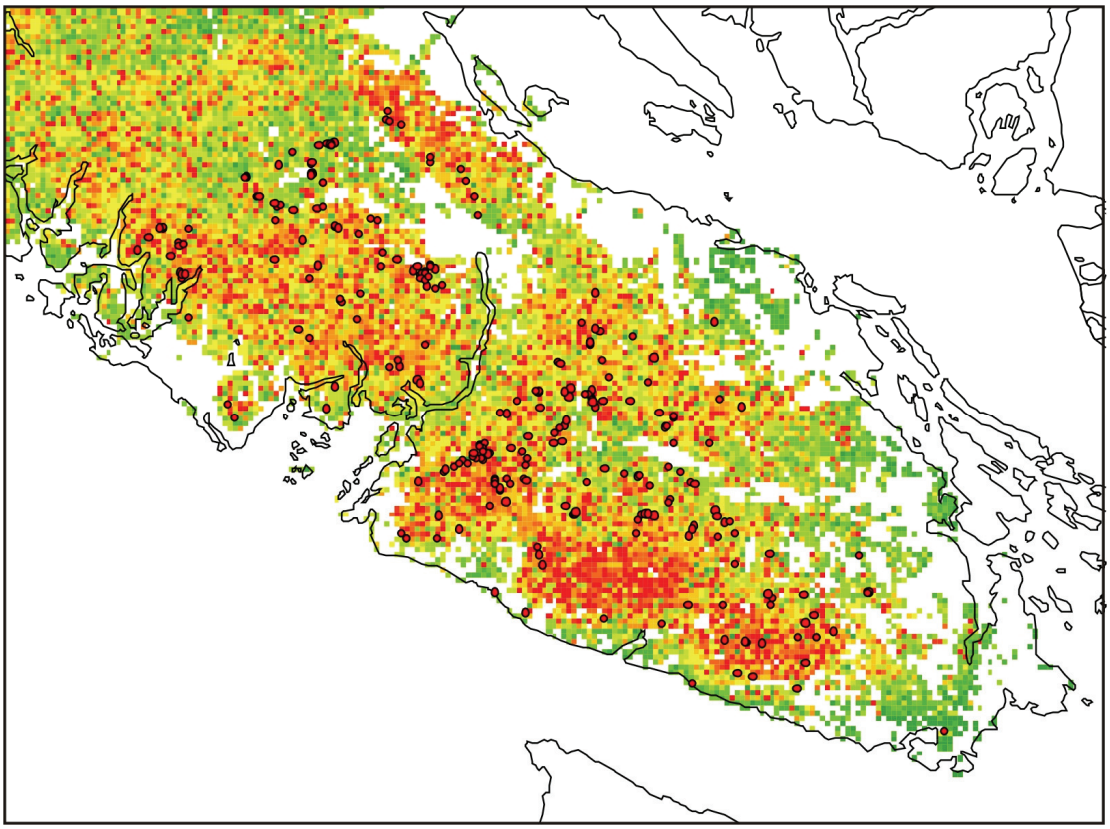

Figure 6.10. November 15th 2006 map of cumulative 24 hour wind-driven rain over areas of potentially unstable terrain. Precipitation grades from green to red in 20 mm increments with red representing anything greater than 200 mm. Dark red dots represent landslides.

Despite a visually similar pattern of rain intensity on the landscape, results of the wind-driven rain analysis over SVI showed markedly concentrated local rainfall, increasing rain in some instances as much as 282 mm, and decreasing others by up to 187 mm. The highest WDR_{24} value on SVI increased to almost 500 mm in 24 hours and the highest value associated with a landslide was 383 mm. This compares to 224 mm in both cases for non-wind-driven rainfall intensity. This analysis of the effect of wind-driven rain while no doubt simplified indicates just how complex and important local effects may be. Interpreted as a measure of actual local rainfall intensity, the WDR_{24} results suggest an increase in the threshold level of rainfall intensity for slope failure of 15.6 mm (Figure 6.9). Almost 40% of landslides occur with >140 mm in 24 hours, and 23% with

>160 mm over the same period. This compares with 21% and 5% respectively for landslides analyzed without considering wind.

Against a backdrop of climate change, return intervals of high-intensity storms are important. Traditional return period analysis for rainfall intensity was conducted for the hydrometric stations indicated as yellow dots on Figure 6.1 by Miles *et al.* (2008). Miles *et al.* (2008) considered both precipitation gauges and instantaneous stream flow records and determined that the return period of the November 2006 storm approached 20 years. Importantly they also found that return periods were grossly overestimated by using traditionally available but outdated data such as the rainfall frequency atlas for Canada (Hogg and Carr 1985) or older intensity-duration-frequency curves (publicly available to 1998). Return intervals are not static, and coastal North America is currently experiencing an overall increase in temperature and precipitation (Rodenhuis *et al.* 2007), and is expected to encounter increased intensity and frequency of winter storms (Yin 2005; Tebaldi *et al.* 2006). As a result, large storms such as the November 15th event will likely recur more frequently than recorded history would lead one to believe.

6.5.3 The impact of rain-on-snow

In addition to wind and rainfall measures, the numerical weather forecasts contain temperature data, and can provide some insights into the location of the freezing level. The role of rain-on-snow events has taken on almost mythical proportions in coastal British Columbia, and anecdotal evidence relating melting snow to landslide occurrence is common. There are, however, few systematic studies that document or analyze this phenomenon. The notable exception was by Harr (1981) almost 30 years ago in western Oregon. Harr (1981) documented peak flows related to rain-on-snow events and for rain alone over 24 years in the H.J. Andrews experimental forest. He demonstrated that the rain-on-snow events produced greater average discharges and more rapid responses within the watershed. He further identified that 85% of all slope failures over the study period were related to snowmelt during rainfall.

It is evident that precipitation leading up to or during the storm is insufficient to fully explain the clusters of landslides that occurred on November 15th 2006 on NVI (Figures

6.4, 6.6A and 6.6B). Similarly, while wind-driven rain calculated for the northern island does result in local concentrations of precipitation, something else is still required to explain the landslide distribution.

Anecdotal evidence from forestry staff corroborated by recorded observations report that there was approximately 0.5 m of new snow over much of the landscape at higher elevations on NVI, and that temperature warmed several degrees beginning on November 14th through November 15th. Field reconnaissance of landslide sites by forest industry professionals immediately after the storm suggested that areas that had snow melt were the hardest hit.

Numerical weather forecast, ground surface temperatures on NVI increased by up to 10 degrees over the period of the storm (Figures 6.5B and 6.5C) bringing average daily temperatures from slightly below zero on November 14th (Figure 6.5A) to slightly above on November 15th (Figure 6.5D). Despite a relatively ripe snow pack, the temperature increase combined with rain was probably insufficient to melt snow in sufficient quantities to create the landslide clusters observed. Recent research by the BC Ministry of Forests on Vancouver Island (Floyd unpublished), however, demonstrates that the contribution of wind to melting snow is significant. Figure 6.11 shows the effect of wind on melting snow during moderately high rainfalls (100 mm /24 hours) on a ripe snow pack under cloud cover; conditions similar to what were likely present on NVI. Wind substantially increases the rate of melt under such conditions particularly in exposed areas (clear cuts for example), and melt is highly dependent on wind speed. Wind speeds were particularly high and sustained during the storm, and over the landslide clusters on NVI average speeds were maintained in excess of 25 $m \cdot s^{-1}$ for over 12 hours (Figure 6.7).

This record represents substantial circumstantial evidence of a significant rain-on-snow event, and a subsequent record of landslides. A warming climate may prolong the shoulder seasons and increase the likelihood of rain-on-snow events when snow is easily melted. Historically, rain-on-snow has been largely overlooked in favour of rainfall analysis for landslide prediction (Crosta and Frattini 2003). Rainfall thresholds are inadequate to predict the impact on the ground from such changes, and more research into the role of snow melt is necessary to develop accurate hazard prediction and warning systems. Similarly, wind played a significant role in all aspects of the storm, and should

be routinely incorporated into landslide hazard models. With the new high resolution spatial datasets and geographic information systems this incorporation is relatively straight-forward.

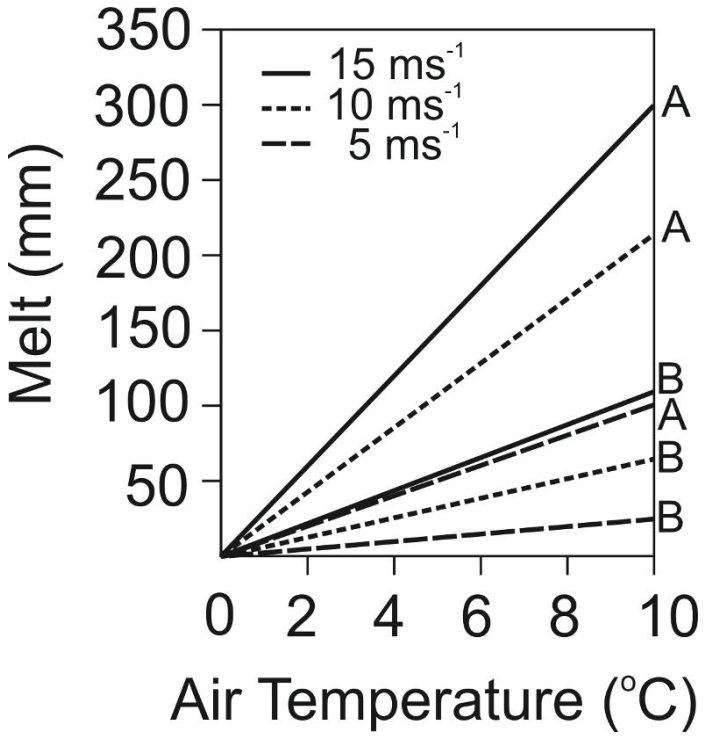

Figure 6.11. The role of wind in melting snow (adapted from Floyd, unpublished data; assumes 100 mm of rain, 101.3 kPa, 100% humidity and cloud cover). A represents wind over open ground, and B represents wind over a closed forest canopy.

6.6 CONCLUSIONS

Spatial analysis of landslide triggering storms is necessary to understand their regional impact and to provide adaptive solutions to expected changes from global warming scenarios. Shallow landslides in British Columbia and the Pacific Northwest, as in many areas worldwide, are intimately related to climate and weather patterns. Precipitation is the most commonly analyzed variable for landslide forecasts. BC has already experienced an average increase in precipitation of +22% this century and GCMs predict a general increase in the intensity and frequency of winter storms. It follows that a

changing climate portends a shift in landslide frequency and subsequent impact to the landscape.

The storm of November 14-15 2006 had an estimated return period of 20 years, and in combination with other less intense storms over the winter of 2006-2007 produced 626 landslides across Vancouver Island. Precipitation, temperature, and wind speed results from hourly numerical weather forecasts with the MM5 model at a resolution of 4 km were used to examine the association of storm characteristics with the spatial pattern of landslides. High-intensity rainfall is associated with the majority of landslides in southern Vancouver Island. Rather than using a minimum threshold for predicting landslide initiation, we recommend that the critical range of landslide-causing precipitation is readily discernable from the plot of cumulative probability of landslides against precipitation intensity. Using this function also enables a probabilistic assessment of landslide activity with storm intensity. This represents a new holistic approach to the analysis of landslide-inducing rainfall focussing on the evolution of a storm, made possible by modern technology.

Wind-driven rain concentrates precipitation in the landscape and is possible to model in the GIS environment using precipitation, wind (speed and direction) and terrain (aspect) variables. Taken as a measure of actual precipitation on the ground, it appears that landslide-causing precipitation is 15.6 mm greater than indicated by non-wind-driven estimates of cumulative precipitation.

Rapid snow melt caused by a combination of ambient temperature, rainfall and wind speed may also have been a contributing factor during the November 14-15 storm event. Rain-on-snow events have long been recognized as important to landslide generation, however, little research in this area has been completed since it was introduced almost 30 years ago. Research detailing the role of snow, air temperature, rain and wind in the rain-on-snow regime remains one of the great challenges if we are to understand the impact that a warming climate will have landslides in coastal mountain watersheds.

Chapter 7: Denudation and landslides in coastal mountain watersheds: 10,000 years of erosion

Based on: Guthrie, R.H. and Brown, K.J., 2008. Denudation and landslides in coastal mountain watersheds: 10,000 years of erosion. Geographica Helvetica, 1/2008, 26-35.

OVERVIEW: A conceptual model of landslide-induced denudation for coastal mountain watersheds spanning 10,000 years of environmental change is presented. The model uses a constructed paleo-climate based on vegetation records and an established relationship between the landslide frequencies and precipitation. Landslide frequencies are determined for the early warm-dry Holocene, the warm wet middle Holocene, and modern climates. Average landslide rates vary between 0.005 landslides$\cdot y^{-1}\cdot km^{-2}$ and 0.008 landslides$\cdot y^{-1}\cdot km^{-2}$. Recent human impacts are calculated by recalculating landslide frequencies for logged areas in the 20th century. The impact of logging during the last 100 years is unambiguous as landslide frequency increased to 0.015 landslides$\cdot y^{-1}\cdot km^{-2}$ suggesting that the impact of logging outpaces that of climatic change. We estimate that debris slides and flows eroded an average of 0.7m$\cdot m^{-2}$ across Vancouver Island during the last 10,000 years.

7.1 INTRODUCTION

Landslides are primary denuders of the landscape since they directly transport sediment from upslope sources to both stream networks and lower more stable positions. Precipitation and earthquake-triggered landslides in coastal British Columbia, Canada, annually erode the surrounding landscape concurrent with other dynamic modes of erosion such as stream incision and runoff. Here, we present a conceptual model of landslide-induced denudation for coastal mountain watersheds spanning 10,000 years of environmental change. Given that climate has varied substantially during the Holocene from warm-dry to cool-wet, the model fosters important insight into the interaction between climate and landslide-induced denudation. Further, the model considers recent and deleterious anthropogenic activity, mainly logging, and provides a framework by which human-induced denudation rates can be contrasted to those of the Holocene.

7.1.1 Setting

Vancouver Island is located off the southwest coast of British Columbia, Canada (Figure 7.1). The island is comprised of 31,788 km^2 of highly variable terrain, with the interior of the island containing the steep and rugged volcanic and intrusive Vancouver Island Ranges (Yorath and Nasmith 1995, Massey *et al.* 2003a, 2003b). The largest mountain peaks attain elevations of ~2,200 m. Average annual precipitation varies longitudinally across the island, with eastern rain shadow areas receiving as little as 700 mm of annual rainfall compared to >3,500 mm of rainfall on the oceanic west coast (Environment Canada 1993, 2007). The moist and mild climate supports widespread temperate rainforest in the lowlands. At high elevation, cooler temperatures coincide with alpine forest and tundra.

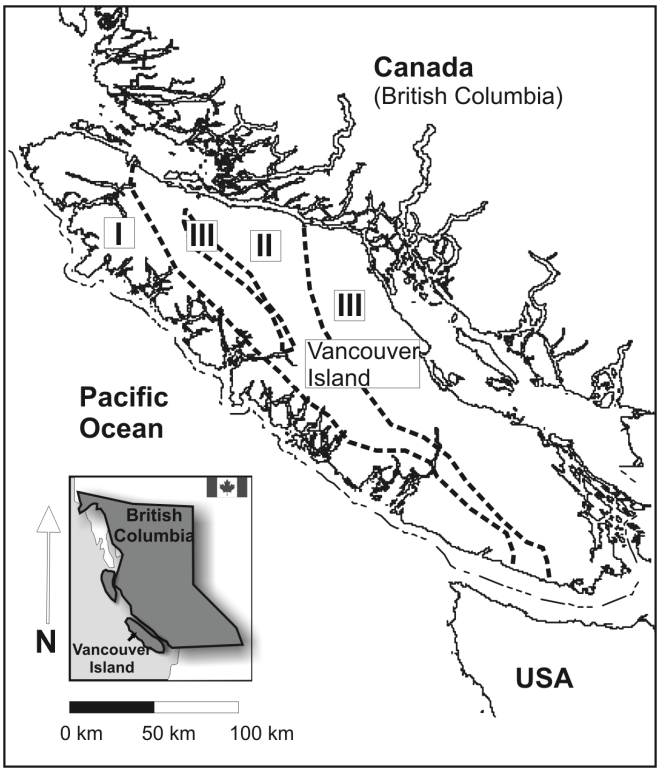

Figure 7.1. Vancouver Island in the southwest corner of British Columbia. The island is divided into three zones related to mass movement potential, discussed in detail in the text.

The aforementioned geologic, physiographic, climatic and tectonic regimes of Vancouver Island have combined to produce a steep, youthful terrain that is generally prone to mass wasting. Landslide types typical to Vancouver Island include slides, slumps, flows, falls and topples in debris and rock according to the Varnes (1978) classification. Debris slides and flows (Figure 7.2A) are most common and almost 20 times more frequent than rock falls in the forested areas (Guthrie 2005). Debris slides and flows are defined as extremely rapid, shallow mass movements of unconsolidated material that usually begin as translational failures. These movements typically break up as velocity or water content increases, ultimately forming an avalanche (dry) or flow (wet). Herein, the term 'landslide' refers to events of this category. Channelized debris flows (CDFs) occur when a debris flow enters a confined channel. CDFs usually travel considerable distances and are common in coastal British Columbia (Figure 7.2B). It is likely that CDFs are under-represented in air photograph interpretations as smaller events of this type tend to have a short persistence time in the landscape. There is not always a clear and objective distinction between channelized and unchannellized events and they are undifferentiated in the following discussions. Finally, rock falls constitute an extremely rapid displacement of rock from a steep surface, usually characterized by some component of falling through the air, bouncing and rolling of material. Rock falls often break up on impact and continue down slope with fluid behaviour, typically referred to as an avalanche or *sturzstrom*. Rock falls range in size from small ($<1m^3$) to large ($>1Mm^3$), with the largest rock fall avalanches initiating in the alpine zone (Guthrie 2005).

Glaciers retreated rapidly at the end of the Pleistocene on Vancouver Island, with most upland areas free of ice by 13,000 radiocarbon years before present (^{14}C y BP, Alley and Chatwin 1979). At this time, the combination of isostatic uplift, exposed bedrock, unconsolidated surface sediments and relatively sparse vegetation allude to a landscape that was likely similar to the present day alpine zone in terms of landslide potential. Guthrie (2005) indicates that the modern alpine zone produces approximately 4 times as many landslides as the wet west coast of Vancouver Island, including a larger number of rock falls and avalanches. Large events such as rock fall-avalanches were likely more

common around 13,000 ^{14}C y BP as the newly debuttressed landscape sought to establish equilibrium.

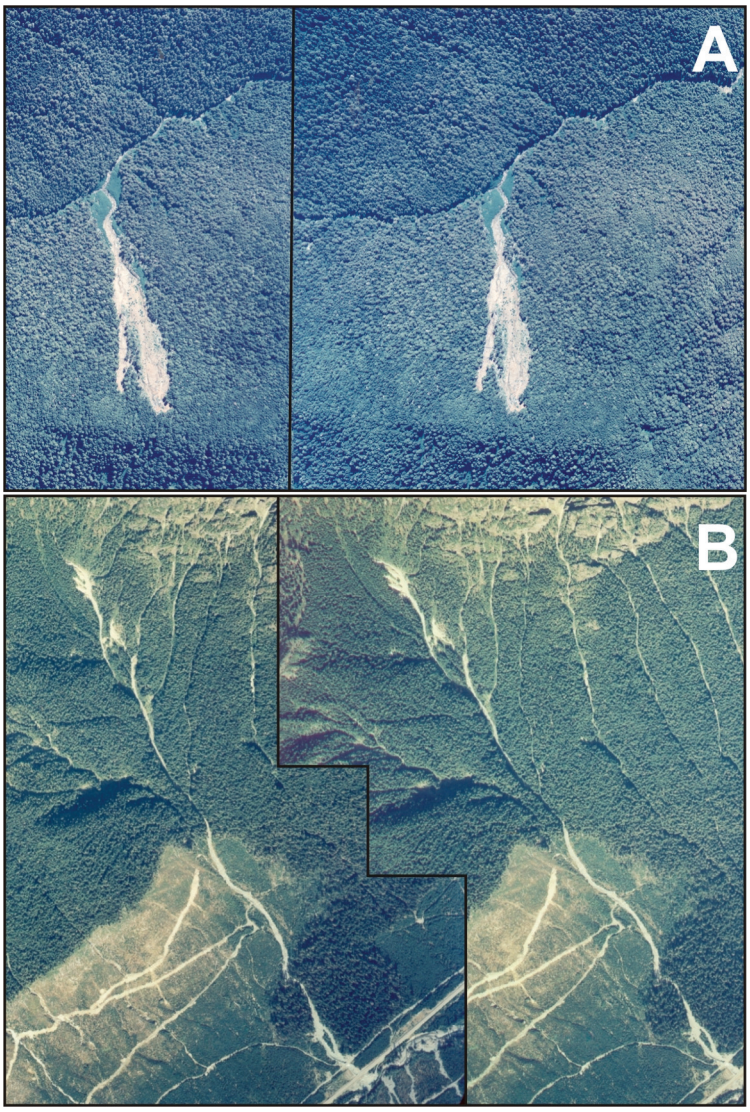

Figure 7.2. Stereo air photograph of typical precipitation caused debris slide (A) and channelized debris flow (B) from Vancouver Island, British Columbia Canada.

Overwhelming evidence reveals that Vancouver Island was ice free, vegetated and dry by 11,700 calendar years before present (y BP), following a rapid rise in temperature (Alley and Chatwin 1979, Carlson 1979, Hebda 1983, Brown *et al.* 2006, Hay *et al.* 2007). Following the warm-dry xerothermic interval (11,700-7,000 y BP), an increase in precipitation coincides with the start of the more moist mesothermic interval (7,000–

4,000 y BP. At this time, western hemlock (*Tsuga heterophylla*) expanded on the island and the vegetated landscape began to resemble that of today. During the last several millennia, precipitation has remained relatively stable. Consequently, it is possible to surmise that the type and form of landslides throughout the Holocene were similar to those of present-day, namely precipitation induced debris slides and debris flows (Figures 7.2A and 7.2B) with rock falls playing a less significant role. It is also conceivable that large rock fall-avalanches were relatively inconsequential in the geomorphological development of the post-glacial landscape as they occurred too infrequently below 800 m (Guthrie and Evans 2007).

7.2 METHODS

7.2.1 Determining Holocene Landslide Rates

Previously, a landslide potential map of Vancouver Island divided the island into four major categories based predominantly on the slope and climatic regime (Table 7.1, Guthrie 2005, Guthrie and Evans 2005). The four categories are described as follows:

Zone I – The wet west coast, characterized by steep fjords, densely vegetated terrain and high precipitation falling as rain in winter months (>2600 $mm \cdot y^{-1}$). Landslides are typically debris slides and flows.

Zone II – The moderately wet central island, characterized by steep terrain, densely vegetated with exposed small outcrops, precipitation between 1600-2600 $mm \cdot y^{-1}$ falling mostly in winter months. Landslides are typically debris slides and flows with minor numbers of rock falls.

Zone III – The moderately dry east coast, characterized by more exposed bedrock and lower rainfall (<1600 $mm \cdot y^{-1}$), increased urbanization and rural development and shallower slope gradients. One quarter of all landslides identified were rock falls.

Zone IV – The alpine zone, characterized by high elevation steep cliffs and plateaus, exposed bedrock, ponded water, steep gorges and sparse vegetation, with most of the precipitation falling as snow in the winter months. Landslides commonly include rock falls, rock avalanches, debris slides and debris flows and regularly result in the accumulation of coalescing talus slopes. Snow avalanches are similarly common and often related to land instability.

Consistent differentiation of landslides in the alpine zone is problematic due to their relatively high frequency and overlapping distribution. Through time, however, the frequency of landslides in the alpine zone is likely to fluctuate in response to changing biogeoclimatic conditions. For example, during the Little Ice Age a drop in temperature of about 1^{o} C caused alpine glaciers on Vancouver Island to advance several hundred meters in mountain valleys (Smith and Laroque 1996, Lewis and Smith 2004). Fewer landslides are expected when slope walls are buttressed by ice, even if there is an increase in glacial erosion, whereas during and after glacial retreat the number of landslides is likely to increase as over-steepened, eroded and weathered slopes become exposed. Ultimately, however, the variability in climate-related landslide potential is expected to be minor in the alpine zone compared to the overall high incidence of landslides that characterize this steep and sparsely vegetated zone.

In contrast to the alpine zone, the three non-alpine landslide zones I-III (Figure 7.1), appear to be highly sensitive to changes in climate, particularly precipitation (Guthrie 2005). A record of Holocene climate for Vancouver Island has been established using vegetation records and climate transfer functions (Figure 7.3, Alley and Chatwin 1979, Carlson 1979, Hebda and Rouse 1979, Hebda 1983, Brown and Hebda 2002a, Brown *et al.* 2006, Hay *et al.* 2007). Brown *et al.* (2006) used a vegetative index that compared the proportional distribution of coastal Douglas fir and coastal western hemlock to quantify temporal changes in Holocene precipitation for the southern part of Vancouver Island. The results yielded precipitation isopleths in 1000-year intervals for the Holocene and showed that overall, temporal changes in precipitation were generally subtle, though a notable increase in precipitation is observed at the end of the Holocene dry period.

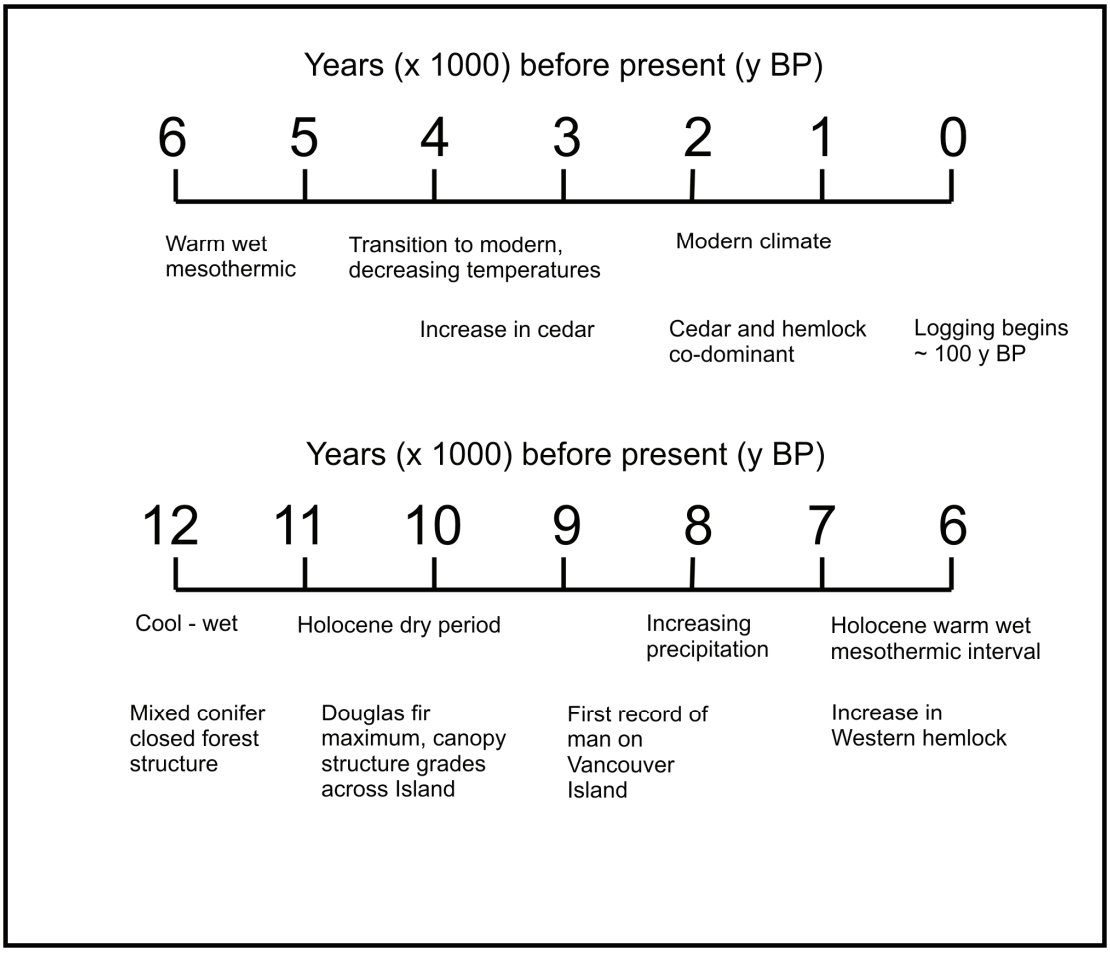

Figure 7.3. A calendar year schematic of vegetation and climate development on Vancouver Island during the Holocene (Alley and Chatwin 1979, Carlson 1979, Hebda and Rouse 1979, Hebda 1983, Brown and Hebda 2002a, Brown *et al.* 2006, Hay *et al.* 2007).

In the development of a conceptual mass wasting model, we incorporated the strong direct linkage between the incidence of landslides and precipitation (Guthrie 2005). Present-day precipitation isopleths were overlain on the mass wasting zones of Guthrie (2005), revealing that the precipitation isopleths are in broad agreement with the mass wasting map (Figure 7.4). Subsequently, each 1000 year interval was assigned an ordinal category of either drier than present, modern, or wetter than present based on the variability of precipitation compared to present-day. The mass wasting potential maps for the wet and dry climatic intervals (Figure 7.5) were established by shifting zones I – III in proportion to the modelled climatic changes, calibrated against the modern analog and taking into account elevation effects. Landslide frequencies were then estimated

using the established rates for each zone (Table 7.1). As previously discussed, the alpine zone was excluded from the analysis. In addition, a physiographic region of low relief and low gradients on the east side of Vancouver Island, the Nanaimo Lowlands, was also excluded since it generally does not contain unstable terrain.

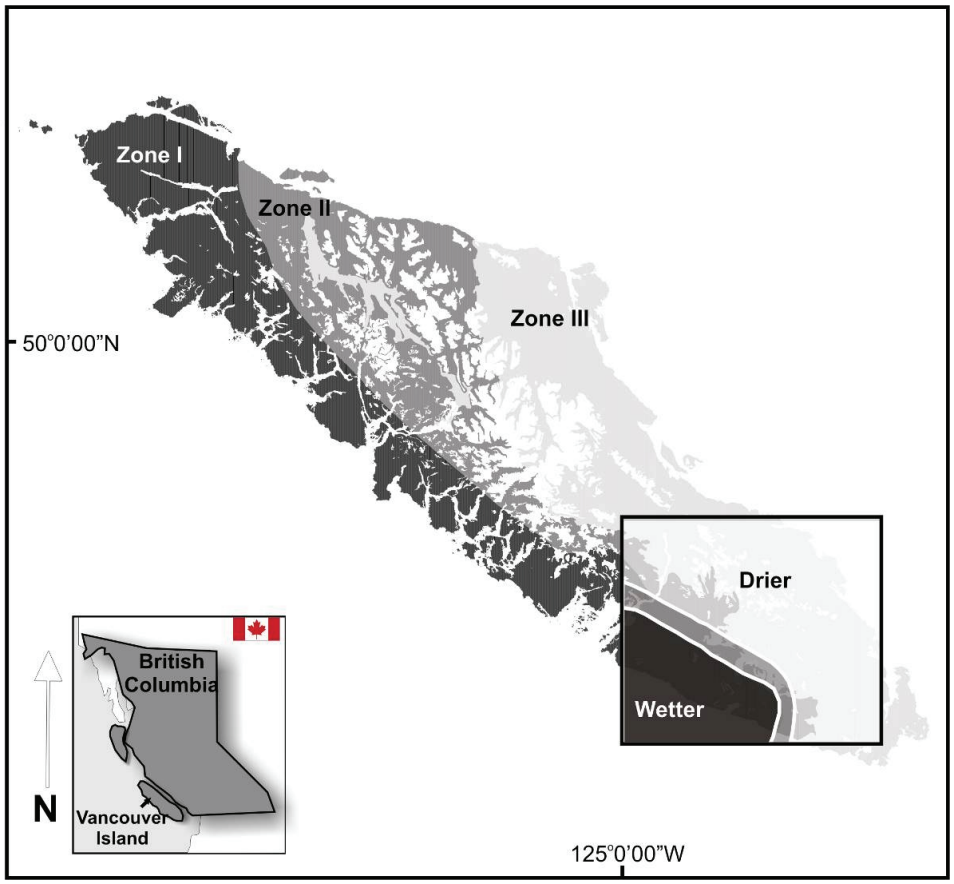

Figure 7.4. Comparison of present-day precipitation isopleths (Brown *et al.* 2006) and mass wasting potential (Guthrie 2005), revealing broad agreement. Zones I – III refer to the mass wasting potential zones discussed in the text.

Table 7.1. Natural landslide frequency tables for zones I-III. Note that the frequency relates to a long term average, the actual failures are typically clustered in both time and space (Guthrie and Evans, 2004a, b).

Zone	Natural landslide frequency ($\#\cdot km^{-2}\cdot y^{-1}$)	Area required for 1 landslide per year (km^2)
I	0.012	83
II	0.007	143
III	0.004	250

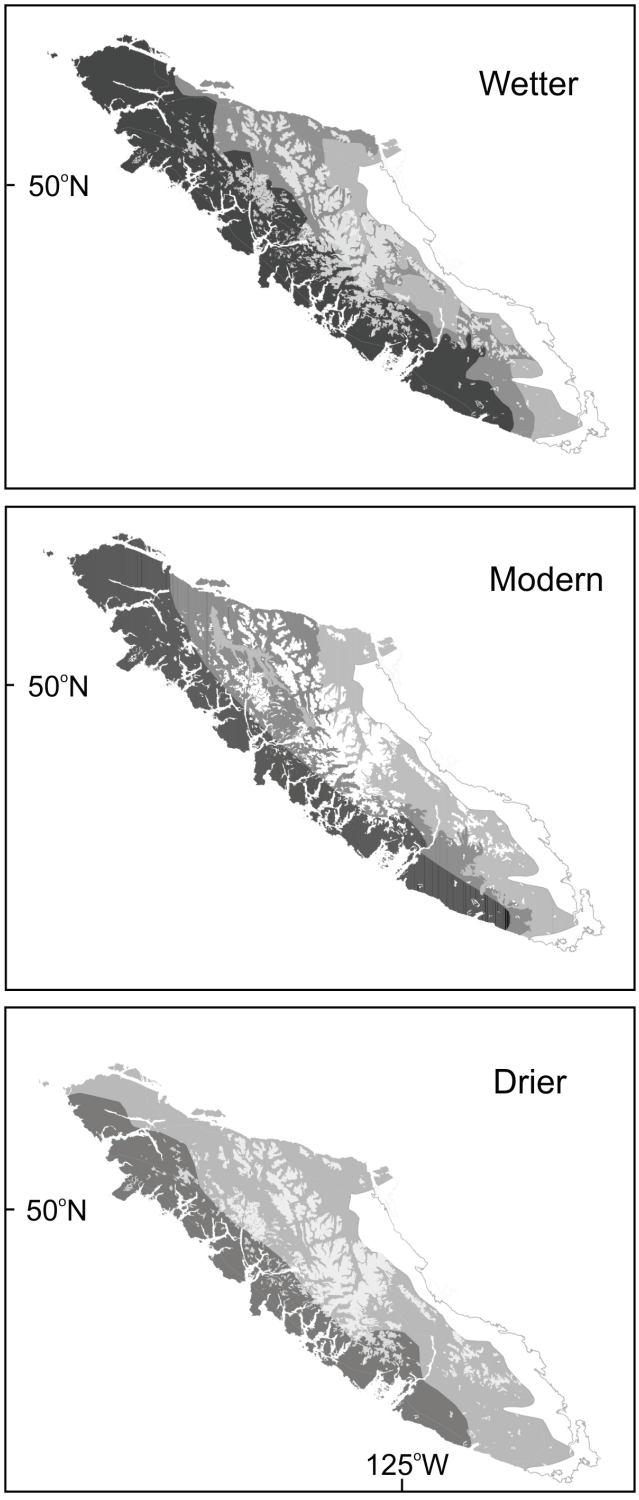

Figure 7.5. Mass movement potential zones for different climatic regimes including a wetter regime present in the middle Holocene, a modern climate, and a drier climate present in the early Holocene. Darkest grey indicates zone I, zone II is the medium grey and the light grey is zone III. Removed from landslide calculations are the alpine zone (white) and the flat Nanaimo lowlands (white).

7.2.2 Determining 20th Century Landslide Rates

Recent logging and road building have significantly altered landslide frequencies in coastal British Columbia, with reported increases ranging between 3-34 times the modern natural rates (Schwab 1983, Rood 1984, Jakob 2000, Guthrie 2002, Jordan 2003, Chatwin 2005, Guthrie 2005). In addition to directly removing forest cover and changing the hydrologic regime, secondary forest harvest activities such as road building can also intercept, concentrate and reroute water to new locations on the hill slope. Guthrie (2005) suggests that an order of magnitude increase in landslide frequencies reasonably reflects the impact of logging.

Widespread commercial logging began on Vancouver Island at the onset of the 20th century and continues today. The rate of logging was established using forest cover maps during two 50-year periods. To determine a landslide frequency that accounts for logging, the natural landslide rates were calculated to incorporate the accumulated area logged renewed each year. Harvested cut-blocks were given a hydrologic recovery time of 25 years, representing the time required for a new forest to establish and exceed 10 m in height. Recovery was limited to 90% of the harvest to account for residual hazards. The total harvested area was subtracted from the unlogged area for each year in each zone, and the frequencies calculated by increasing the numbers of landslides in the area harvested by an order of magnitude (Guthrie 2005). Landscape recovery was simultaneously calculated. Once again, the Alpine zone and the Nanaimo Lowlands were excluded from all calculations.

7.3 RESULTS AND DISCUSSION

7.3.1 10,000 years of Denudation

A conceptual model of primary denudation for Vancouver Island over the last 10,000 years is realized by compiling the 1000-year mass wasting potential maps (Table 7.2, Figure 7.6). During the early Holocene dry period, the landslide rate for the entire island below the alpine zone (approximately 26 497 km^2) was 121 landslides$\cdot y^{-1}$ or an average

of 0.005 landslides·y^{-1}·km^{-2}. This rate increased considerably to approximately 221 landslides·y^{-1} (0.008 landslides·y^{-1}·km^{-2}) during the warm wet Mesothermic interval. Thereafter the rate declined slightly during the late
Holocene to about 191 landslides·y^{-1} (0.007 landslides·y^{-1}·km^{-2}). It should be noted that the landslide frequency in the wet millennia may be slightly underestimated on the outer west coast of Vancouver Island as there is no analog with which to increase the frequency of the outer portion of Zone I for wetter conditions.

Table 7.2. Estimated average annual landslide frequency for Vancouver Island below the Alpine zone.

Climatic regime	Millennia before present	Landslide frequency (#·km^{-2}·y^{-1})	Total annual landslide count
Drier	8-10	0.005	121
Modern	0-3, 7	0.007	191
Wetter	4-6	0.008	221
	Years before present		
Human influence	99-50	0.011	303
Human influence	0-49	0.015	402

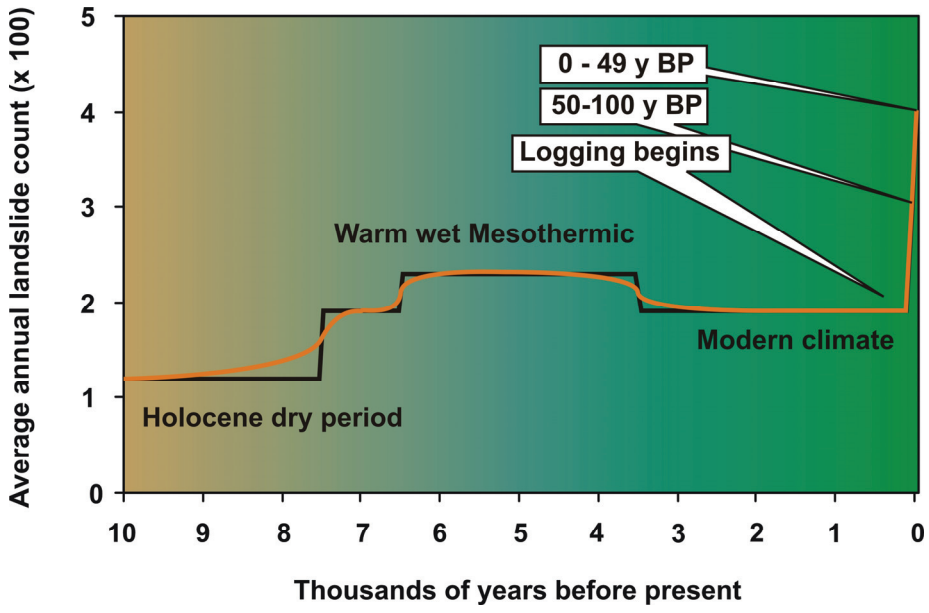

Figure 7.6. Annual average landslide count for Vancouver Island below the alpine zone (below about 800 m) for 10,000 years.

7.3.2 The influence of humans

Earliest records of humans on Vancouver Island date back to approximately 8000 y BP (Carlson 1979, Hebda 1983). At about 2000 years ago, people started to modify the landscape through burning, as evidenced by an increase in fossil charcoal (Brown and Hebda 2002b). The activities of these early people on landslide potential was likely negligible. A more pronounced impact by people, particularly on steep slopes, is clearly evident during the last 100 years as a result of human-induced landscape modification. Approximately 56% of Vancouver Island has been altered in some way by agricultural activity, urbanization or logging. As the most prominent, logging has been both widespread and extensive, with some plantations in their third rotation. As a consequence of these activities, much of the remaining old-growth forest is located in protected parks and reserves as well as in other areas with uneconomic timber. At high elevation, some old-growth forest remains in areas with difficult access, typically on slopes steeper than 30^{o}.

By fifty years ago, the island wide total landslide rate was an estimated 303 landslides$\cdot y^{-1}$, with the rate increasing to modern levels of about 402 landslides$\cdot y^{-1}$ or 0.015 landslides$\cdot y^{-1} \cdot km^{-2}$. These figures reveal that the average landslide rate (below the alpine zone) in the last 50 years is close to twice the highest average landslide rate in the last 10,000 years. Thus, the impact of modern human action such as logging must be recognized as having a significant, and perhaps deleterious, affect that may exceed all previous variation in natural landslide rates.

Given the nature of the human impact compared to past climatic shifts, one can argue that an improvement in logging practices is perhaps the single most effective way to adapt to any future climate change scenarios.

7.3.4 Sediment yield

Magnitude-frequency characteristics of debris slides and debris flows on Vancouver Island were derived previously (Guthrie and Evans 2004, Guthrie 2005), enabling an estimation of the total landslide impact in terms of area affected and volume of sediment

delivered. The mean total area of debris slides and debris flows is about 9,500 m^2 on Vancouver Island, though ranging between 7,500 - 11,500 m^2. Guthrie and Evans (2004) determined a conservative estimate of volume for shallow debris slides and debris flows:

$$V = 0.1549A^{1.0905} \quad (12)$$

where V = landslide volume in m^3 and A = total area in m^2.

Multiplying the annual frequency by the mean total area and volume, and summing over the last 10,000 years yields a total of 1.75×10^{10} m^2 and 6.2×10^9 m^3 respectively, with approximately 1.2×10^8 m^3 of material eroded from the slopes in the last 100 years alone. Further, a total of 9,385 km^2 on Vancouver Island is susceptible to landslides, given that 37% of Vancouver Island is designated as having landslide potential (Guthrie 2005). An estimate of total down-wasting by landslides can be calculated by dividing the total estimated volume by the area available for landslide initiation, yielding 0.7 m of down-wasting on the steep slopes of Vancouver Island during the past 10,000 years. The reader is reminded, however, that this is an averaged result, and that the landscape will erode preferentially on steep sites with sufficient available sediment.

7.4 CONCLUSIONS

Landslides in coastal British Columbia are dominated by precipitation-induced shallow debris slides and flows. These events are responsible for much of the primary erosion by slope failure and play a significant role in shaping the landscape by transporting sediment from upslope sources to lower more stable positions or into stream networks where the material can be removed.

Landslide frequencies were estimated for the past 10,000 years on Vancouver Island by examining climatic shifts in the vegetative record and, using modern conditions and associated frequencies as an analog, comparing those shifts to expected changes in landslide potential. The results suggest an initially low incidence of landslides in the

early Holocene, followed by a substantial increase in landslide frequency between the Holocene dry period and the warm wet mesothermic interval in the mid Holocene. Thereafter, there is a slight reduction in landslide frequency at 3000 y BP; after which landslide frequency remains relatively constant until recent human action drastically altered the landslide regime. Landslide rates varied between 0.005 - 0.008 landslides$\cdot y^{-1}\cdot km^{-2}$ during that time.

The impact of logging during the last 100 years is unambiguous as landslide frequency increased to 0.015 landslides$\cdot y^{-1}\cdot km^{-2}$. This increase reveals that the impact of logging outpaces that of climatic change. Thus, improving logging practices will help offset any potential increase in landslide incidence induced by climate change.

Based on a mean landslide size it is estimated that debris slides and flows eroded an average of 0.7m$\cdot m^{-2}$ across the Vancouver Island during the last 10,000 years.

Chapter 8: Synthesis

8.1 INTRODUCTION

This thesis represents a body of research that seeks to describe and analyze the occurrence and behavior of rainfall-triggered landslides in coastal British Columbia. In particular, it focuses on the analysis of landslide temporal and spatial distributions and magnitudes, and considers the major controls that influence regional landslide behavior. Implicit in the research is the understanding that the landscape of coastal BC is managed, and that landslides, in addition to occurring naturally may be caused by, and certainly impact, resources that are important to British Columbians. Underlying each chapter is the rationale that by better understanding the causes of, and controls on landslide distributions, statistical, spatial and temporal, we can reduce the socioeconomic impacts as well as the impacts on the landscape and lower the risk associated with their activity. To this end, the main conclusions from each chapter are summarized below.

8.2 MAGNITUDE-FREQUENCY CHARACTERISTICS

Chapter 2 examined the practical application of magnitude-frequency characteristics of landslides on Vancouver Island. It showed that by using quantifiable data from complete landslide inventories, a regional hazard map could be generated that can begin to answer the important questions: How big, how likely and how often? Differences in landscape sensitivity across Vancouver Island were revealed based on several landslide inventories, and mapped as four major zones of mass movement potential with different magnitude-frequency characteristics. Differences in landslide type and frequency for each of the zones were caused primarily by differences in climate. Natural landslides were three times more common in the wet zone, with total precipitation > 2.6 $m \cdot y^{-1}$, than the relatively dry zone and occurred on average, once per 83 $km^2 \cdot y^{-1}$. The dry zone, in contrast, had an average annual natural landslide rate of one per 250 $km^2 \cdot y^{-1}$ associated with average precipitation < 1.6 $m \cdot y^{-1}$. Finally, a moderately wet zone was identified between the dry and the wet and associated with a natural landslide frequency of 143 $km^2 \cdot y^{-1}$.

Logging-related landslides frequencies were about 10 times higher than natural frequencies.

Distribution of landslide size can be derived from the magnitude-frequency relation for the west coast watersheds, and it was evident that rainfall-triggered landslides tended toward larger sizes, controlled by slope angle and slope length until about 10,000 m^2. The statistical distribution of landslides greater than 10,000 m^2 was constrained by the landscape itself. Understanding the underlying controls of this M-F distribution was the subject of subsequent chapters.

8.3 A PHYSICAL BASIS FOR M-F CURVES

Chapter 3 explored the physical basis for the shape of M-F curves in coastal BC. Using a simple deterministic model of landslide runout and a model based on cellular automata, the behavior of landslides were simulated to examine the assertion that physiographic controls dominate the landslide M-F distribution.

The deterministic model helped to explain why, for rain-triggered landslides, the rollover might exist. However, the results remained inconclusive for landslides greater than the rollover.

In contrast, the cellular automata model, however, provided corroborative evidence that the main controls on landslide M-F distribution, for both the power law component and the component below the rollover, are indeed governed by the physical conditions related to slope angle, slope distance of the potential path and the redistribution of mass within landslides. Based on empirically based rules for scour, deposition, movement and mass spread, the model produced results that compared favorably to actual landslide data.

Chapter 3 concluded that the M-F distributions of landslides, including both the rollover and the power law components, are a result not of a data bias, but of actual physiographic limitations related to slope angle, slope distance travelled and the distribution of mass within landslides.

8.4 CONTROLS ON RUNOUT AND LANDSLIDE MOBILITY

Chapter 4 explored the relationship between slope angle, slope path distance and debris mass balance in the field to better define rules concerning the relationships observed in Chapter 3 and to try to characterize the mobility of debris flows for coastal BC. Using 1700 field observations, and data from 331 debris flows obtained from air photograph interpretation, probabilistic rules for entrainment and deposition within landslide paths were developed. Overall, deposition and scour occurred on steeper and flatter slopes respectively than previously reported, though mean net deposition and scour were similar. The onset of net deposition occurred on slopes between 18^{o} and 24^{o} for open slope failures and between 12^{o} and 15^{o} for gullied or channelized debris flows. The entrainment volumes for a full range of slope angles along a debris flow path were calculated, and by using these values, runout can now be rapidly estimated in the field or by using a GIS. A simple rule based methodology for estimating debris flow runout was derived and tested in the Klanawa study on Vancouver Island. Predicted results matched very well with the observed. Further analysis of the data concluded that landslides entering stream channels at an acute angle to the main channel direction were significantly more likely to have longer runout distances. Analysis of forest barriers demonstrated that mature timber was effective at stopping debris flows within 40 m of the forest boundary almost 50% of the time, and within 50 m 72% of the time. Debris flow widths were reduced after passing through a mature timber boundary 88% of the time, indicating that forests can act as a substantial barrier. Roads stopped debris flows in 52% of the cases and reduced the debris flow width almost 72% of the time. However, landslides that breached roads and continued onto steep slopes continued to entrain material and grow in volume.

8.5 LANDSLIDES AND LANDSCAPE EVOLUTION

Landslides exist in a sympathetic relationship with the landscape; while physiographic drivers control the behavior and distribution of landslides, the landslides in turn have a major influence on landscape evolution in steep terrain. Chapter 5 identified the event magnitudes of landslides that are geomorphically effective in the landscape.

Effectiveness was examined in terms of work (material transported a given distance), persistence (residence time), and formativity (effectiveness in shaping the landscape).

Chapter 5 concluded that the most geomorphic work in the landscape was performed by "moderate-sized" landslides defined by a work peak (the product of frequency and magnitude) on a probability distribution. The definition of moderate-sized is variable between landscapes depending on physiographic, climatic, and geotechnical settings, but consistent within a region.

Landslide persistence was estimated over nearly six orders of magnitude and described by a power law. Persistence times were found to be substantially different for rock slides and rock avalanches (P_{RS}) compared to debris slides and debris flows (P_{DS}).

Finally, Chapter 5 defined a catastrophic landslide as an event of sufficient magnitude to persist above the background noise of the work done by more moderate-sized events in the landscape. The degree to which an event is individually formative was given by the persistence ratio (P_F). Where $P_F \geq 10$, a catastrophic event has occurred and the geomorphic system has been overwhelmed.

8.6 WEATHER AND LANDSLIDES

In Chapter 6 the regional distribution and characteristics of 626 landslides, most of which occurred during a late fall storm in 2006, were determined using change detection of SPOT imagery across Vancouver Island. This event provided a unique opportunity to more precisely examine the relationships between landslide occurrence and cause.

Precipitation, temperature, and wind speed results from hourly numerical weather forecasts with the MM5 model at a resolution of 4 km were used to examine the association of storm characteristics with the spatial pattern of landslides. High-intensity rainfall was associated with the majority of landslides in southern Vancouver Island. However, rather than using a minimum threshold for predicting landslide initiation, a critical range of landslide-causing precipitation was readily shown on a cumulative probability plot of landslides and precipitation intensity. Increased concentration of landslide-triggering rain as a result of driving winds was demonstrated. Taken as a measure of actual precipitation on the ground, wind and rain together produced an average 15.6 mm more rain at landslide locations than precipitation measured alone.

Rapid snow melt caused by a combination of ambient temperature, rainfall and wind was shown to be a contributing factor during the fall storm for landslides on northern Vancouver Island. Rain-on-snow events have long been recognized as important to landslide generation; however, little research in this area has been completed since it was introduced almost 30 years ago.

8.7 CLIMATE AND LANDSLIDES

Chapter 7 brings together several concepts from previous chapters to derive a model of landscape erosion over the Holocene. The Vancouver Island landslide zones from Chapter 2 were combined with a millennial scale climate record based on a vegetative index that extended back over 10,000 years. Landslide frequencies were estimated using modern conditions and associated frequencies as a benchmark and by comparing climate shifts to expected changes in landslide potential. The results suggested an initially low incidence of landslides in the early Holocene, followed by a substantial increase in landslide frequency between 7000 and 4000 y BP. From 3000 y BP landslide frequency remains relatively constant until drastically increased logging in the 20th century. The impact of logging during the last 100 years is unambiguous as landslide frequency approximately doubled from the wettest, warmest period in the last 10 000 years to 0.015 landslides$\cdot$km$^{-2}\cdot$ y^{-1}. The impact of logging outpaced that of recent climatic change and improving logging practices will help offset potential increases in landslide incidence induced by global warming.

Based on a mean landslide size it is estimated that debris slides and flows have resulted in surface lowering of 0.7 m across Vancouver Island during the last 10,000 years.

8.8 FUTURE WORK

Three major changes in the way we view landslides in coastal British Columbia are underway. Each will require new research, new methods and new knowledge in addition to what has already been produced in this and other studies.

The first is a move from hazard mapping to risk mapping. As hazard mapping matures in BC, economic drivers are forcing practitioners to recognize that all landslides are not created equal, and the risk from some of them exceeds the risk from others. It is my belief that risk will be better managed as more accurate estimates of landslide magnitudes and frequencies are determined. In this thesis I have established a baseline that relates M-F and climate, but additional inventories should be able to refine those estimates. In addition, there needs to be a measure of what risks are tolerable given the nature of BC's considerable remote terrain. Without this information it is difficult to establish how much effort should go into preventing and mitigating landslides and we are left, each of us, guessing based on our personal set of values. I have attempted to begin the discussion of tolerability and social values around landslides in coastal BC, and the initial results are presented in Appendix A. However, this work is far from complete, and it is my hope that it will be taken up by a group of professionals.

The second major change is one of technology. The availability of high-resolution imagery, digital elevation models, weather data, GIS, and high-capacity computing power means we are able to look at landslides in their environmental context in a way that has never existed before in history. In this thesis alone, several technological firsts were claimed including, (a) the first wide scale use of change detection from satellite imagery to identify landslides down to less than 1000 m^2 across a large landscape, and (b) the first use of a cellular automata model to describe the regional behavior of landslides rather than the behavior a single event. In many ways these and other technologies will vastly increase our understanding of landslide behavior; much emphasis will necessarily be put on refining knowledge. However, technology does not yet replace experience on the ground in what remains a highly judgmental discipline. In my opinion, however, there is a danger that primary fundamental data will not be considered useful in a technologically rich world.

Finally, the third major change is change itself. We exist in a dynamic environment, recently emphasized by the growing awareness of a warming planet. Landslide research is not a static science, and we need to look across the landscape to identify areas that are likely to be substantially impacted by geomorphological shifts in response to drivers such

as climate, resource development and major tectonic events. The clues are written in the landscape, we need only see them.

References

Adams, J. 1984. Active deformation of the Pacific Northwest continental margin. Tectonics, 3, 449-472.

Aleotti, P. 2004. A warning system for rainfall-induced shallow failures. Engineering Geology, 73, 247-265.

Alley, N.F. and Chatwin, S.C. 1979. Late Pleistocene history and geomorphology, southwestern Vancouver Island, British Columbia. Canadian Journal of Earth Sciences 16, 1645-1657.

Andrews, E.D. and Nankervis, J.M. 1995. Effective discharge and the design of channel maintenance flows for gravel-bed rivers. Geophysical Monograph, American Geophysical Union 89, 151-164.

Association of Professional Engineers and Geoscientists of British Columbia, 2003. Guidelines for Terrain Stability Assessments in the Forest Sector. APEGBC, Vancouver, BC.

Atwater, B.F. 1987. Evidence for great Holocene earthquakes along the outer coast of Washington. Science 236, 942-944.

Avolio MV, Di Gregorio S, Mantovani F, Pasuto A, Rongo R, Silvano S, Spataro W. 2000. Simulation of the 1992 Tessina landslide by a cellular automata model and future hazard scenarios. JAG, 2, 41-50.

Ayotte, D., Evans, N., Hungr, O., 1999. Runout analysis of debris flows and avalanches in Hong Kong. Proceedings 13th Vancouver Geotechnical Society Symposium, Vancouver, BC, 39-46.

Bak, P., 1996. How Nature Works. The Science of Self-organized Criticality. Springer-Verlag, New York, NY.

Bak, P., Tang, C., Wiesenfeld, K., 1988. Self-organized criticality. Physical Review A38, 364-374.

Benda, L.E. and Cundy, T.W., 1990. Predicting deposition of debris flows in mountain channels. Canadian Geotechnical Journal, 27, 409-417.

Blais-Stevens, A., Clague, J. J. and Rogers, G. C. 2003. Earthquake signature in Late Holocene sediments in Saanich Inlet, British Columbia. In: Proceedings of the 3rd Canadian Conference on Geotechnique and Natural Hazards, Sheraton Hotel, June 09-10, Edmonton, Alberta, The Canadian Geotechnical Society, Alliston, Ontario, 69-75.

Bonnard, C. and Corominas, J. 2005. Landslide hazard management practices in the world. Landslides, 2, 245-246.

Brardinoni, F., Slaymaker, O. and Hassan M.A. 2003. Landslides inventory in a rugged forested watershed: a comparison between air photo and filed survey data. Geomorphology, 54, 179-196.

British Columbia Ministry of Forests and Ministry of Environment, 1999. Forest Practices Code of British Columbia, Mapping and Assessing Terrain Stability Guidebook, Second Edition. Government of British Columbia, Victoria, BC.

Brown, A. S. 1968. Geology of the Queen Charlotte Islands, British Columbia, Bulletin no. 54, British Columbia Department of Mines and Petroleum Resources, Victoria, BC.

Brown, K.J. and Hebda R.J. 2002a. Origin, development, and dynamics of coastal temperate conifer rainforests of southern Vancouver Island, Canada. Canadian Journal of Forest Research, 32, 353-372.

Brown, K.J. and Hebda R.J. 2002b. Ancient fires on southern Vancouver Island, British Columbia Canada: A change in causal mechanisms at about 2000 ybp. Environmental Archeology, 7, 1-12.

Brown, K.J., Fitton, R.J., Schoups, G., Allen, G.B., Wahl, K.A. and Hebda R.J. 2006. Holocene precipitation in the coastal temperate rainforest complex of southern British Columbia, Canada. Quaternary Science Reviews 25, 2762-2779.

Brunsden, D., 1993. The persistence of landforms. Zeitschrift für Geomorphologie N.F., 93, 13-28.

Brunsden, D., 2001. A critical assessment of the sensitivity concept in geomorphology. Catena, 42, 99-123.

Bunn, J. T. and Montgomery D. R. 2000. Patterns of wood and sediment storage along debis-flow impacted headwater channels in old-growth and industrial forests of the Olympic Mountains, Washington. In: Riparian Vegetation and Fluvial Geomorphology, edited by Bennett, S. J. and Simon, A., American Geophysical Union, Washington, DC, 99-112.

Caine, N. 1976. A uniform measure of subaerial erosion. Geological Society of America Bulletin 87, 137-140.

Caine, N. 1980. The rainfall intensity-duration control of shallow landslides and debris flows. Geografiska Annaler Series, A62, 23-27.

Cannon, S.H., 1993. An empirical model for the volume-change behavior of debris flows. In: Proceedings, Hudraulic Engineering ,93, edited by H.W. Shen, S.T. Su, and F. Wen. American Society of Civil Engineers, New York, 1768-1773.

Cardinali, M., Reichenbach, P., Guzzetti, F., Ardizzone, F., Antonini, G., Galli, M., Cacciano, M., Castellani, M., Slavati, P., 2002. A geomorphological approach to estimate landslide hazard and risk in urban and rural areas in Umbria, central Italy. Natural Hazards and Earth Systems Science 2, 57-72.

Carlson, C. 1979. The early component at Bear Cove. Canadian Journal of Archaeology 3,177-194.

Cassidy, J.F., Ellis, R.M. and Rogers G.C. 1988. The 1918 and 1957 Vancouver Island earthquakes. Bulletin of the Seismological Society of America 78, 617-635.

Castro, J.M. and Jackson, P.L., 2001. Bankfull discharge recurrence intervals and regional hydraulic geometry relationships: Patterns in the Pacific Northwest, USA. Journal of the American Water Resources Association 37, 1248-1262.

Chang, K., Chiang, S. and Lei, F. 2008. Analysing the relationship between typhoon-triggered landslides and critical rainfall conditions. Earth surface Processes and Landforms, 33, 1261-1271.

Chatwin, S.C. 2005. Managing Landslide Risk from Forest Practices in British Columbia. Forest Practices Board Special Investigation Report, FPB/SIR/14, Victoria, BC.

Chatwin, S.C., Howes, D.E., Schwab, J.W. and Swanston, D.N. 1994. A Guide for Management of Landslide-Prone Terrain in the Pacific Northwest, Second Edition. British Columbia Ministry of Forests Land Management Handbook 18, Victoria, BC.

Chen C., Yu F., Lin S., and Cheung K. 2007. Discussion of landslide self-organized criticality and the initiation of debris flow. Earth Surface Processes and Landforms, 32, 197-209.

Chiang, S. and Chang, K. 2009. Application of radar data to modeling rainfall-induced landslides. Geomorphology, 103, 299-309.

Chung, C., Bobrowsky, P.T. and Guthrie, R.H. 2002. Quantitative prediction model for landslide hazard mapping: Tsitika and Schmit Creek watersheds, Northern Vancouver Island, British Columbia, Canada. *In*: Geoenvironmental Mapping: Methods, Theory and Practice, edited by P.T. Bobrowsky, A.A. Balkema Publishers, Lisse, Netherlands, 697-716.

Church, M. and Miles, M. J. 1987. Meterological antecedents to debris flow in southwestern British Columbia; some case studies. *In*: Debris Flows/Avalanches: Process, Recognition, and Mitigation, edited by J. E. Costa and G. F. Wieczorck. Geological Society of America, Reviews in Engineering Geology, 7: 63-79.

Clague, J.J. and James T.S. 2002. History and isostatic effects of the last ice sheet in southern British Columbia. Quaternary Science Reviews, 21, 71-87.

Clague, J.J. and Bobrowsky, P.T. 1999. The geological signature of great earthquakes off of Canada's West Coast. Geoscience Canada, 26, 1-15.

Clerici A. and Perego S. 2000. Simulation of the Parma River blockage by the Corniglio landslide (Northern Italy). Geomorphology, 33, 1-23

Corominas, J. 1996. The angle of reach as a mobility index for small and large landslides. Canadian Geotechnical Journal, 33, 260-271.

Corominas, J., Copons, R., Vilaplana, J. M., Altimir, J. and Amigó, J. 2004. Integrated Landslide Susceptibility Analysis and Hazard Assessment in the Principality of Andorra. Natural Hazards, 30, 421-435.

Crosta, G.B. and Frattini, P. 2003. Distributed modelling of shallow landslides triggered by intense rainfall. Natural Hazards and Earth System Sciences, 3, 81-93.

Crosta, G.B. and Frattini, P. 2008. Preface: Rainfall-induced landslides and debris flows. Hydrological Processes, 22, 473-477.

Crozier, M.J. 1999. The frequency and magnitude of geomorphic processes and landform behaviour. Zeitschrift für Geomorphologie N.F. 115, 35-50.

Cruden, D.M. and Varnes D.J. 1996. Landslide types and processes. *In:* Landslides, Investigation and Mitigation, edited by Turner A.K. and Schuster R.L., Transportation Research Board, National Research Council, Special Report 247, Washington DC, 36-75.

Czirok A., Somfai E. and Vicsek T. 1994. Self-affine roughening in a model experiment on erosion in geomorphology. Physica A, 205, 355-366.

D'Ambrosio D., Di Gregorio S., Iovine G., Lupiano V., Rongo R. and Spataro W. 2003. First simulations of the Sarno debris flows through cellular automata modeling. Geomorphology, 54, 91-117.

Dai, F.C., Lee, C.F., 2001. Frequency-volume relation and prediction of rainfall-induced landslides. Engineering Geology 59, 253-266.

De Lima, J.L.M.P. 1990. The effect of oblique rain on inclined surfaces: a nomograph for the rain-gauge correction factor. Journal of Hydrology, 115, 407-412.

Di Gregorio S., Rongo R., Siciliano C., Sorriso-Valvo M. and Spataro W. 1999. Mt. Ontake landslide simulation by the cellular automata model SCIDDICA-3. Physics and Chemistry of the Earth (A), 24, 131-137

Doyle, M.W.and Julian, J.P. 2005. The most-cited works in Geomorphlogy. Geomorphology 72, 238-249.

Dragert, H. 1987. The fall (and rise) of central Vancouver Island: 1930-1985. Canadian Journal of Earth Sciences 24, 689-697.

Dudhia, J. 2005. MM5 Version 3.7 (The Final Version). Paper 1.1 presented at the 6thWRF/15thMM5 Users'Workshop, National Center for Atmospheric Research, June 27–30, 2005, Boulder, Colorado.

Dunne, T. 1998. Critical data requirements for prediction of erosion and sedimentation in mountain drainage basins. Journal of the American Water Resources Association, 34, 795-808.
Dury, G.H. 1980. Neocatastrophism? A further look. Progress in Physical Geography, 4, 391-413.
Emmett, W.W. and Wolman, G.M. 2001. Effective discharge and gravel-bed rivers. Earth Surface Processes and Landforms 26, 1369-1380.
Environment Canada 1993. Canadian climate normals, 1961-90 British Columbia. Canadian Climate Program. Atmospheric Environment Services, Ottawa, ON.
Environment Canada 2007. Canadian climate normals, 1971-2000 British Columbia. Environment Canada online resource – http://climate.weatheroffice.ec.gc.ca/climate_normals/stnselect_e.html accessed August 2007.
Erpul, G., Gabriels, D., Corelis, W.M., Samray, H.N. and Guzelordu, T. 2008. Sand detachment under rains with varying angle of incidence. Catena, 72, 413-422.
Erpul, G., Norton, L.D. and Gabriels, D. 2002a. The effect of wind on raindrop impact and rainsplash detachment. Transactions of the American Society of Agricultural Engineers, 45, 51-62.
Erpul, G., Norton, L.D. and Gabriels, D. 2002b. Raindrop-induced and wind-driven soil particle transport. Catena, 47, 227-243.
Evans, S. G. 1989. The Mount Colonel Foster rock avalanche and associated displacement wave, Vancouver Island, British Columbia, Canadian Geotechnical Journal, 26, 452-477.
Evans, S.G., 2003. Characterizing landslide risk in Canada. 3rd Canadian Conference on Geotechnique and Natural Hazards. Canadian Geotechnical Society, Edmonton, AB, 35-50.
Evans, S.G., 2006. Single event landslides resulting from massive rock slope failure: Characterising their frequency and impact on society. *In:* Proceedings of the NATO Advanced Research Workshop on Massive Rock Slope Failure: New Models for Hazard Assessment, Celano, Italy, 16-21 June, 2002.
Fannin, R. J. and Rollerson, T. P. 1993. Debris flows: some physical characteristics and behaviour. Canadian Geotechnical Journal, 30, 71-81.
Fannin, R. J. and Rollerson T.P. 1996. Assessing debris flow hazard in coastal British Columbia: runout behaviour. *In:* Proceedings of the 9th Pacific Northwest Skyline Symposium, International Union of Forest Research Organizations, 3.06, Forest operations under mountainous conditions, 30-44.
Fannin, R.J. and Wise, M.P., 2001. An empirical-statistical model for debris flow travel distance. Canadian Geotechnical Journal, 38, 982-994.
Fenger, M., Manning, T., Cooper, J., Guy, S. and Bradford, P. 2006. Wildlife and Trees in British Columbia. Lone Pine Publishing, Edmonton AB.
Finlay, P. J., Mostyn, G. R. and Fell, R. 1999. Landslide risk assessment: prediction of travel distance. Canadian Geotechnical Journal, 36, 556-562.
Fujii, Y. 1969. Frequency distribution of the magnitude of the landslides caused by heavy rainfall. Journal of the Seismological Society of Japan 22, 244-247.
Gabet, E.J., Burbank, D.W., Putkonen, J.K., Pratt-Situala, B.A. and Ojha, T. 2004. Rainfall thresholds for landsliding in the Himalayas of Nepal. Geomorphology, 63, 131-143.
Gimbarzevsky, P. 1988. Mass wasting on the Queen Charlotte Islands – a regional inventory. British Columbia Ministry of Forests Land Management Report 29, Victoria, BC.

Government of British Columbia, 2004. Forest Planning and Practices Regulation, Forest and Range Practices Act.

Grant, G.E. and Swanson, F.J. 1995. Morphology and Processes of Valley Floors in Mountain Streams, Western Cascades, Oregon. Geophysical Monograph 89, American Geophysical Union, Corvallis, Oregon, 83-101.

Guthrie, R.H., 1997. The characterization and dating of landslides in the Tsitika River and Schmidt Creek watersheds, northern Vancouver Island, British Columbia. M.S. thesis, University of Victoria, Victoria, BC.

Guthrie, R.H. 2002. The effects of logging on frequency and distribution of landslides in three watersheds on Vancouver Island, British Columbia. Geomorphology 43, 275-294.

Guthrie R.H. 2005. Geomorphology of Vancouver Island: mass wasting potential. Research Report No. RR01, British Columbia Ministry of Environment Victoria, BC.

Guthrie, R.H. and Brown, K.J. 2008. Denudation and landslides in coastal mountain watersheds. Geographica Helvetica, 63, 26-35.

Guthrie, R.H. and Evans, S.G. 2004a. Analysis of landslide frequencies and characteristics in a natural system, Coastal British Columbia. Earth Surface Processes and Landforms 29, 1321-1339.

Guthrie, R.H. and Evans, S.G. 2004b. Magnitude and frequency of landslides triggered by a storm event, Loughborough Inlet, British Columbia. Natural Hazards and Earth System Sciences, 4, 475-483.

Guthrie, R.H. and Evans S.G. 2005. The role of magnitude-frequency relations in regional landslide risk analysis. *In:* Landslide Risk Management, edited by Hungr, O., Fell R., Couture, R., and E. Eberhardt. A.A. Balkema Publishers, London, UK, 375-380.

Guthrie, R.H. and Evans, S.G. 2007. Work, persistence, and formative events: The geomorphic impact of landslides. Geomorphology, 88, 266-275.

Guthrie, R. H., Deadman, P. J., Cabrera, A.R, and Evans, S.G.: Exploring the magnitude-frequency distribution: a cellular automata model for landslides, Landslides, 5, 151-159, 2008.

Guzzetti, F., Reichenbach, P., Cardinali, M., Ardizzone, F. and Galli, M. 2002a. Impact of landslides in the Umbria Region Central Italy. Natural Hazards and Earth System Science, 3, 469-486

Guzzetti, F., Reichenbach, P., Cardinali, M., Ardizzone, F. and Galli, M. 2002b. Power-law correlations of landslide areas in Central Italy. Earth and Planetary Science Letters, 195, 169-183

Guzzetti, F., Reichenbach, P. and Wieczorek, G.F. 2003. Rockfall hazard and risk assessment in the Yosemite valley, California, USA. Natural Hazards and Earth System Sciences 3:491-503.

Guzzetti, F., Reichenbach, P., and Ghigi, S. 2004. Rockfall hazard and risk assessment along a transportation corridor in the Nera Valley, Central Italy. Environmental Management 34:191-208.

Guzzetti, F., Reichenbach, P., Cardinali, M., 2005. Probabilistic landslide hazard assessment at the basin scale. Geomorphology, 72, 272-299.

Guzzetti, F., Peruccacci, S., Rossi, M. and Stark, C.P. 2008. The rainfall intensity-duration control of shallow landslides and debris flows: an update. Landslides, 5, 3-17.

Hall, K.J. 1992. Fractal geometry of global change in earth history. Proceedings of the 29th International Geological Congress, Kyoto, Japan, 24 August–3 September, 10.

Harp, E. and Jibson, R.L. 1995. Inventory of Landslides Triggered by the 1994 Northridge California Earthquake. Open File Report 95-213, U.S. Geological Survey, Denver, Colorado.

Harr, R.D. 1981. Some characteristics and consequences of snowmelt during rainfall in western Oregon. Journal of Hydrology, 53, 277-304.

Hartman, G.F., Scrivener, J.C. and Miles, M.J. 1996. Impacts of logging in Carnation Creek, a high-energy coastal stream in British Columbia, and their implication for restoring fish habitat. Canadian Journal of Fisheries and Aquatic Sciences, 53, 237-251.

Hay, M.B., Dallimore, A., Thomson, R.E., Calvert, S.E. and Reinhard P. 2007. Siliceous microfossil record of late Holocene oceanography and climate along the west coast of Vancouver Island, British Columbia (Canada). Quaternary Research 67, 22-49.

Hebda, R.J. 1983. Late-glacial and postglacial vegetation history at Bear Cove Bog, northeast Vancouver Island, British Columbia. Canadian Journal of Botany 61, 3172-3192.

Hebda, R.J. and Rouse G.E. 1979. Palynology of two Holocene cores from the Hesquiat Peninsula, Vancouver Island, British Columbia. Syesis 12, 121-129.

Heim, A. 1932. Der Bergsturz und Menschenleben: Zurich, Fretz and Wasmuth Verlag, 218 p.

Hickin, E.J. 1989. Contemporary Squamish River sediment flux to Howe Sound, BC. Canadian Journal of Earth Science 26, 1953-1963.

Hirano, M. and Ohmori, H. 1989. Magnitude-frequency distribution for rapid mass movements and its geomorphological implication. Transactions, Japanese Geomophological Union, 10, 95-111

Hogan, D. L., and Schwab, J. W. 1990. Precipitation and runoff characteristics, Queen Charlotte Islands, British Columbia Ministry of Forests, Land Management Report, 60, Ministry of Forests, Victoria, BC.

Hogan, D. L., and Schwab, J. W. 1991. Meteorological conditions associated with hillslope failures on the Queen Charlotte Islands British Columbia Ministry of Forests, Land Management Report 73, Victoria, BC.

Hogg, W.D. and Carr, D.A. 1985. Rainfall frequency atlas for Canada. Canadian Climate Program, Environment Canada, Atmospheric Environment Service, Ottawa, ON.

Holland, S. S. 1976. Landforms of British Columbia: A Physiographic Outline. The Government of the Province of British Columbia, Bulletin 48, Victoria, BC.

Horel, G. 2007. Overview-level landslide runout study: Western Forest Products Inc., Tree Farm Licence 6. Streamline Watershed Management Bulletin, 10, 15-24.

Houghton, J.T., Jenkins, G.J., and Ephraums J.J. (eds) 1990. Climate change: The IPCC scientific assessment. Cambridge University Press, Cambridge, UK.

Hovius. N., Stark, C.P., Allen, P.A., 1997. Sediment flux from a mountain belt derived by landslide mapping. Geology 25, 231-234.

Hovius, N., Stark, C.P., Hao-Tsu, C., Jiun-Chuan, L., 2000. Supply and removal of sediment in a landslide-dominated mountain belt: Central Range, Taiwan. Journal of Geology 108, 73-89.

Howes, D.E. 1981. Terrain inventory and geological hazards: Northern Vancouver Island. Province of British Columbia, Ministry of Environment, APD Bulletin 5, Victoria, BC.

Howes, D.E. 1987. A method for predicting terrain susceptible to landslides following forest-harvesting: a case study from the southern Coast Mountains, British

Columbia. Forest Hydrology and Watershed Management. Proceedings of the International Association of Hydrological Sciences Symposium, XIX General Assembly of the International Union of Geodesy and Geophysics August 19-22, University of British Columbia, Vancouver, BC, 167, 143-154.

Howes, D.E. and Kenk, E. 1997. Terrain Classification System for British Columbia, Version 2. British Columbia Ministry of Environment Manual 10, Victoria, BC.

Howes, D.E. and Sondheim, M. 1988. Quantitative definitions of stability classes as related to post-logging clearcut landslide occurrence. Part II, Proceedings of the 10th B.C. Soil Science Workshop. British Columbia Ministry of Forests Land Management Report 56. British Columbia Ministry of Forests, Victoria BC, 167-184.

Hsu, K.J. 1975. Catastrophic debris streams (sturzstroms) generated by rockfalls. Geological Society of America Bulletin, 86, 129-140,

Hsu, K.J., 1983. Actualistic catastrophism. Sedimentology 30, 3-9.

Hungr, O., 1995. A model for the runout analysis of rapid flow slides, debris flows and avalanches. Canadian Geotechnical Journal 32, 610-623.

Hungr, O. and Evans, S.G. 2004. Entrainment of debris in rock avalanches: An analysis of a long run-out mechanism. Geological Survey of America Bulletin 116, 1240-1252.

Hungr, O., Morgan, G. C. and Kellerhals, R. 1984. Quantitative analysis of debris torrent hazards for design of remedial measures. Canadian Geotechnical Journal 21, 663-676.

Hungr, O., Evans, S.G., and Hazzard, J. 1999. Magnitude and frequency of rock falls and rock slides along the main transportation corridors of southwestern British Columbia. Canadian Geotechnical Journal 36, 224-238.

Hungr, O., Corominas, J. and Eberhardt E., 2005. Estimating landslide motion mechanisim, travel distance and velocity. In: Landslide Risk Management, edited by O. Hungr, R. Fell, R. Couture and E. Eberhardt, O., A.A. Balkema Publishers, London, UK, 99-128.

Hungr, O., McDougall, S., Wise, M., Cullen, M. 2008. Magnitude-frequency relationships of debris flows and debris avalanches in relation to slope relief, Geomorphology, 96, 355-365.

Hürlimann, M., Rickenmann, D., Medina, V. and Bateman, A., 2008. Evaluation of approaches to calculate debris-flow parameters for hazard assessment. Engineering Geology, 102, 152-163.

Hutchinson, I., Guilbault, J.P., Clague, J.J. and Bobrowsky, P.T. 2000. Tsunamis and tectonic deformation at the northern Cascadia margin: a 3000 year record from Deserted Lake, Vancouver Island, British Columbia. The Holocene, 10, 429-439.

Innes, J.L., 1983. Lichenometric dating of debris-flow deposits in the Scottish Highlands. Earth Surface Processes and Landforms 8, 579-588.

Innes, J.L., 1985. Magnitude-frequency relations of debris flows in Northwest Europe. Geografiska Annaler 67A, 23-32.

Iovine, G., Di Gregorio, S., Lupiano, V. 2003. Debris-flow susceptibility assessment through cellular automata modeling: an example from 15-16 December 1999 disaster at Cervinara and San Martino Valle Caudina (Campania, southern Italy). Natural Hazards and Earth System Sciences, 3, 457-468

IPCC, 2007. Summary for policymakers. Climate change 2007: climate change impacts, adaptation and vulnerability. Contribution of Working Group II to the Fourth Assessment Report of the Intergovernmental Panel on Climate Change. Cambridge University Press, Cambridge, UK.

Jakob, M. 2000. The impacts of logging on landslide activity at Clayoquot Sound, British Columbia. Catena 38: 279-300.
Jakob, M. and Wetherly, H. 2003. A hydroclimatic threshold for initiation on the North Shore Mountains of Vancouver, British Columbia. Geomorphology, 54, 137-156.
Johnson, A.C., Swanston, D.N. and McGee, K.E. 2000. Landslide initiation, runout, and deposition within clearcuts and old-growth forests of Alaska. Journal of the American Water Resources Association, 36,17-30.
Jordon, P. 2003. Landslide and terrain attribute study in the Nelson forest region. Final report to Ministry of Forests Research Branch, Nelson, BC.
Keefer, D.K. 1984. Landslides caused by earthquakes. Geological Society of America Bulletin, 95. 406-421.
Korup, O. 2005. Distribution of landslides in southwest New Zealand. Landslides 2, 43-51.
Kwan, J.S.H. and Sun, H.W. 2006. An improved landslide mobility model. Canadian Geotechical Journal, 43, 531-539.
Lancaster, S. T., Hayes, S.K. and Grant, G. 2003. Effects of wood on debris flow runout in small mountain watersheds. Water Resources Research 39, 1168.
Lee, E.M. and Jones, D.K.C. 2004. Landslide Risk Assessment. Thomas Telford, London. 454 p.
Leonard, L.J., Hyndman, R.D., and Mazzotti, S. 2004. Coseismic subsidence in the 1700 great Cascadia earthquake: Coastal estimates versus elastic dislocation models. Geological Society of America Bulletin, 116, 665-670.
Leopold, L.B., Wolman, M.G., Miller, J.P., 1964. Fluvial Processes in Geomorphology. W.H. Freeman and Company, San Francisco, California.
Lewis, D.H., and Smith D.J. 2004. Little Ice Age glacial activity in Strathcona Provincial Park, Vancouver Island, British Columbia, Canada. Canadian Journal of Earth Sciences, 41, 285-297.
Lister, D.R., Morgan, G.C., VanDine, D.F. and Kerr, J.G.W., 1984. Debris torrents in Howe Sound, British Columbia. *In*: Proceedings, 4th International Symposium on Landslides, Toronto ON, p649-654.
Locat, P., Couture, R., Leroueil, S., Locat, J. and Jaboyedoff, M. 2006. Fragmentation energy in rock avalanches. Canadian Geotechnical Journal, 43, 830-851.
Luino, F. 2005. Sequence of instability processes triggered by heavy rainfall in the northern Italy. Geomorphology, 66, 13-39.
Malamud, B.D. and Turcotte, D.L. 2000. Cellular Automata models applied to natural hzards. IEEE Computing in Science and Engineering, 2, 42-51.
Malamud, B.D., Turcotte, D.L., Guzzetti, F., Reichenbach, P., 2004a. Landslides, earthquakes and erosion. Earth and Planetary Science Letters 229, 45-59.
Malamud, B.D., Turcotte, D.L., Guzzetti, F., Reichenbach, P., 2004b. Landslide inventories and their statistical properties. Earth Science Processes and Landforms 29, 687-711.
Martin, Y., Rood, K., Schwab, J.W. and Church, M. 2002. Sediment transfer by shallow landsliding in the Queen Charlotte Islands, British Columbia. Canadian Journal of Earth Sciences 39, 189-205.
Massey, N.W.D., MacIntyre D.G. and Desjardins, P.J. 2003a. Digital map of British Columbia: Tile Nm 10, Southwest British Columbia. Geofile 2003-3, British Columbia Ministry of Energy and Mines, Victoria, BC.
Massey, N.W.D., MacIntyre D.G. and Desjardins P.J. 2003b. Digital map of British Columbia: Tile Nm 9, Southwest British Columbia. Geofile 2003-4, British

Mathews, W.H. 1979. Landslides of Central Vancouver Island and the 1946 earthquake. Seismological Society of America, Bulletin, 69, 445-450.

May, C. L. and Gresswell, R. E. 2003. Processes and rates of sediment and wood accumulation in headwater streams of the Oregon Coast Range, USA. Earth Surface Processes and Landforms, 28, 409-424.

McClung, D.M., 1999. Extreme avalanche runout in space and time. Canadian Geotechnical Journal 37, 161-170.

McDougall, S. and Hungr, O. 2004. A model for the analysis of rapid landslide motion across three-dimensional terrain. Canadian Geotechnical Journal, 41, 1084-1097.

Miles, M., Allegretto, S. and Goldsworthy, L. 2008. Storm return periods associated with flooding and sediment movement in the Beaufort Ranges: January 2006 to December 2007. Report to TimberWest Forest Corporation. Mike Miles and Associates Limited, Victoria, BC.

Millard, T.H. 1999. Debris flow initiation in coastal British Columbia gullies. British Columbia Ministry of Forests Technical Report, TR-002, Vancouver Forest Region, Nanaimo, BC 22 p.

Miller, D.J. and Burnett, K.M. 2008. A probabilistic model of debris-flow delivery to stream channels, demonstrated for the Coast Range of Oregon, USA. Geomorphology, 94, 184-205,

Mitchell, S.J., Lanquaye-Opoku, N., Modzelewski, H., Shen, Y., Stull, R., Jackson, P. Murphy, B. and Ruel, J.C. 2008. Comparison of wind speeds obtained using numerical weather prediction models and topographic exposure indices for predicting windthrow in mountainous terrain. Forest Ecology and Management, 254, 193-204.

Montgomery, D.R. and Dietrich, W.E. 1994. A physically based model for topographic control on shallow landsliding. Water Resources Research, 30, 1153-1171.

Nadim, F. and Lacasse, S. 2004. Mapping of landslide hazard and risk along the pipeline route, Terrain and geohazard challenges facing onshore oil and gas pipelines. International Centre for Geohazards contribution 41, Thomas Telford publishing, London, 12 p.

Nicoletti, P., and Sorriso-Valvo, M. 1991. Geomorphic Controls of the Shape and Mobility of Rock Avalanches. Geological Society of America Bulletin, 103, 1365-1373.

Noever, D.A., 1993. Himalayan sandpiles. Physics Review E47, 724-725.

Ohmori, H., Hirano, M., 1988. Magnitude, frequency and geomorphological significance of rocky mud flows, landcreep and the collapse of steep slopes. Zeitschrift für Geomorphologie. N.F. 67, 55-65.

Pack, R.T., Tarboton, D.G. and Goodwin, C.N., 1998. The SINMAP approach to terrain stability mapping. *In*: 8th Congress of the International Association for Engineering Geology and the Environment Volume II, edited by Moore, D.P. and Hungr, O., A.A. Balkema Publishers, Rotterdam, Netherlands, 1157-1165.

Page, M.J., Reid, L.M. and Lynn I.H. 1999. Sediment production from Cyclone Bola landslides, Waipaoa catchment. Journal of Hydrology (NZ), 38, 289-308.

Pedersen, H.S. and Hasholt, B. 1995. Influence of wind speed on rainsplash erosion. Catena, 24, 39-54.

Pelletier, J.D., Malamud, B.D., Blodgett, T., Turcotte, D.L., 1997. Scale-invariance of soil moisture variability and its implications for the frequency-size distribution of landslides. Engineering Geology 48, 255-268.

Perline, R., 2005. Strong, weak and false power laws. Statistical Science 20, 68-88.

Philip, H., Ritz, J., 1999. Gigantic paleolandslide associated with active faulting along the Bogd fault (Gobi-Altay, Mongolia). Geology 27, 211-214.

Pike, R.J. and Sobieszczyk, S. 2008. Soil slip/debris flow localized by site attributes and wind-driven rain in the San Francisco Bay region storm of January 1982. Geomorphology, 94, 290-313.

Reichenbach, P., Galli, M., Cardinali, M., Guzzetti, F., Ardizzone, F. 2005. Geomorphologic mapping to assess landslide risk: concepts, methods and applications in the Umbria Region of central Italy. *In:* Landslide Hazard and Risk, edited by Glade, T., Anderson, M.G., Crozier, M.J., John Wiley, 429-468.

Reid, L.M., Page, M.J. 2002. Magnitude and frequency of landsliding in a large New Zealand catchment. Geomorphology 49; 71-88.

Rickenmann, D., 1999. Empirical relationships for debris flows. Natural Hazards, 19, 47-77.

Robison, E.G., Mills, K.A., Paul, J., Dent, L., and Skaugset, A. 1999. Storm Impacts and Landslides of 1996, Oregon Department of Forestry. Forest Practices Monitoring Program, Forest Practices Technical Report 4, Salem, OR,

Rodenhuis, D. Bennett, K.E., Werner, A.T., Murdock, T.Q. and Bronaugh, D. 2007. Climate overview 2007: Hydro-climatology and future climate impacts in British Columbia. Pacific Climate Impacts Consortium Report, University of Victoria, Victoria, British Columbia.

Rogers, G.C. 1980. A documentation of soil failure during the British Columbia earthquake of 23 June, 1946. Canadian Geotechnical Journal, 17, 122-127.

Rollerson, T.P. 1992. Relationships between landscape attributes and landslide frequencies after logging: Skidegate Plateau, Queen Charlotte Islands, Land Management Report no. 76, BC Ministry of Forests Research Branch, Victoria, BC.

Rollerson, T.P., Thomson, B. and Millard, T. 1997. Identification of Coastal British Columbia terrain susceptible to debris flows. *In:* Proceedings of the 1st International Symposium on Debris Flows, August 7-9, San Francisco. United States Geological Survey and the American Society of Civil Engineers: San Francisco, CA.

Rollerson, T.P., Jones, C., Trainor, K. and Thomson, B. 1998. Linking post-logging landslides to terrain variables: Coast Mountains, British Columbia – preliminary analyses. *In:* Proceedings of the 8th International Congress of the International Association for Engineering Geology and the Environment. Balkema Rotterdam; 3, 1973-1979.

Rollerson, T.P., Millard, T. and Thomson, B. 2002. Using terrain attributes to predict post-logging landslide likelihood on southwestern Vancouver Island. Forest Research Technical Report TR-015. Research Section, Vancouver Forest Region, BC Ministry of Forests, Nanaimo, BC.

Rood, K.M., 1984. An aerial photograph inventory of the frequency and yield of mass wasting on the Queen Charlotte Islands, British Columbia. Ministry of Forests Lands Management Report 34, Victoria, BC.

Rulli, M.C., Meneguzzo, F. and Rosso, R. 2007. Wind control of storm-triggered shallow landslides. Geophysical Research Letters, 34, L03402, 1-5.

Ryder, J.M., and Clague, J.J. 1989. Chapter 1: British Columbia (Quaternary stratigraphy and history, Cordilleran Ice Sheet). *In:* Quaternary Geology of Canada and Greenland, edited by: Fulton R.J. Geological Survey of Canada, Geology of Canada 1, 48-53.

Salathé, E.P. 2006. Influences of a shift in North Pacific storm tracks on western North American precipitation under global warming. Geophysical Research Letters, 33, L19820.

Salathé, E.P., Steed, R., Mass, C.F. and Zahn, P.H. (in press). A high-resolution climate model for the United States Pacific Northwest: Mesoscale feedbacks and local responses to climate change. *Journal of Climate.*

Satake, K. 1995. A possible Cascadia earthquake of January 26, 1700 as inferred from tsunami records in Japan. *In:* Program and Abstracts of the 1995 Geological Association of Canada/Minieralogical Association of Canada Annual Meeting: A-93.

Sauder, E.A. Krag, R.K. and Welburn, G.V. 1987. Logging and mass wasting in the Pacific Northwest with application to the Queen Charlotte Islands, B.C. British Columbia Ministry of Forests Land Management Report 53, Victoria, BC.

Scheidegger, A. E. 1973. On the prediction of the reach and velocity of catastrophic landslides. Rock Mechanics, 5, 231-236,

Schmidt, K.M. and Montgomery, D.R. 1995. Limits to relief. Science, 270: 617-620.

Schwab, J.W. 1983. Mass wasting: October-November 1978 storm, Rennell Sound, Queen Charlotte Islands, British Columbia. British Columbia Ministry of Forests, Research Note 91, Victoria BC,

Segre, E. and Deangeli, C. 1995. Cellular automaton for realistic modeling of landslides. Nonlinear Processes in Geophysics, 2, 1-15

Sharon, D. 1980. The distribution of hydrologically effective rainfall incident on sloping ground. Journal of Hydrology, 46, 165-188.

Singh, N.K. and Vick, S.G. 2003. Probabilistic rockfall hazard assessment for roadways in mountainous terrain. Proceedings of 3rd Canadian Conference on Geotechnique and Natural Hazards, Canadian Geotechnical Society, Edmonton, 253-260.

Smith, D.J., and Laroque, C.P. 1996. Dendroglaciological dating of a little ice age glacial advance at Moving Glacier, Vancouver Island, British Columbia. Géographie physique et Quaternaire, 50, 47-55.

Smith, R.B., Commandeur, P.R., Ryan, M.W. 1986. Soils, Vegetation, and Forest Growth on Landslides and Surrounding Logged and Old-growth Areas on the Queen Charlotte Islands. British Columbia Ministry of Forests Land Management Report 41. British Columbia Ministry of Forests, Victoria, BC.

Soeters, R. and van Westen, C.J. 1996. Slope instability recognition, analysis and zonation. *In*: Landslides, Investigation and Mitigation, edited by Turner A.K. and Schuster R.L., Transportation Research Board, National Research Council, Special Report 247, Washington DC, 129-177.

Somfai, E., Czirok, A. and Vicsek,T. 1994. Power-law distribution of landslides in an experiment on the erosion of a granular pile. Journal of Physics A: Mathematical and General 27, L757-L763.

Stark, C.P. and Hovius, N., 2001. The characterization of landslide size distributions. Geophysical Research Letters 28, 1091-1094.

Sterling, S.M. 1997. The influence of bedrock type on magnitude, frequency and spatial distribution of debris torrents on northern Vancouver Island. MSc Thesis, University of British Columbia, Vancouver, BC.

Sugai, T. and Ohmori, H., 2001. Magnitude-frequency distribution of landslide mass in uplifting mountains. Transactions, Japanese Geomorphological Union 22, 229.

Sugai, T., Ohmori, H., Hirano, M., 1994. Rock control on magnitude-frequency distribution of landslide. Transactions, Japanese Geomorphological Union 15, 233-251.

Swanston, D. N., and Howes, D. E. 1994. A technique for stability hazard assessment. Chapter 2 In: A Guide for Management of Landslide Prone Terrain in the Pacific Northwest, edited by S. C. Chatwin, D. E., Howes, J. W. Schwab, and D. N.

Swanston. British Columbia Ministry of Forests, Land Management Handbook, 18, Victoria, BC.
Takahashi, T. 1981. Debris flows. Annual Review of Fluid Mechanics, 13, 57-77.
Tebaldi, C., Hayhoe, K., Arblaster, J.M. and Meehl, G.A. 2006. Going to the extremes: an intercomparison of model-simulated historical and future changes in extreme events. Climatic Change, 79, 185-211.
Thomson, B. 1987. Chapman Creek landslide inventory. 1:20,000 scale map with legend. British Columbia Ministry of Environment, Lands and Parks technical report, Victoria BC.
Trustrum, N.A., Gomez, B., Page, M.J., Reid, L.M. and Hicks, D.M., 1999. Sediment production, storage and output: The relative role of large magnitude events in steepland catchments. Zeitschrift für Geomorphologie. N.F. 115, 71-86.
Turcotte, D. L., Malamud, B. D., Guzzetti, F. and Reichenbach, P. 2002. Self-organization, the cascade model, and natural hazards, Proceedings of the National Academy of Sciences of the USA, 19: 2530-2537.
Turner, K.A and Schuster, R.L. (eds.) 1996. Landslides, Investigation and Mitigation. Transportation Research Board Special Report 247, National Research Council, Washington, D.C.: National Academy Press.
VanDine, D.F., 1985. Debris flows and debris torrents in the southern Canadian Cordillera. Canadian Geotechnical Journal, 22, 44-68.
Varnes, D. J. 1978. Slope movement types and processes. *In:* Landslides; analysis and control, edited by, Schuster, R.L. and Krizck, R.J., Transportation Research Board National Academy of Sciences Special Report 176, Washington, DC, 11-33.
Von Neumann, J. 1966. Theory of self-reproducing automata, University of Illinois Press, Urbana.
Wang, T., Hamann, A., Spittlehouse, D. L. and Aitken, S. N. 2006. Development of scale-free climate data for Western Canada for use in resource management. International Journal of Climatology, 26, 383-397.
Wemple, B.C., Swanson, F.J., and Jones, J.A. 2001. Forest roads and geomorphic process interactions, Cascade Range, Oregon. Earth Surface Processes and Landforms 25, 191-204.
Wise, M. P. 1997. Probabilistic modelling of debris flow travel distance using empirical volumetric relationships. M.Sc. thesis, Department of Civil Engineering, Universitiy of British Columbia, Vancouver, British Columbia.
Wolfram, S. 1984. Cellular automata as models of complexity. Nature, 311, 419-424.
Wolman, M.G. and Gerson, R., 1978. Relative scales of time and effectiveness of climate in watershed geomorphology. Earth Surface Processes and Landforms 3, 189-208.
Wolman, M.G. and Miller, J.P., 1960. Magnitude and frequency of forces in geomorphic processes. Journal of Geology 68, 54-74.
Wörner, G., Uhlig, D., Kohler, I. and Seyfried, H. 2002. Evolution of the West Andean Escarpment at 8^{o}S (N. Chile) during the last 25 Ma: uplift, erosion and collapse through time. Tectonophysics 345, 183-198.
Yin, J.H. 2005. A consistent poleward shift of the storm tracks in simulations of 21st century climate. Geophysical Research Letters, 32 L18701.
Yorath, C.J. and Nasmith, H.W. 1995. The Geology of Southern Vancouver Island: A Field Guide. Orca Book Publishers, Victoria, British Columbia.
Zhang, X., Vincent, L.A., Hogg, W.D. and Niitsoo, A. 2000. Temperature and precipitation trends in Canada during the 20th century. Atmosphere-Ocean, 38, 395-429.

Zhou, C.H., Lee, C.F., Li, J. and Xu, Z.W. 2002. On the spatial relationship between landslides and causative factors on Lantau Island, Hong Kong. Geomorphology, 43, 197-207.

Appendix A: A discussion on forestry and landslides: What is acceptable in BC?

Based on: Guthrie, R.H., 2009. Forestry and Landslides: What is acceptable in BC? Forestry Chronicle, 85, 25-31.

OVERVIEW: Landslides are unavoidably linked to forestry operations in coastal BC. A neglected component of landslide risk assessment is the degree to which impacts from landslides may be acceptable. One hundred and thirteen professionals in the BC forest industry, including foresters, biologists, geoscientists and engineers, examined landslide tolerability criteria. Despite differences by sector, there was general agreement that landslides resultant of ignoring expert advice or where an expert was clearly at fault were unacceptable, and penalties were high. In more ambiguous cases, increased consequences resulted in increased scrutiny and it was clear that experts should expect to be held responsible for their decisions by government officiators and the public.

A.1. INTRODUCTION

The Canadian Cordillera lies almost entirely within British Columbia (BC), and is comprised of approximately 800,000 km^2 of rugged mountainous terrain and interior plateaus. Population density is low; with 4.3 million people living largely in affluence in urban centers, and resource availability is high with about half the province considered merchantable timber. British Columbia demands extraction of its considerable resources, but not at any price. The people of BC have long focussed on environmental values: clean running water, scenic vistas, clean air and unmarred ground. Local forest professionals are faced with the daunting task of building roads and harvesting forests in some of the most rugged conditions in the world, all while minimizing impacts. In no place is this truer than the west coast of British Columbia. Arboreal giants, like the coastal Douglas-fir tower up to 85 m tall (Parish and Thomson, 1994) in glacially over-steepened watersheds, approximately a third of which are steeper than 60% by area (Guthrie, 2005). Natural landslides are frequent, up to 1 landslide/year/83 km^2 on average in wetter landscapes,

and large, approaching 1 ha in total average size, as they exploit long slopes and considerable relief (Guthrie, 2005, Guthrie and Evans, 2004a, 2004b). Historically, the impact of logging has been an increase in landslide frequency of about 10 times (Guthrie, 2002, 2005) though the range has been recorded from 4 – 34 times (Schwab 1983, Jakob, 2000, Jordan 2003). Recent practices may be improving these numbers, but the amount is still high (Chatwin 2005, Horel 2006). As British Columbia moves fully into a results based legislative regime, where the responsibility and liability for landslide impacts falls on the forest licensees who in turn ask for guidance from qualified registered professionals, an examination of risk and risk tolerance is necessary.

A.2. RISK AND TOLERABILITY

In landslide studies, Risk is broadly defined as: "The likelihood of specified adverse consequences arising from an event, circumstance or action within a stated period and area" (Lee and Jones, 2004 p. 3-4). More specific definitions included: a "measure of the probability and severity of an adverse effect to life, heath, property, or the environment" (Fell *et al.*, 2005 p. 4, Fell and Hartford, 1997, p. 52) and "the chance of injury or loss as defined as a measure of the probability and the consequence of an adverse effect to health, property, the environment, or other things of value" (Wise *et al.*, 2004, p. 6). In each case Risk combines the probability of some hazard and the adverse consequences of that hazard to things that human's value (lives, property, environment, infrastructure, economic activity, services and so forth). This is often expressed in a simplified algebraic form as:

$$R = H \times C \qquad (13)$$

where R = Risk, H = Hazard and C = Consequence. A brief look at the literature behind landslide Risk reveals that the equation may be broken into many more component parts and increasingly complex definitions.

Several studies point out that for Risk Management, a degree of risk is acceptable (Fell, 1994, Findlay and Fell, 1997, Lee and Jones, 2004, Wise *et al.*, 2004, Leroi *et al.*, 2005). An acceptable risk is defined as one where everyone affected is prepared to accept the risk to which they are exposed with no changes or modifications to reduce or control that risk (Fell and Hartford, 1997, Wise *et al.*, 2004, Leroi *et al.*, 2005) and typically occurs when the risk is either considered negligible (Findlay and Fell, 1997) or the benefits of a particular event, circumstance or action grossly overshadow the perceived cost to improve the risk.

Tolerable Risk on the other hand is the risk society or affected members of society are willing to take to secure some net benefit. There is generally a notion that the risk is limited, under constant review, and generally being reduced where possible (Fell, 1994, Wise *et al.*, 2004, Fell *et al.*, 2005, Leroi *et al.*, 2005). There is considerable literature to suggest that tolerance to voluntary risks (for example: the chance of a driver getting into a car accident in which he is responsible) are substantially higher than involuntary risks (the chance of a driver getting into an accident because of a flaw in the car design) (Fell, 1994, Leroi *et al.*, 2005). In terms of landslides the evidence implies that society will tolerate higher risks from natural events, than those from engineered slopes or slopes altered by human activity (particularly where that alteration has increased the hazard).

The principle As Low As Reasonably Practicable (ALARP) applies such that where incremental risk from a hazard occurs, it is reduced to the extent that is reasonably practical. A risk becomes tolerable, under this principle, only if the effort to reduce it is impracticable or the cost is grossly disproportionate to the improvement gained (HSE 1992). The simplest and most often used measure of tolerable risk is the expected loss of life due to some hazard. This is typically a plot of the cumulative probability (F) that N or more lives will be lost and is known as an F-N plot (Figure A.1).

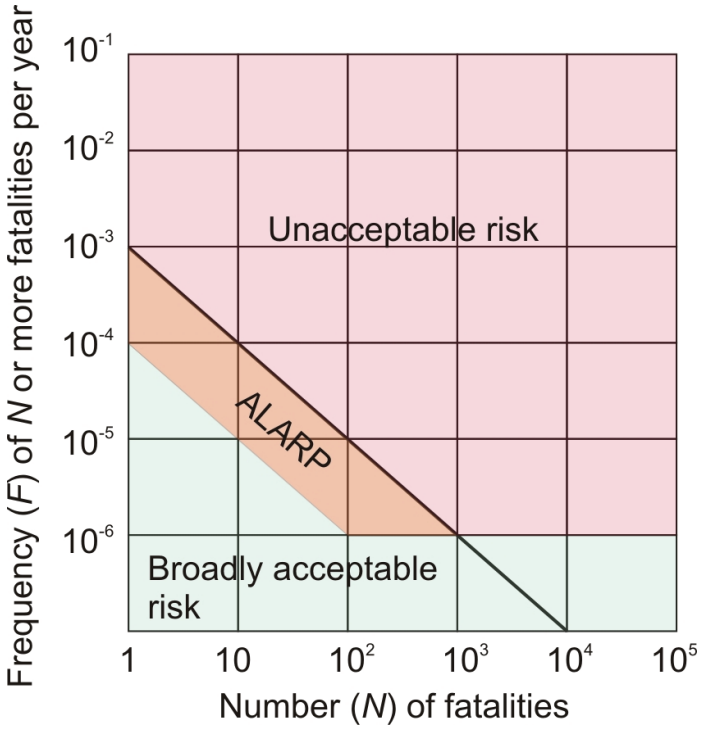

Figure A.1. F-N plot showing colored areas of broadly acceptable risk, unacceptable risk and ALARP (as low as reasonably practicable) region (ANCOLD, 2003). Heavy line is the line used by BC Hydro (1993) for dam failures (above the line being intolerable, below being tolerable). Hong Kong accepts no risk where fatalities exceed 10,000 and has an additional intense scrutiny region between 1,000 and 10,000 fatalities (Ho *et al.*, 2000).

A.3. BC: A UNIQUE CASE

Despite the general definition, tolerability criteria are often applied exclusively against the potential loss of life. There is currently no research that indicates for British Columbia how tolerability might relate to the other values including: property, environment, infrastructure, economic activity and services. Consider that half of British Columbia's population lies in the Greater Vancouver Regional District and that most of the remainder live in a few cities scattered near to the US border. Most of the approximately 1,000,000 km^2 province is essentially empty. The vast majority of landslide risk from forest practices then, deals almost entirely with those other values.

A new draft guideline for the management of terrain stability in the forest sector (APEGBC and ABCFP, 2007) recommends establishing guidance around what is

acceptable risk. In addition, there is a global precedent whereby the industry that understands geotechnical hazard and risk establish, at least in part, tolerability criteria.

The objective herein is to initiate a first look at tolerability to logging-related landslide hazards and consequences by a group of professional of engineers, geoscientists, foresters and biologists engaged in the forestry industry in BC. It should be recognized up front that tolerability is fundamentally subjective and values based. The results below do not represent actual tolerability criteria, but instead are a stepping stone towards them.

A.4. METHODS

One hundred and forty nine professionals from the forest industry, government and private practice participated in a full day course on forestry related landslide hazards and risk (http://www.forrex.org/events/lfvoi/) that took place in 5 locations (Victoria, Nanaimo, Port Alberni, Campbell River and Port Hardy) from November 14 – 17, 2006 and January 25, 2007 (Figure A.2). Each day ended with a discussion and an exercise around tolerability of varying risks posed by landslide hazards. One hundred and thirteen participants voluntarily submitted their results and preliminary analysis is shown here.

The exercise consisted of 13 scenarios (Table A.1), and 14 possible responses to each scenario (Table A.2). Participants were asked to assign to each question one and only one action (response). They were instructed that additional (hypothetical) actions would not be taken in each scenario and the action they assigned should be considered the total response. In addition, participants were asked, in assigning actions, to choose to assign them to the expert or the company, but not both. Several of the questions were ambiguous or lacked detail. In such cases participants were asked to assign responses based on their best estimation about what happened. Participants chose not to answer questions less than 2% of the time (22 of 1430 possible responses were either intentionally not answered, or assigned more than one answer and consequently excluded from the calculations).

The scenarios in Table A.1 form a range of possible events with increasing consequences or decreasing professional care, however, they were scrambled and shown to participants individually to limit a pattern bias of grading from best to worst. Answers

were expected to contain considerable variability where questions were ambiguous or where values differed between respondents and post survey discussions were held discussing some of the assumptions around the answers.

Actions were also ordered by increasing severity and results were therefore calculated including mode (the most common response), mean (a general indication of tolerability by the overall group) and range (an indication of differences in assumptions and values). The position of the mean relative to the overall range is a reasonable measure of the extent to which there were outliers in values.

A.5. RESULTS AND DISCUSSION

The mean and modal results of the survey are given in Figures A.3 and A.4 respectively. Figure A.3 shows each centre's mean plotted within the range of responses at Port Hardy (the selection of Port Hardy was arbitrary but the overall range in responses from each centre was similar). A qualitative first look at the results suggests that there is substantial agreement with scenarios 1-4, 8 and 12-13. There appears to be reasonable agreement with scenarios 5 and 7, and dispersion around scenarios 6, 9, 10 and 11.

Mean and modal responses suggest that for relatively low consequences or for a hazard that was explicitly not predictable (residual hazard) the risk is tolerable. Scenarios 1, 3 and 13 were of this type: landslides sizes were small (1,000 m^2) and the impact was either low or unforeseeable.

There was general agreement amongst all groups and all centres that risks were intolerable where expert advice was ignored and consequences were relatively high. Scenarios 4, 8 and 12 reflect this (Figure A.5). Evidently, increasing the risk by ignoring expert advice is less tolerable than high consequences alone. Figure A.6 shows considerably more variation and lower mean and modal scores for scenarios that resulted in deaths but were more ambiguous than those that were assumed to be a direct result of ignoring the expert. This is probably related to the extent of perceived certainty around cause by the participants in each scenario. In each scenario where a company ignored expert advice the company was considered responsible. In each case, the action increased

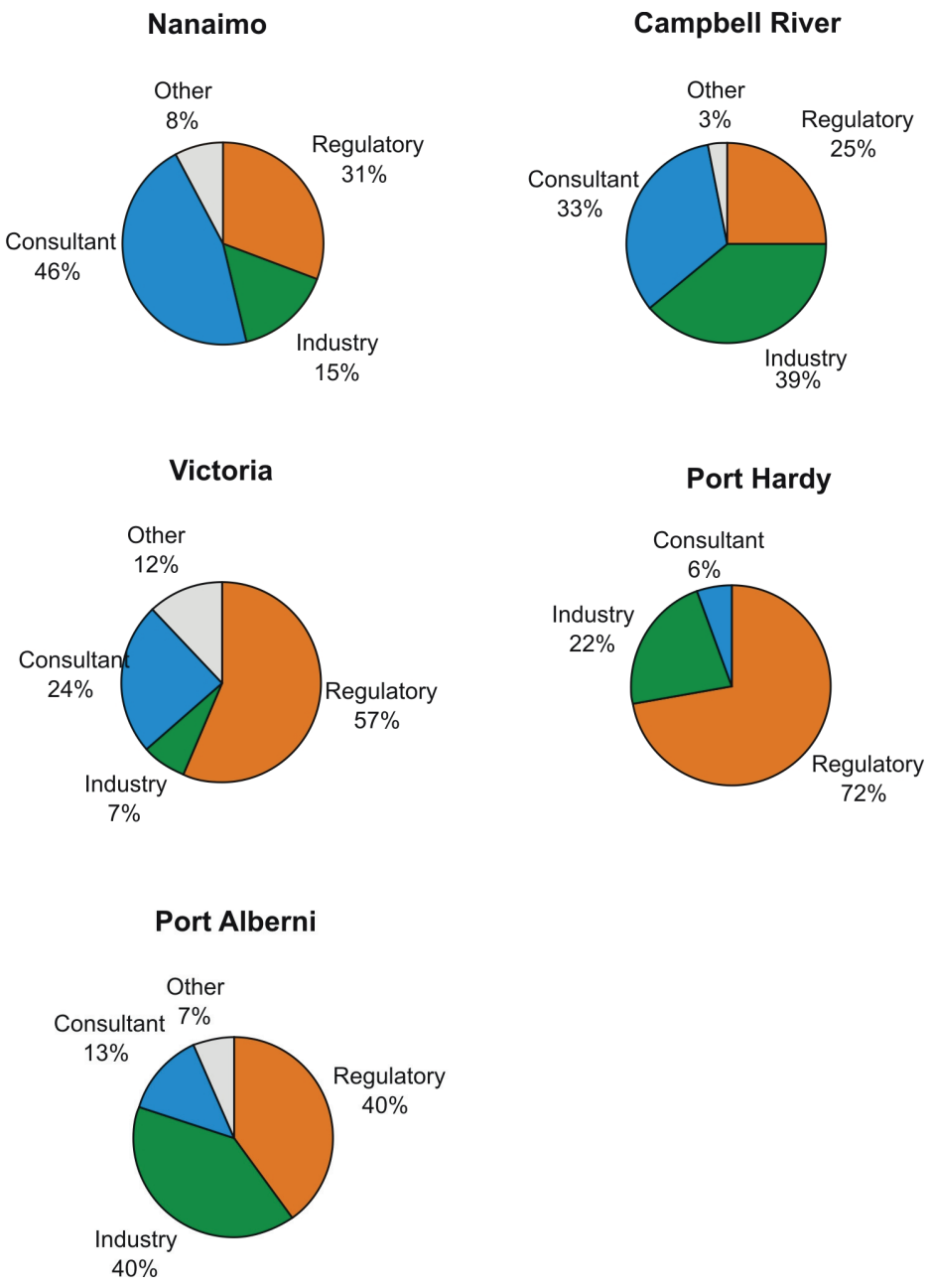

Figure A.2. Distribution of professionals participating in the survey at each of five centres. Consultants were typically engineers, geoscientists and infrequently biologists. The regulatory category consisted of municipal, provincial and federal employees who dealt with the forest industry as part of their job (predominantly foresters, biologists, engineers, and geoscientists) and industry consisted largely of foresters and engineers. The other category is self explanatory included academics and the interested public individuals. Numbers of participants for each of the centres were 41, 39, 15, 36, and 18 for Victoria, Nanaimo, Port Alberni, Campbell River and Port Hardy respectively, with 76% of participants voluntarily submitting their results for analysis.

Table A.1. Thirteen possible landslide scenarios used to consider tolerability.

Q1. A 1,000 m2 landslide occurs following the logging of a steep block in otherwise stable terrain. The landslide does not hit a stream.

Q2. An expert says that there is a low likelihood of landslides in a proposed block, despite a steep slope, and several post logging failures in adjacent blocks. The expert has pulled out a small area from the block immediately around the headscarp of a natural landslide. A 100,000 m2 landslide occurs following logging of the block and buries a fish bearing stream for 1 km.

Q3. A 1,000 m2 landslide occurs following logging of otherwise stable terrain. The landslide hits a fish bearing stream. Experts agree the landslide was not predictable.

Q4. Against expert advice, a block is logged on unstable terrain. Following logging a landslide occurs, wipes out a mainline road, buries and kills three members of the public in their car.

Q5. An expert says that there is a low likelihood of landslides in a proposed block, despite a steep slope, and several post logging failures in adjacent blocks. The expert has pulled out a small area from the block immediately around the headscarp of a natural landslide. A 10,000 m2 landslide occurs following logging of the block. The landslide does not hit a stream.

Q6. A 10,000 m2 landslide occurs following the logging of a steep block in otherwise stable terrain. The landslide crosses a road and kills a vehicle passenger and hospitalizes the driver of a car.

Q7. A 1,000 m2 landslide occurs following the logging of a steep block in otherwise stable terrain. The landslide hits a fish bearing stream.

Q8. Against expert advice, a block is logged on unstable terrain. Following logging a 10,000 m2 landslide occurs and buries a fish bearing stream for 100 m.

Q9. An expert says that there is a low likelihood of landslides in a proposed block, despite a steep slope, and several post logging failures in adjacent blocks. The expert has pulled out a small area from the block immediately around the headscarp of a natural landslide. During logging a landslide occurs killing a machine operator.

Q10. An expert says that there is a low likelihood of landslides in a proposed block, despite a steep slope, and several post logging failures in adjacent blocks. The expert has pulled out a small area from the block immediately around the headscarp of a natural landslide. A 10,000 m2 landslide occurs following logging of the block and buries a fish bearing stream for 100 m.

Q11. A 100,000 m2 landslide occurs following the logging of a steep block in otherwise stable terrain. The landslide buries a fish bearing stream for 1 km.

Q12. Against expert advice, a block is logged on unstable terrain. Following logging a 100,000 m2 landslide occurs and buries a fish bearing stream for 1 km.

Q13. A 1,000 m2 landslide occurs following the logging of a steep block in otherwise stable terrain. The landslide hits a stream 1 km above fish bearing water.

Table A.2. Possible penalties/actions (note, for penalties 5 and greater, landslide rehabilitation is assumed) assigned to each scenario (maximum of one action considered) in Table A.1.

1. No action.
2. No action, landslides sometimes occur.
3. Landslide should be mitigated (hydro-seeding, planting etc…)
4. Landslide should be mitigated (hydro-seeding, planting etc…) and hazards reassessed, possibly affecting adjacent proposals.
5. Small financial penalty levied against the expert (<$1,000.00)
6. Small financial penalty levied against the company (<$1,000.00)
7. Moderate financial penalty levied against the expert (<$10,000.00)
8. Moderate financial penalty levied against the company (<$10,000.00)
9. Large financial penalty levied against the expert (>$10,000.00)
10. Large financial penalty levied against the company (>$10,000.00)
11. Very large financial penalty levied against the expert (>$100,000.00)
12. Very large financial penalty levied against the company (>$100,000.00)
13. The expert faces jail time.
14. Responsible company representatives face jail time.

in severity as the consequence increased. A 10,000 m^2 landslide that hit and buried 100 m of a fish bearing stream resulted in a large financial penalty, a 100,000 m^2 landslide that buried a fish-stream for 1 km resulted in a very large financial penalty, and loss of life resulted in jail time. When presented with limited choices, participants indicated a clear response of lower tolerance to increased consequences.

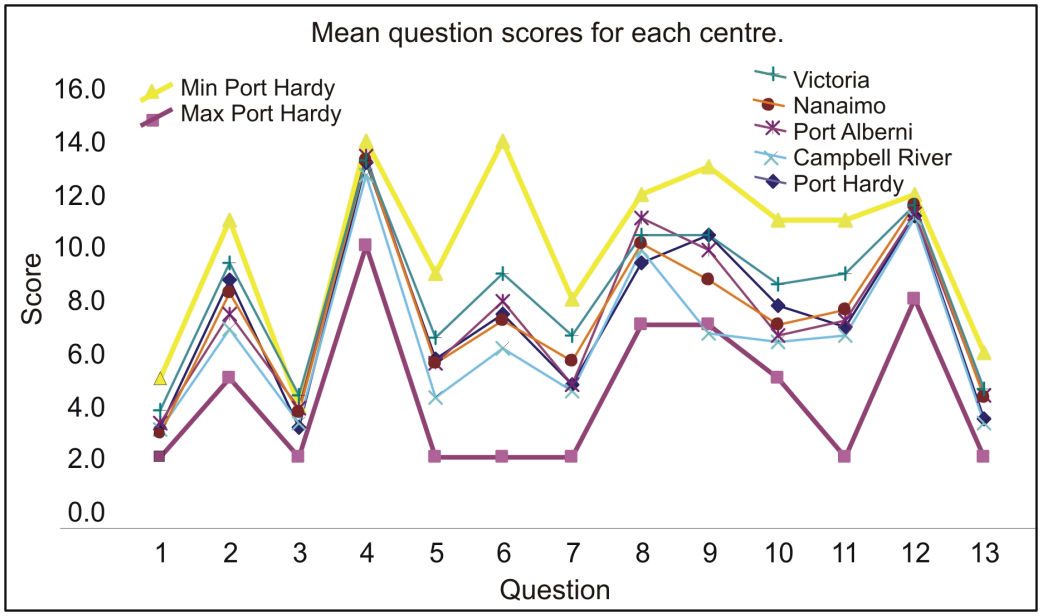

Figure A.3. Mean response of participants to 13 scenarios for forestry related landslides (see Tables A.1 and A.2 for questions and responses). Range is arbitrarily taken from the Port Hardy centre but is similar to ranges at each centre.

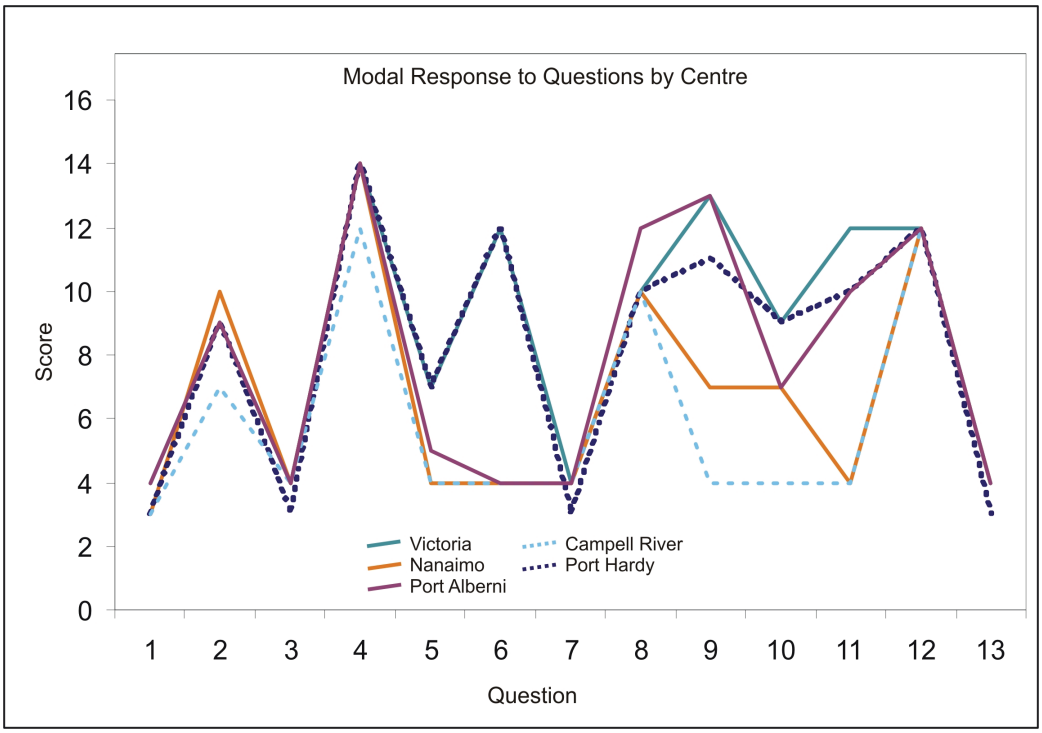

Figure A.4. Modal response of participants to 13 scenarios for forestry related landslides (see Tables A.1 and A.2 for questions and responses).

Scenarios 5 and 7 resulted in similar agreement and scores for two very different situations. In the first case a small landslide from otherwise stable terrain hit a stream, and another had a larger landslide in an explicitly assessed block that did not. Cause of the landslide was ambiguous in both cases. Modal responses for both cases indicated landslides should be mitigated and hazards reassessed. The exceptions in scenario 5 were for the Victoria and Port Hardy centres where professionals from the regulatory and other categories comprised almost 75% of the participants. Within these groups, there was a tendancy to assume that if the expert had looked at the block, pulled out an area of hazard and a landslide followed, that it occurred in an area deemed stable by the expert and the expert was therefore liable. This is indicated by the modal response in both those centres of a moderate financial penalty against the expert. Mean response in both cases suggests that there is an expectation that if terrain is considered stable, that it has been correctly assessed by an expert. While the modal response indicates some recognition of residual hazard, sufficient liability was assigned to either the expert or the company to raise the mean above the no direct penalty options in each centre but Campbell River. This is a good indication that we are in the ALARP region.

Scenarios 7, 10 and 2 are reasonably self similar with the impact to a fish bearing stream increasing in that order. Mean scores increase similarly at each centre, suggesting again that when presented with limited choices, participants indicated a clear response of lower tolerance to increased consequences, even in the face of ambiguous cause.

Question ambiguity was intentional and an attempt to illicit value judgements from participants. Answers were expected to, and did, contain variability; however, there is much to learn from the answers in any case. Questions 6, 9, 10 and 11 had considerable variation both within and between centres (mean versus modal scores). Based on the results, the breakdown of participants and the post survey discussions (discussions occurred when results had been handed in and could not be changed) it was clear that government regulators and special interest groups (the ‘other’ category) had lower risk tolerances than industry and consultants. To see this, one need only compare the scores and composition of Nanaimo and Campbell River to those of Victoria and Port Hardy.

Consultants (professional engineers and geoscientists) were, in particular, reluctant to be tough in the scenarios that could be seen to be implicitly or symbolically self-

incriminating; a dilemma not encountered by either the regulators or the 'other' group. Consultants tended to argue that there were several legitimate and logically consistent ways in which a landslide could occur that would indemnify the expert despite the scenario. Poor road construction for example could result in a landslide despite a block that an expert had deemed stable. There was a general consensus that if one could say definitively, "It was the experts fault", then penalties would be severe.

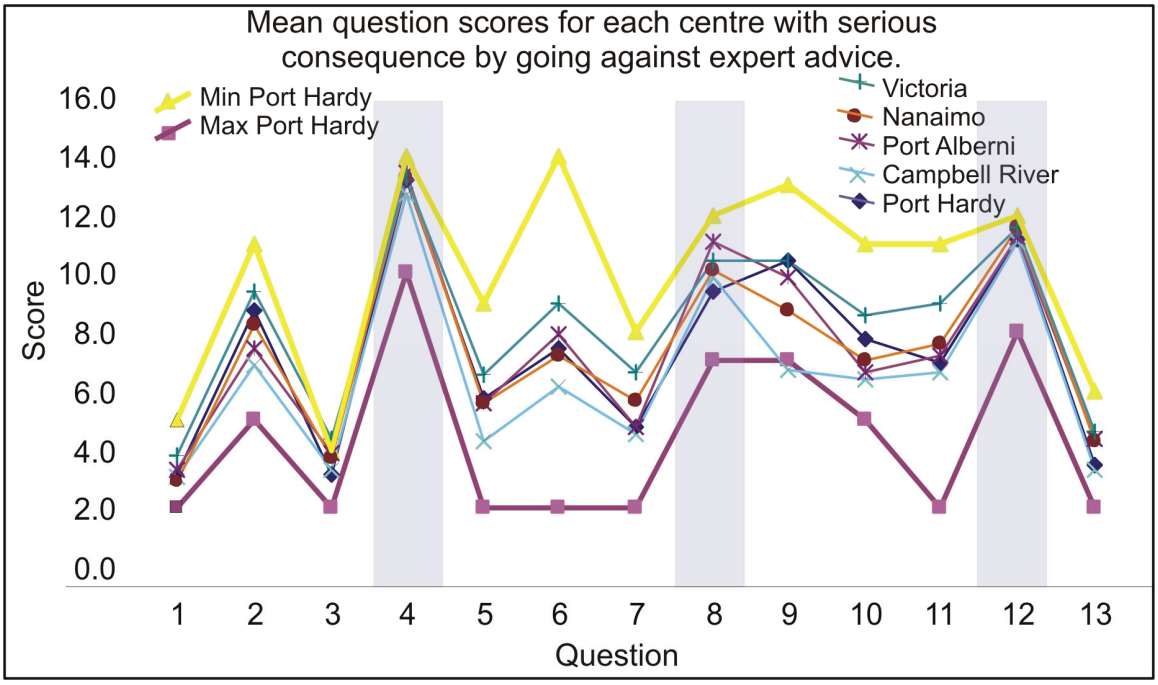

Figure A.5. Mean response of participants to scenarios where a consequence followed a company ignoring expert advice (shaded regions: see Tables A.1 and A.2).

Industry, in contrast, while also demonstrating that different assumptions would indemnify both groups (company and expert), also had several examples where they assumed company liability, similar to the previous example of road construction, and levied a penalty against the company rather than the expert (remembering that only one could be chosen). Part of the responses by both consultants and industry reflect direct knowledge of the difficulties in doing the work, and of residual and unknown hazards that may occur despite their best efforts.

Several government regulators did note that assumptions were required to assign liability and occasionally chose not to do so, however, as an overall group appeared more

likely to assign a penalty to either the expert or the company. The regulator group was concerned with results and held an underlying belief that if the experts and the companies were doing their jobs correctly that man-induced landslides, and particularly landslides with severe consequences, wouldn't occur.

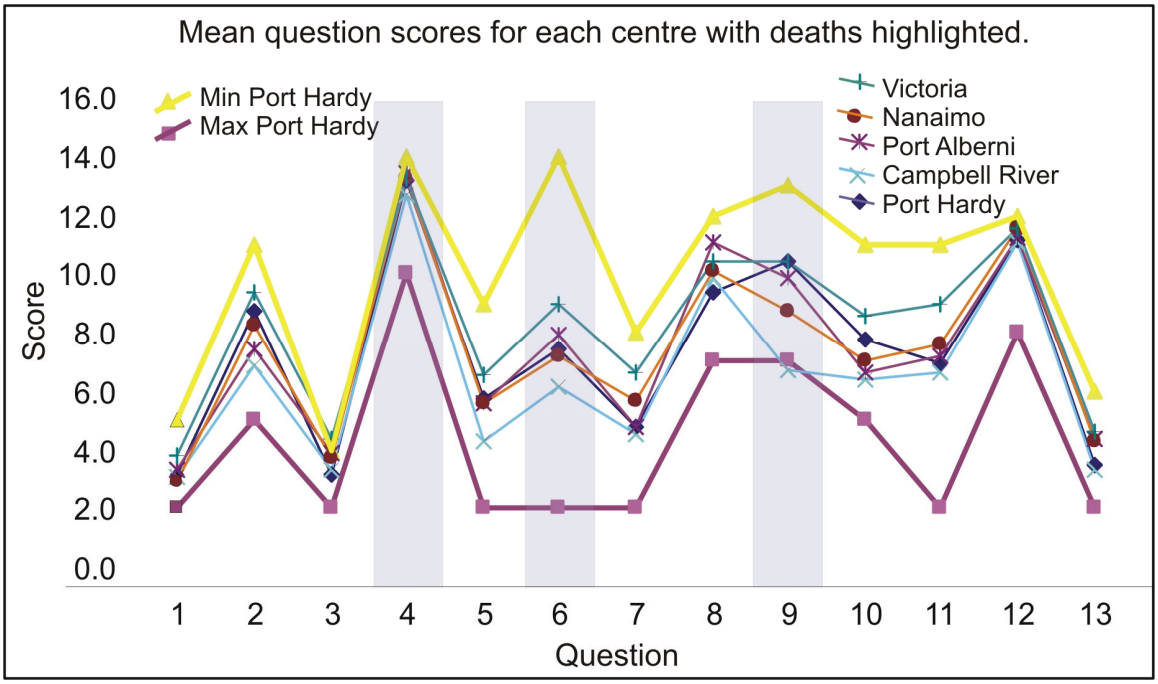

Figure A.6. Mean response of participants to scenarios where the consequence was loss of life (shaded regions: see Tables A.1 and A.2). Note increased variation in response and lower scores than those highlighted in Figure A.5.

Despite a variety of possible assumptions, all groups had been exposed to several case histories earlier in the day where landslides did occur in terrain that had been deemed to have low landslide potential, with consequences varying from the removal of soil on a small portion of a slope to burying a fish stream for more than 1 km. In other words, ambiguous or not, all of the non life-threatening scenarios have occurred recently in coastal BC. In addition, there are few events that occur in the natural world that don't have some ambiguity associated with them to a greater or lesser degree.

The results of the survey suggest that there is a low tolerance to landslides with consequences by governing authorities and a high expectation of the professional's ability

to correctly assess landslide hazard, and of industry to follow that advice. This reinforces the need for Professional Engineers and Geoscientists to quantify and calibrate, wherever possible, the results of their work against their expert judgement, clearly outlining the limitations of their approach.

Despite assumptions, the response for actions dipped only infrequently below a score of 4 which indicates general agreement within and between centres that forestry related landslides should be mitigated, and that hazards should be reassessed, even if it affects neighbouring proposals. While this feedback loop is possibly happening in some areas, particularly within blocks and during road construction, there is ample evidence that it is not happening everywhere. Nonetheless, it constitutes a critical part of the ALARP principle. New information needs to be incorporated to keep landslide risk as low as reasonably practicable.

Combined, the results of the exercise can give us a first look at tolerability for the types of consequence scenarios that may occur in BC (Figure A.7).

A.6. CONCLUSIONS

One hundred and thirteen forest professionals, comprised largely of foresters, biologists, engineers and geoscientists, grouped as government, industry, and consultants, considered the question of tolerability to landslide risk in British Columbia. British Columbia is unique in that the majority of risks posed by landslide hazards relate to environmental values across a massive, rugged and remote landscape.

There was general agreement amongst all participants that risks were intolerable where a landslide had material impact and was a consequence of expert advice being ignored or where experts were clearly at fault. In the examples tested, given limited options, the professional community was willing to set the penalties high (including the maximum penalty available in the example). Loss of life or severe material adverse

affects (burying of a fish stream for example) from an assessed block put the expert consultant or industry under intense scrutiny, with a likelihood of penalty increasing with consequence. Even in ambiguous cases, tolerance among the participants dropped with increasing consequences.

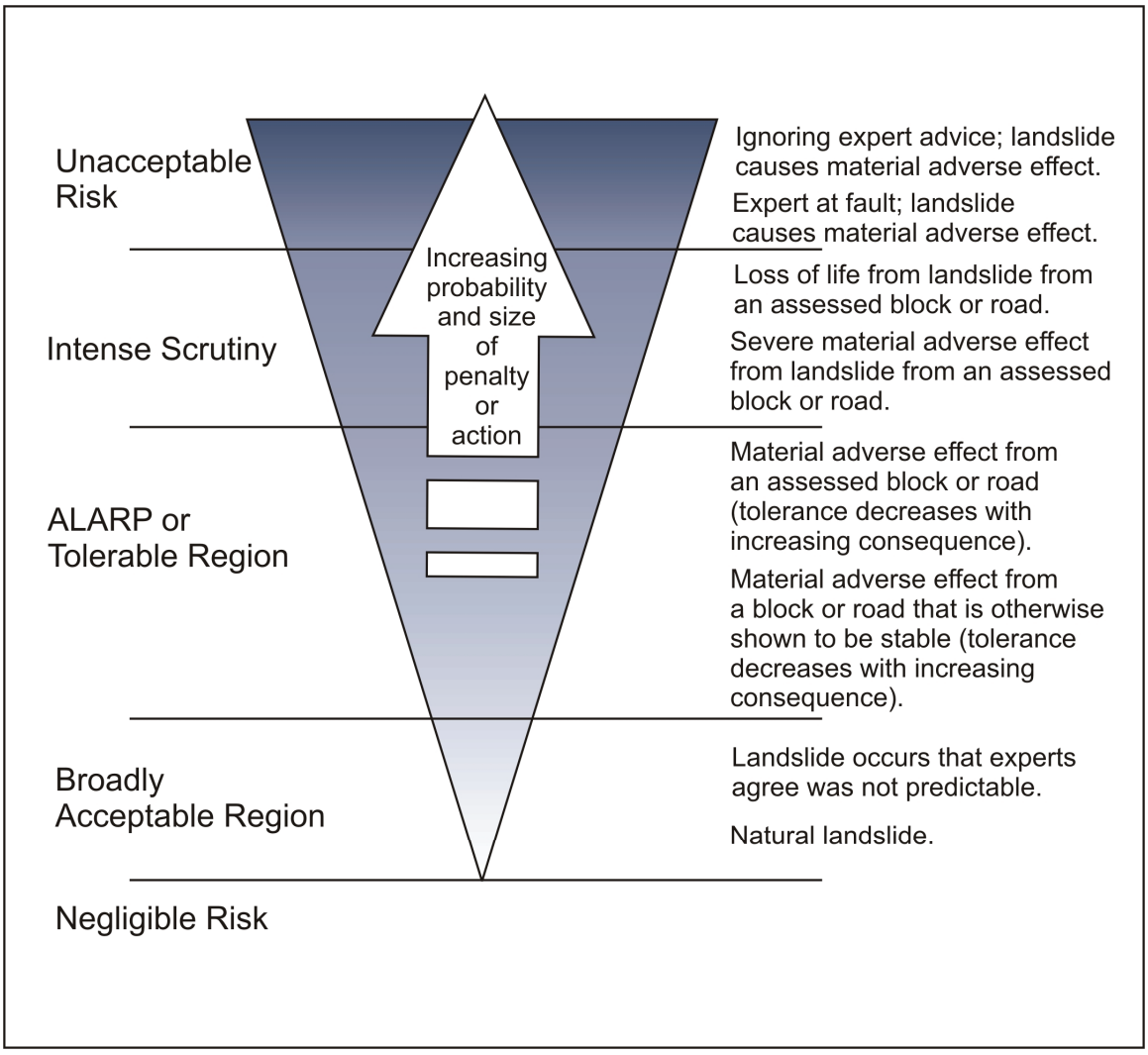

Figure A.7. A qualitative look, based on the results of surveyed professionals, at landslide tolerability criteria in British Columbia.

Overall, penalties were higher against companies than experts, however, it should be noted that in BC there has been a recent case of an expert penalized by a professional association that exceeds all but the very large fine (>$100,000.00) or jail time example penalties. In other words, these penalties might not be an accurate reflection of a real

result, but probably do reflect an actual tolerance, and the differences may be about scope rather than scale. The cautionary comment to experts is that they (as a group) lowered the overall penalty scores for questions that related to their practice. In contrast, the government group (as well as the 'other' group) was concerned primarily with results. These groups held an underlying belief that if the experts and the companies were doing their jobs correctly that man-induced landslides, and particularly landslides with severe consequences, wouldn't occur.

The results of the survey suggest that there is a low tolerance to landslides with consequences by governing authorities and a high expectation of the professional's ability to correctly assess landslide hazard, and of industry to follow that advice. This reinforces the need for Professional Engineers and Geoscientists to quantify and calibrate, wherever possible, the results of their work against their expert judgement, clearly outlining the limitations of their approach. This is particularly true considering that each of the non life-threatening scenarios have occurred recently in coastal BC, and that under the new legislative framework, the liability for the dramatic increase in landslide activity is borne by industry and the expert.

A.7. REFERENCES

ANCOLD, 2003. Guidelines on risk assessment. Australian National Committee on Large Dams, Melbourne, Australia.

APEGBC and ABCFP, 2007 (draft). Guidelines for the management of terrain stability in the forest sector. Association of Professional Engineers and Geoscientists, Vancouver BC.

BC Hydro, 1993. Interim guidelines for consequence-based dam safety evaluation and improvements. Report by the BC Hydro hydroelectric engineering division.

Chatwin, S. 2005. Managing Landslide Risk from Forest Practices in British Columbia. Forest Practices Board, Victoria, BC, 26p.

Fell, R. 1994. Landslide risk assessment and acceptable risk. Canadian Geotechnical Journal, 31, 261-272.

Fell, R. and D. Hartford, 1997. Landslide risk management. *In:* Landslide Risk Assessment, edited by: Cruden and Fell. Balkema Book Publishers, Rotterdam, Netherlands, 51- 109.

Fell, R., Ho, K.K.S., Lacasse, S. and E. Leroi, 2005. A framework for landslide risk assessment and management. *In:* Landslide Risk Management, edited by: Hungr, Fell, Couture and Eberhardt. Balkema Book Publishers, London, UK, 3-25.

Finlay, P.J., and R. Fell, 1997. Landslides: risk perception and acceptance. Canadian Geotechnical Journal, 34, 169-188.

Guthrie, R.H. 2002. The effects of logging on frequency and distribution of landslides in three watersheds on Vancouver Island, British Columbia. Geomorphology, 43, 275-294.

Guthrie, R.H. 2005. Geomorphology of Vancouver Island: mass wasting potential (includes maps). British Columbia Ministry of Environment Research Report No. RR01. British Columbia Ministry of Environment, Victoria, BC.

Guthrie, R.H. and S.G. Evans, 2004a. Analysis of landslide frequencies and characteristics in a natural system, coastal British Columbia. Earth Surface Processes and Landforms, 29:1321-1339.

Guthrie, R.H., and S.G. Evans, 2004b. Magnitude and frequency of landslides triggered by a storm event, Loughborough Inlet, British Columbia. Natural Hazards and Earth Systems Science, 4, 475-483.

Ho, K.K.S., Leroi, E. and B. Roberds, 2000. Quantitative risk assessment: application, myths and future direction. *In:* Thirty years of slope safety practice in Hong Kong, edited by: Chan *et al.*, 2007. Geotechnical Engineering Office, Civil Engineering and Development Department, HK, 521-559.

Horel, G. 2006. Summary of landslide occurrence on northern Vancouver Island. Streamline, 10, 1-9.

HSE (Health and Safety Executive, United Kingdom) 1992. The tolerability of risk from nuclear power stations, Her Majesty's Stationary Office, London.

Jakob M. 2000. The impacts of logging on landslide activity at Clayoquot Sound, British Columbia. Catena 38, 279-300.

Jordan, P. 2003. Landslide and terrain attribute study in the Nelson Forest region. Final report to Ministry of Forests Research Branch, project number: KB97202-0RE1. Nelson, BC, 60p.

Lee, E.M. and D.K.C. Jones, 2004. Landslide Risk Assessment. Thomas Telford Publishing, London, UK, 454 p.

Leroi, E., Bonnard, C., Fell, R. and R. McInnes, 2005. Risk assessment and management. *In:* Landslide Risk Management, edited by: Hungr, Fell, Couture and Eberhardt. Balkema Book Publishers, London, UK, 159-198.

Parish, R., and S. Thomson, 1994. The tree book: learning to recognize the trees of British Columbia, Canadian Forest Service and the British Columbia Ministry of Forests, Victoria, BC, 183 p.

Schwab, J. W. 1983. Mass wasting: October-November 1978 storm, Rennell Sound, Queen Charlotte Islands, British Columbia. British Columbia Ministry of Forests Research Note No. 91, Victoria, BC.

Wise, M.P., Moore, G. and D. VanDine, (eds). 2004. Landslide risk case studies in forest development planning and operations. British Columbia Ministry of Forests Forest Science Program. Land Management Handbook No.56, Victoria, BC.

Appendix B: Constructing a M-F curve

Magnitude-frequency curves are used throughout this thesis as a way of quantifying the probability that for a population of landslides, each individual event will be of a particular size. The probability distribution describes attributes of the population and is independent of variables such as time or space, but can be incorporated into either. Magnitude-frequency (M-F) curves may be plotted cumulatively or as a probability density. However, the cumulative plot is most commonly used in this thesis.

A cumulative M-F plot is constructing by ranking landslide magnitudes (area for example) in a complete inventory from greatest to smallest and plotting that same magnitude against the cumulative probability of occurrence defined as:

$$\Sigma P = m / n + 1 \qquad (14)$$

Where: P = Probability, m = the rank order of magnitude, and n = the sample size.

The example below, Table B1 is the calculation from a single storm in Loughborough Inlet in coastal BC (see Chapter 3 for details), and the resulting M-F curve with magnitude equal to area, is shown in Figure B1.

Table B.1. Calculation of cumulative magnitude-frequency curve for 101 landslides in Loughborough Inlet, British Columbia.

Slide Identification Number	Area in m^2	Rank	Cumulative Probability (Rank/n+1)
L11	409231	1	0.009803922
L45	99963	2	0.019607843
L24	75532	3	0.029411765
L68	72763	4	0.039215686
L46	60429	5	0.049019608
L71	60099	6	0.058823529
L59	58785	7	0.068627451
L48	58349	8	0.078431373
L67	52421	9	0.088235294
L47	43154	10	0.098039216
L84	39963	11	0.107843137
L52	38032	12	0.117647059
L82	33715	13	0.12745098
L41	33679	14	0.137254902
L51	31718	15	0.147058824
L65	31270	16	0.156862745

L23	27962	17	0.166666667
L36	27878	18	0.176470588
L26	27461	19	0.18627451
L27	26400	20	0.196078431
L09	22971	21	0.205882353
L49	22874	22	0.215686275
L32	22072	23	0.225490196
L39	21698	24	0.235294118
L42	20547	25	0.245098039
L44	19500	26	0.254901961
L53	18767	27	0.264705882
L28	18357	28	0.274509804
L29	18219	29	0.284313725
L03	18171	30	0.294117647
L43	17989	31	0.303921569
L73	17915	32	0.31372549
L64	17767	33	0.323529412
L33	17660	34	0.333333333
L66	15769	35	0.343137255
L08	15637	36	0.352941176
L75	15204	37	0.362745098
L83	15164	38	0.37254902
L02	14900	39	0.382352941
L93	14397	40	0.392156863
L01	13838	41	0.401960784
L80	12905	42	0.411764706
L10	12378	43	0.421568627
L86	12279	44	0.431372549
L78	12275	45	0.441176471
L05	12187	46	0.450980392
L76	12118	47	0.460784314
L87	11744	48	0.470588235
L20	11513	49	0.480392157
L55	11486	50	0.490196078
L91	11188	51	0.5
L88	10753	52	0.509803922
L21	10706	53	0.519607843
L38	10512	54	0.529411765
L63	10341	55	0.539215686
L85	10273	56	0.549019608
L81	10204	57	0.558823529
L92	10170	58	0.568627451
L97	9224	59	0.578431373
L50	9100	60	0.588235294
L74	8365	61	0.598039216
L60	8106	62	0.607843137
L57	7740	63	0.617647059
L72	7310	64	0.62745098
L62	7057	65	0.637254902
L35	7022	66	0.647058824
L16	6961	67	0.656862745
L18	6774	68	0.666666667

L96	6252	69	0.676470588
L19	6164	70	0.68627451
L37	6158	71	0.696078431
L30	5957	72	0.705882353
L89	5510	73	0.715686275
L06	5498	74	0.725490196
L25	5488	75	0.735294118
L79	4516	76	0.745098039
L12	4391	77	0.754901961
L54	4200	78	0.764705882
L56	3859	79	0.774509804
L61	3654	80	0.784313725
L34	3589	81	0.794117647
L69	3583	82	0.803921569
L94	3534	83	0.81372549
L70	3509	84	0.823529412
L40	3289	85	0.833333333
L90	3216	86	0.843137255
L22	2983	87	0.852941176
L14	2906	88	0.862745098
L31	2903	89	0.87254902
L13	2327	90	0.882352941
L17	2085	91	0.892156863
L99	2051	92	0.901960784
L100	1936	93	0.911764706
L98	1739	94	0.921568627
L04	1722	95	0.931372549
L58	1609	96	0.941176471
L07	1526	97	0.950980392
L95	1429	98	0.960784314
L101	1325	99	0.970588235
L77	1320	100	0.980392157
L15	1124	101	0.990196078

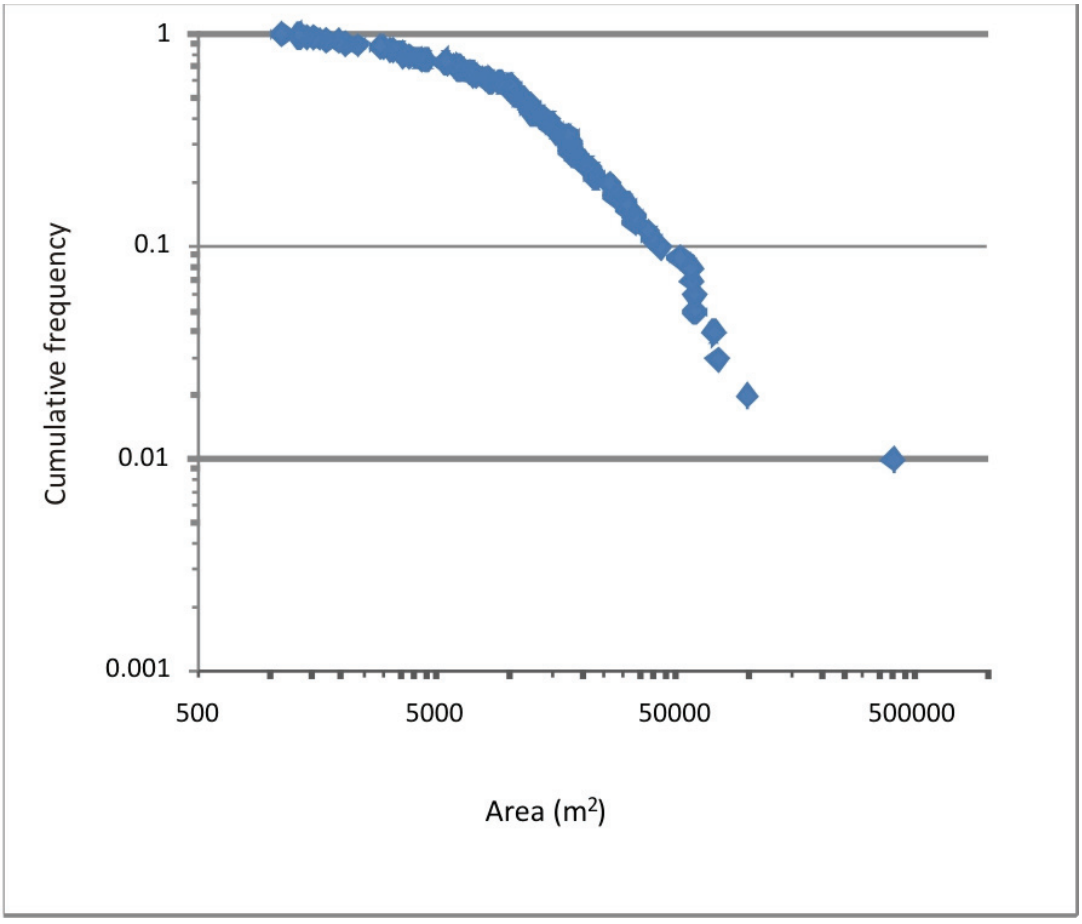

Figure B.1. The results of a cumulative magnitude-frequency calculation for 101 landslides in Loughborough Inlet, British Columbia (see Chapter 3 for more detailed discussion).